Application of Green's Functions to Self-Gravitating and Rotating Planets

and Modelling the Gravitational Field of the Earth

L. Koorevaar

Delft University of Technology

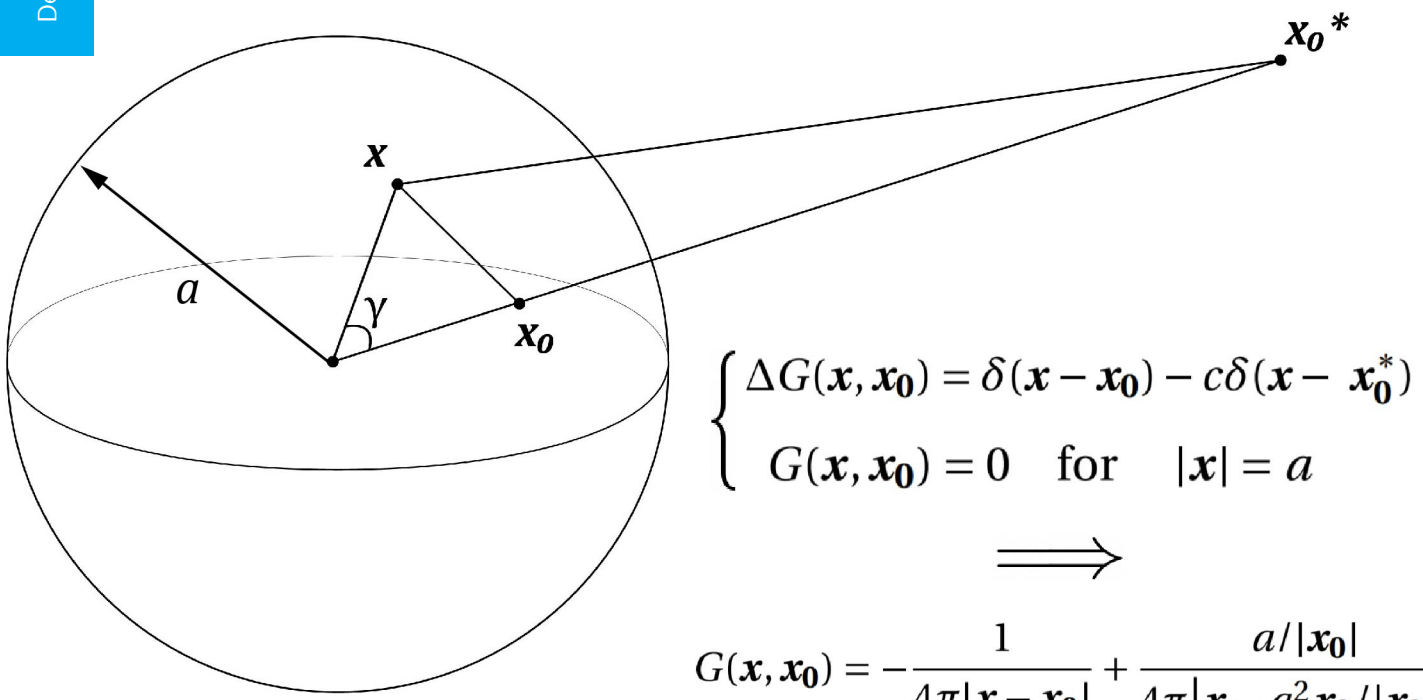

$$\begin{cases} \Delta G(\boldsymbol{x}, \boldsymbol{x_0}) = \delta(\boldsymbol{x} - \boldsymbol{x_0}) - c\delta(\boldsymbol{x} - \boldsymbol{x_0^*}) \\ G(\boldsymbol{x}, \boldsymbol{x_0}) = 0 \quad \text{for} \quad |\boldsymbol{x}| = a \end{cases}$$

$$\Longrightarrow$$

$$G(\boldsymbol{x}, \boldsymbol{x_0}) = -\frac{1}{4\pi|\boldsymbol{x} - \boldsymbol{x_0}|} + \frac{a/|\boldsymbol{x_0}|}{4\pi\left|\boldsymbol{x} - a^2\boldsymbol{x_0}/|\boldsymbol{x_0}|^2\right|}$$

TU Delft Delft University of Technology

Challenge the future

Application of Green's Functions to Self-Gravitating and Rotating Planets

and Modelling the Gravitational Field of the Earth

by

L. Koorevaar

in partial fulfilment of the requirements for the degree of
Bachelor of Science
in Applied Mathematics and Applied Physics
at Delft University of Technology.

Student number:	4598474
Project duration:	February, 2020 – July, 2020
Supervisors:	Dr. ir. R. van der Toorn
	Dr. ir. D.J. Verschuur
Committee Members:	Dr. ir. W. G. M. Groenevelt
	Dr. B. Rieger

TU Delft Delft University of Technology

ABSTRACT

This thesis focuses on the application of Green's functions to solve Poisson's law for gravity in the case of self-gravitating and rotating planets. The outlined theory is demonstrated in detail by applying it to the gravitational potential and acceleration for a spherical Earth.

For a self-gravitating and rotating planet to exist the following three conditions need to be satisfied:

1. The gravitational potential needs to be continuous across the surface of the planet.
2. The normal derivative of the gravitational potential needs to be continuous across the surface of the planet.
3. The surface of the planet is an equipotential surface (geoid).

For satisfying the third condition the sum of the gravitational potential and centrifugal potential needs to be constant on the surface. Introducing this constant on the surface -called the geopotential constant- and calculating the centrifugal potential, it was demonstrated that the third condition could be translated to an inhomogeneous Dirichlet boundary condition complementary to Poisson's law for gravity. The solution of Poisson's law for gravity -given by the gravitational potential $\phi(\boldsymbol{x})$- and this complementary boundary condition are written down in an integral expression with the help of Green's functions $G(\boldsymbol{x}, \boldsymbol{x_0})$.

The Green's function $G(\boldsymbol{x}, \boldsymbol{x_0})$ could physically be interpreted as the field at an observer point $\boldsymbol{x}$ from a unit source at $\boldsymbol{x_0}$. In the integral expression of the gravitational potential two different integrals could be found. The first integral could be interpreted as the field at position $\boldsymbol{x}$ caused by the density distribution $\rho(\boldsymbol{x_0})$ in product with the unit field from this source $G(\boldsymbol{x}, \boldsymbol{x_0})$ over the whole range of sources $\boldsymbol{x_0}$ in the volume D. The second integral could be interpreted as the effects from the boundary at a position $\boldsymbol{x}$ from a source distribution $f(\boldsymbol{x_0})$ on the boundary -given by the Dirichlet boundary condition- in product with the unit flux given by the derivative of the Green's function to the boundary $\frac{\partial G(\boldsymbol{x}, \boldsymbol{x_0})}{\partial n_0}$ over the whole boundary ∂D. The sum of these integrals gives the gravitational potential $\phi(\boldsymbol{x})$ at a position $\boldsymbol{x}$ in- or outside this volume D. Outside this volume D the source distribution is 0, therefore the whole field outside this volume could be thought of as generated only by the second boundary integral.

When this Green's function formalism, as outlined so far, is applied to a spherically symmetrical mass distribution of a rotating planet, some theoretical discrepancy in the results is to be expected, because as a result of centrifugal effects, a rotating planet in equilibrium cannot be spherically symmetric. Hence, provided that the theory is physically complete and consistent, a spherically symmetric mass distribution should not render a physically consistent solution of the gravitational field.

It is not a priori clear however that the discrepancy should come in the form of significant observable effects, as compared to, for example, the numerical accuracy of the numerical methods involved.

It is demonstrated that, when this Green's functions based methodology is applied to a homogeneous density, a linear spherical density and the PREM density profiles (where all density profiles are spherically symmetric), then discontinuities occur in the acceleration of gravitation across the surface of the Earth, in the range of 0.01 %- 0.13 %.

Such an effect is a symptom of incompatibility with the laws of physics for geostatical equilibrium, and it is certainly significant as compared to the numerical accuracy of the solution. Moreover, the discrepancy is dependent on geographical latitude, as was to be expected, because it somehow reflects the centrifugal effect.

The conclusion is made that this method is indeed capable of detecting, and even quantifying, the incompatibility of spherically symmetric mass distributions with the fundamental laws of physics for self-gravitating and rotating planets. This opens a way -and this is one of the main results- to computing corrections to spherically symmetric mass distributions, such as the PREM model. Based on this method, a further way forward to this end is suggested.

CONTENTS

INTRODUCTION

A geomagnetic reversal is a change in the Earth's magnetic field such that the magnetic north-pole and magnetic south-pole switch in polarity. These interchanges of the magnetic field are statistically random and the latest reversal, the Brunhes-Matuyama reversal, occurred approximately 780.000 years ago (Singer et al. (2019)). The duration of such a reversal is a widely varying subject, where the average is estimated around 7000 years, with a spread of 2000 to 12000 years (Clement (2004)).

The study that occupies itself with the source of the internal magnetic field is called geodynamo theory. The large spread in the estimation of the reversal of the poles comes from the fact that the strength and structure of the Earth's internal magnetic field are poorly known (Buffett (2010)). Although many self-consistent dynamo models do exist, there are significant differences between them, in the results these models produce, and in the manner they were constructed (Glatzmaier (2013); Glatzmaier and Roberts (1996)).

When it comes to developing a well-founded understanding of important phenomena such as the dynamics of the Earth's magnetic field, which in itself will depend on the virtually inaccessible ingredients and processes in the interior of the Earth, a well-portrayed energy distribution model at the Earth's core is needed. In the pursuit of these facts, mathematical -physical modelling is among the best tools that we have at our disposal.

In the mathematical physical modelling of the energy profile at the depths of the Earth's source of magnetic fields, a good understanding of the structure and strength of gravity is needed. In the best-known estimation of the strength of the Earth's internal magnetic field, the gravity and the shape of the nickel-iron inner core were neglected (Buffett (2010)). It is because of this reason that the self-consistent model of gravity will be revisited and quantified. The best model of the appropriate sources of the Earth's gravitational field -namely the mass densities at appropriate depths- is given by the PREM model (Dziewonski and Anderson (1981)). In this report, a self-consistent mathematical physical model for a self-gravitating and rotating planet's gravitational field will be constructed. This self-consistent model will use the formalism of Green's functions, which are coupled to Poisson's law for gravity that obeys the perceptible geoid condition on the surface of our planet, to generate the inaccessible gravitational field at the core of this planet.

In the first part of this report, the mathematical construction of the Green's function will be derived and evaluated for a Poisson's equation. In the first chapter, the definition of the Poisson's equation complementary with Dirichlet boundary conditions is evaluated and this expression is then used to define the Green's function. Then, in the second chapter, Green's functions on an infinitely large domain are evaluated. These infinite space Green's functions are then used in the third chapter, with a technique called the method of images, to solve for the Green's function on a spherical volume.

In the second part of this report, a look will be given to the usage of these expressions on the gravitational potential of a self-gravitating and rotating planet. Therefore, in chapter 4 the Poisson's equation for the gravitational potential will be derived. Also in this chapter, continuity constraints for the physical shapes of a self-gravitating and rotating planet will be evaluated. Subsequently, in chapter 5, this defined model using the Green's function will be tested to gain a better understanding of the gravitational field of the Earth. Thereafter, in chapter 6 the discussion of the results is presented and recommendations for further

research are given. And in the last chapter, the conclusion is given.

This report is part of the completion of the bachelor of science programs of Applied Mathematics and Applied Physics, provided at Delft University of Technology. To this end, this report contributes as a bachelor thesis in both study programs simultaneously.

List Of Constants

In this chapter, some important constants that will be used in the modelling of the Earth are written down. The basic parameters underlying these constants are summarized by the International Astronomical Union (IAU) and the latest version of these constants was uploaded in the following paper Luzum et al. (2011). In the next table the constants, their description, their value, their standard uncertainty, and their references are listed:

Constant	Description	Value	Uncertainty	Reference
$\mathcal{G}$	Gravitational Constant	$6.67430\ 10^{-11}$ m ^{3} kg $^{-1}$ s $^{-2}$	$0.00015\ 10^{-11}$ m ^{3} kg $^{-1}$ s $^{-2}$	Milyukov and Fan (2012)
M_e	Mass of Earth	$5.9722\ 10^{24}$ kg	$0.0006\ 10^{24}$ kg	Luzum et al. (2011)
K	Potential of the Geoid	$6.26368560\ 10^{7}$ m ^{2} s $^{-2}$	$8.0\ 10^{-9}$ m ^{2} s $^{-2}$	Moritz (1988)
ω	Angular Velocity	$7.2921150\ 10^{-5}$ rad s $^{-1}$	$0.0000001\ 10^{-5}$ rad s $^{-1}$	Groten (1999)
a	Semi-Major Axis/ Equatorial radius of the Earth	$6.3781366\ 10^{6}$ m	$1\ 10^{-1}$ m	Burša et al. (1998)
b	Semi-Minor Axis	$6.3567523\ 10^{6}$ m	$1\ 10^{-1}$ m	Groten (1999)
R	Radius Of Spherical Earth (Same Volume)	$6.3710008\ 10^{6}$ m	$1\ 10^{-1}$ m	Moritz (1988)

In the table above, the radius of the Earth is chosen in such a manner that the the volume of a spherical Earth is equivalent to the volume of the spheroidal Earth (Moritz (1988)). This radius of the Earth R is given by the following formulae:

$$R = \sqrt[3]{a^2\ b}.$$

For the uncertainty of this radius α_R, the calculus based approximation can be used (Ifan G. Hughes (2010)):

$$\alpha_R = \sqrt{\left(\frac{\partial R}{\partial a}\alpha_a\right)^2 + \left(\frac{\partial R}{\partial b}\alpha_b\right)^2} = \frac{1}{R^2}\sqrt{\left(\frac{2ab}{3}\alpha_a\right)^2 + \left(\frac{a^2}{3}\alpha_b\right)^2} = 7.4502 \cdot 10^{-2}\ \text{m} \approx 1 \cdot 10^{-1}\ \text{m},$$

where α_a is the uncertainty in the semi-major axis a and α_b is the uncertainty in the semi-minor axis b.

Part I: Mathematical Constructions

1

Mathematical Introduction to Green's Functions for Poisson's Equations

In this chapter, the mathematical concept of Green's function will be defined and explored for certain partial differential equations, which are called Poisson's equations. Firstly a Poisson's equation will be defined in the first section, then in the second section, an important integral expression is derived, which is going to be used in defining the Green's function in the third section.

1.1. Definition of the Poisson's Equation with Boundary Condition

Definition of the Poisson's Equation

The necessity for the reason why Green's function will only be solved for the Poisson's equation lies in the fact that in the physical counterpart of this report an important physical Poisson's equation arises. This important Poisson's equation is an equation where the gravitational potential $\phi(\boldsymbol{x})$ is given by a certain density distribution $\rho(\boldsymbol{x})$, by Poisson's law for gravity, given in the following expression:

$$\Delta\phi(\boldsymbol{x}) = -4\pi\mathscr{G}\rho(\boldsymbol{x}). \tag{1.1}$$

In this equation, $\mathscr{G}$ is the universal gravitational constant of Newton, and Δ is the Laplace operator. The Laplace operator in a 3-dimensional space, given by coordinates (x, y, z), is a differential operator on a function, and is defined by:

$$\Delta = \frac{\partial^2}{\partial x^2} + \frac{\partial^2}{\partial y^2} + \frac{\partial^2}{\partial z^2}. \tag{1.2}$$

Every partial differential equation that can be written in a way, where a function $u(\boldsymbol{x})$ needs to be found on a certain volume D, and the left-hand side is given by $\Delta u(\boldsymbol{x})$ and the right-hand side by another function $Q(\boldsymbol{x})$ is called a Poisson's equation. For a better understanding of these Poisson's equations, let us summarize these facts in the following definition:

Definition 1.1 (Poisson's Equation)**.** Let $D \subset \mathbb{R}^3$ be a volume, $u : D \to \mathbb{R}$ be a twice continuously differentiable function and $Q : D \to \mathbb{R}$ be a function, often known as the source term. A Poisson's equation is a Partial Differential Equation on this volume D that for all $\boldsymbol{x} \in D$ satisfies:

$$\Delta u(\boldsymbol{x}) = Q(\boldsymbol{x}).$$

In the case that the source term is zero-valued i.e. $Q(\boldsymbol{x}) = 0$ for all $\boldsymbol{x} \in D$, then this particular Poisson's equation is also called a Laplace's equation.

If in the above definition the functions $u(\boldsymbol{x})$ and $Q(\boldsymbol{x})$ are respectively given by $\phi(\boldsymbol{x})$ and $-4\pi\mathcal{G}\rho(\boldsymbol{x})$, then it can easily be seen that the equation in (1.1) is a Poisson's equation.

BOUNDARY CONDITION ON POISSON'S EQUATION

In the mathematical construction part of this report, one specific boundary condition will be complementary to the Poisson's equation in definition (1.1), and for this boundary condition, Poisson's equation will be solved with the help of an appropriate function called the Green's function. The boundary condition that will be considered is of Dirichlet type. The reason why only Dirichlet boundary conditions -in contrast to Neumann boundary conditions and mixed/Robin conditions- are considered, is the fact that in the physical counterpart a Dirichlet boundary condition arises. However, the reader could be interested, out of mathematical curiosity, in the case of a Neumann boundary condition and therefore the case of a Neumann boundary condition can be found in the Appendix. With a Dirichlet boundary condition, a specific distribution of the function $u(\boldsymbol{x})$ is prescribed on the boundary of our volume D, denoted by ∂D. The Poisson's equation of definition (1.1) together with the Dirichlet boundary condition will be the main subject to solve in the first part of the report, and is therefore formally denoted in the following problem:

Problem 1.1. *Let $D \subseteq \mathbb{R}^3$ be a closed bounded set with piecewise smooth boundary ∂D, let $u : D \to \mathbb{R}$ be a twice continuously differentiable function, and let $Q : D \to \mathbb{R}$ be a function known as the source term. The problem that needs to be solved is the following Poisson's equation:*

$$\Delta u(\boldsymbol{x}) = \frac{\partial^2 u(\boldsymbol{x})}{\partial x^2} + \frac{\partial^2 u(\boldsymbol{x})}{\partial y^2} + \frac{\partial^2 u(\boldsymbol{x})}{\partial z^2} = Q(\boldsymbol{x}) \quad \textit{for} \quad \boldsymbol{x} \in D,$$

with the appropriate Dirichlet boundary condition:

$$u(\boldsymbol{x}) = f(\boldsymbol{x}) \quad \textit{for} \quad \boldsymbol{x} \in \partial D.$$

1.2. INTEGRAL EXPRESSION FOR GREEN'S FUNCTION

In the manner the Green's function is going to be defined and why this definition is useful, it is recommended to first look at a special integral expression. This integral expression will give a lot of insight in why the Green's functions are used in solving Poisson's equations. For constructing this integral expression, let u and v be twice differentiable functions and let the operator Δ be given by the Laplace operator. Notice that, because the Laplace operator is the sum of differential operators and the linearity property of differentiation, the Laplace operator must also be a linear operator. Now let us take a look at an integral over a certain volume D and over the integrand $u\,\Delta v - v\,\Delta u$:

$$= \int_D u\,\Delta v - v\,\Delta u\,dV. \tag{1.3}$$

In making a useful expression out of this integral expression the following intermezzo given in (1.2) is needed.

Intermezzo 1.2. *Let $D \subseteq \mathbb{R}^3$ and let $u, v : D \to \mathbb{R}$ be continuously differentiable functions, then*

$$u\,\Delta v - v\,\Delta u = \nabla \cdot (u\,\nabla v - v\,\nabla u).$$

Before stating the proof, let us look of how the ∇ operator behaves in the above expression. Notice that u, v are scalar functions, therefore ∇ is the gradient operator and ∇u, ∇v are vector fields. Moreover, it follows that $u\,\nabla v - v\,\nabla u$ is the sum of products of scalar functions and vector fields and is, thus, also a vector field. On this vector field $u\,\nabla v - v\,\nabla u$, the nabla operator $\nabla\cdot$ acts as the divergence operator, and the scalar function $\nabla\cdot(u\,\nabla v - v\,\nabla u)$ is obtained.

Proof. Assume that $D \subset \mathbb{R}^3$ is a volume and $u, v : D \to \mathbb{R}$ are continuously differentiable functions, then:

$$\begin{aligned}\nabla\cdot(u\,\nabla v - v\,\nabla u) &= \nabla\cdot(u\,\nabla v) - \nabla\cdot(v\nabla u)\\ &= \nabla u\cdot\nabla v + u\,\nabla\cdot(\nabla v) - \nabla v\cdot\nabla u - v\,\nabla\cdot(\nabla u)\\ &= u\,\Delta v - v\,\Delta u.\end{aligned}$$

Where in the first line the linearity of ∇ was used, in the second line the dot product rule and the associative property of ∇ were used, and in the third line the definition of the Laplacian $\Delta = \nabla^2 = \nabla\cdot\nabla$ was used. □

If the intermezzo of (1.2) is used in the integral expression of (1.3), then one can find the following expression:

$$\int_D u\,\Delta v - v\,\Delta u\,dV = \int_D \nabla\cdot(u\nabla v - v\nabla u)\,dV. \tag{1.4}$$

To make further simplifications to this integral expression the divergence theorem of Gauss given in de Pagter and Groenevelt (2015) is going to be used:

Theorem 1.3 (Divergence Theorem of Gauss)**.** *Let $U \subseteq \mathbb{R}^3$ be an open set and $\boldsymbol{f} : U \to \mathbb{R}^3$ a continuously differentiable vector field. Let $D \subseteq U$ be a closed bounded subset with a piecewise smooth boundary ∂D, then:*

$$\int_D \nabla\cdot\boldsymbol{f}(\boldsymbol{x})\,dV = \int_{\partial D}\boldsymbol{f}(\boldsymbol{x})\cdot\hat{\boldsymbol{n}}\,dS,$$

where dV stands for a volume integral, dS for a surface integral and $\hat{\boldsymbol{n}}$ is the outgoing surface unit vector on dS.

The proof of this theorem is beyond the scope of this report. If the divergence theorem (1.3) is applied to the integral expression in (1.4), then the following expression can be found:

$$\int_D \nabla\cdot(u\,\nabla v - v\,\nabla u)\,dV = \int_{\partial D}(u\,\nabla v - v\,\nabla u)\cdot\hat{\boldsymbol{n}}\,dS = \int_{\partial D} u\,\frac{\partial v}{\partial n} - v\,\frac{\partial u}{\partial n}\,dS. \tag{1.5}$$

In the last step of (1.5) the abbreviation was used for a scalar function u that $(\nabla u)\cdot\hat{\boldsymbol{n}} = \frac{\partial u}{\partial n}$. The abbreviation stands for the directional derivative of this function u in the direction of the normal vector $\hat{\boldsymbol{n}}$ on the boundary ∂D. The integral expression of (1.5) is going to be used in determining the definition of Green's function for the Dirichlet boundary condition for our Poisson's equation at the problem of (1.1).

1.3. DEFINITION OF GREEN'S FUNCTION

In this section, a definition of Green's function will be given in the precise manner such that the problem of (1.1) with Dirichlet boundary condition could be solved. Before this evaluation can be done, it is helpful to first define a particular function called the Dirac-Delta function.

1.3.1. DIRAC-DELTA FUNCTION

For the definition of the Green's function, a helpful other function is needed, this function is called the Dirac-delta function and is defined in the following definition. [1]

Definition 1.2 (Dirac-Delta Function)**.** Let $U \subseteq \mathbb{R}$ and let $\delta : U \to \mathbb{R}$ be the Dirac-delta function. This function satisfies the following properties:

$$\delta(x) = \begin{cases} \infty & \text{if } x = 0 \\ 0 & \text{elsewhere} \end{cases}$$

and

$$\int_{\mathbb{R}} \delta(x)\,dx = 1.$$

One can think of $\delta(x - x_i)$ as a concentrated source or impulsive force at $x = x_i$. An important property of this function which will be stated without proof is the following:

$$f(x) = \int_{\mathbb{R}} f(x_i)\delta(x - x_i)\,dx_i\,, \tag{1.6}$$

where the assumption was made that $f(x)$ is a well-defined function. For 3-dimensional problems, a 3-dimensional delta function is going to be needed. This 3-dimensional Dirac-delta function is given in the following definition.

Definition 1.3 (3-Dimensional Dirac-Delta Function)**.** Let $D \subseteq \mathbb{R}^3$ and let $\delta : D \to \mathbb{R}$ be the 3-dimensional Dirac-delta function. If the source is concentrated at $\boldsymbol{x_0} = (x_0, y_0, z_0)^T$, then the 3-dimensional Dirac-delta function is defined as:

$$\delta(\boldsymbol{x} - \boldsymbol{x_0}) = \delta(x - x_0) \cdot \delta(y - y_0) \cdot \delta(z - z_0),$$

where in the product the 1-dimensional Dirac-delta function was used.

The same property as in equation (1.6) can be constructed for the 3-dimensional case. Using the definition in (1.3) and a well-defined function $f : D \to \mathbb{R}$, then the following can be found:

$$\begin{aligned}
\int_{\mathbb{R}^3} f(\boldsymbol{x_0})\delta(\boldsymbol{x} - \boldsymbol{x_0})\,dV_0 &= \int_{-\infty}^{\infty}\int_{-\infty}^{\infty}\int_{-\infty}^{\infty} f(\boldsymbol{x_0})\delta(\boldsymbol{x} - \boldsymbol{x_0})\,dx_0\,dy_0\,dz_0 \\
&= \int_{-\infty}^{\infty}\int_{-\infty}^{\infty}\int_{-\infty}^{\infty} f(x_0, y_0, z_0)\delta(x - x_0)\delta(y - y_0)\delta(z - z_0)\,dx_0\,dy_0\,dz_0 \\
&= \int_{-\infty}^{\infty}\int_{-\infty}^{\infty} f(x, y_0, z_0)\delta(y - y_0)\delta(z - z_0)\,dy_0\,dz_0 \\
&= \int_{-\infty}^{\infty} f(x, y, z_0)\delta(z - z_0)\,dz_0 \\
&= f(x, y, z) \\
&= f(\boldsymbol{x}).
\end{aligned}$$

Hence, it follows that:

$$f(\boldsymbol{x}) = \int_{\mathbb{R}^3} f(\boldsymbol{x_0})\delta(\boldsymbol{x} - \boldsymbol{x_0})\,dV_0. \tag{1.7}$$

[1] Actually, mathematically spoken, this function is not a function but a measure (Haberman (2003)), however, these details will not be of significant value in this report.

1.3.2. DEFINING THE GREEN'S FUNCTION FOR THE DIRICHLET PROBLEM

The Poisson's equation with Dirichlet boundary condition constructed in section (1.1) is copied below:

$$\Delta u(\boldsymbol{x}) = Q(\boldsymbol{x}) \quad \text{for} \quad \boldsymbol{x} \in D,$$
$$u(\boldsymbol{x}) = f(\boldsymbol{x}) \quad \text{for} \quad \boldsymbol{x} \in \partial D.$$

The main result of section (1.2) was the last integral expression (1.5):

$$\int_D u\,\Delta v - v\,\Delta u\,dV = \int_{\partial D} u\,\frac{\partial v}{\partial n} - v\,\frac{\partial u}{\partial n}\,dS. \tag{1.8}$$

Let us first propose the definition of the Green's function for this problem. The reason why this definition is chosen in this precise manner will become clear when the subsequent steps are evaluated. The definition of the Green's function for a Poisson's equation with Dirichlet boundary condition is given to be:

Definition 1.4 (Green's Function for Dirichlet Boundary Condition)**.** Let $D \subseteq \mathbb{R}^3$ be the same closed bounded subset with piece-wise smooth boundary ∂D as given in problem (1.1). The Green's function, for the Dirichlet boundary condition, given by $G : D \times D \to \mathbb{R}$ is defined in the following manner:

$$\Delta G(\boldsymbol{x}, \boldsymbol{x_0}) = \delta(\boldsymbol{x} - \boldsymbol{x_0}) \quad \text{for} \quad \boldsymbol{x}, \boldsymbol{x_0} \in D,$$
$$G(\boldsymbol{x}, \boldsymbol{x0}) = 0 \quad \text{for} \quad \boldsymbol{x} \in \partial D, \boldsymbol{x_0} \in D.$$

Now let the functions u and v in the integral expression shown in (1.8) be given respectively by the function of the Poisson's problem $u(\boldsymbol{x})$ and the recently defined Green's function $G(\boldsymbol{x}, \boldsymbol{x_0})$. At this moment, when filling in the conditions of the Poisson's equation and the boundary conditions of $u(\boldsymbol{x})$ and $G(\boldsymbol{x}, \boldsymbol{x_0})$ in the integral expression of (1.8), then one would end up with the following result:

$$\int_D u(\boldsymbol{x})\,\delta(\boldsymbol{x} - \boldsymbol{x_0}) - G(\boldsymbol{x}, \boldsymbol{x_0})\,Q(\boldsymbol{x})\,dV = \int_{\partial D} f(\boldsymbol{x})\,\frac{\partial G(\boldsymbol{x}, \boldsymbol{x_0})}{\partial n} - 0\,\frac{\partial u(\boldsymbol{x})}{\partial n}\,dS. \tag{1.9}$$

Notice that on $\int_D u(\boldsymbol{x})\delta(\boldsymbol{x} - \boldsymbol{x_0})dV$ the result for the 3-dimensional delta function of (1.7) can be used, such that this integral expression is equivalent to $u(\boldsymbol{x_0})$, and hence after rearranging, the following result shown in (1.10) could be deduced:

$$u(\boldsymbol{x_0}) = \int_D G(\boldsymbol{x}, \boldsymbol{x_0})Q(\boldsymbol{x})dV + \int_{\partial D} f(\boldsymbol{x})\frac{\partial G(\boldsymbol{x}, \boldsymbol{x_0})}{\partial n}dS. \tag{1.10}$$

An important property of Green's function, which is proved in Haberman (2003), is that for the Green's function the following result is valid:

$$\text{for all} \quad \boldsymbol{x}, \boldsymbol{x_0} \in D: \quad G(\boldsymbol{x}, \boldsymbol{x_0}) = G(\boldsymbol{x_0}, \boldsymbol{x}).$$

This result is called the symmetric property for Green's function and is a property for all Green's functions coupled to certain different partial differential equations, and is not only a specific property for the Green's function coupled to the Poisson's equation.

If the above property of Green's function is used when interchanging $\boldsymbol{x}$ and $\boldsymbol{x_0}$ in expression (1.10), then the following result could be obtained:

$$u(\boldsymbol{x}) = \int_D G(\boldsymbol{x}, \boldsymbol{x_0})Q(\boldsymbol{x_0})dV_0 + \int_{\partial D} f(\boldsymbol{x_0})\frac{\partial G(\boldsymbol{x}, \boldsymbol{x_0})}{\partial n_0}dS_0. \tag{1.11}$$

Notice that in the first integral of this result one finds the product of the Green's function $G(\boldsymbol{x}, \boldsymbol{x_0})$ with the function that made the Poisson's equation inhomogeneous $Q(\boldsymbol{x})$, and at the second integral one finds the product of the outgoing derivative of Green's function to the boundary $\frac{\partial G(\boldsymbol{x},\boldsymbol{x_0})}{\partial n_0}$ with the function that made the Dirichlet boundary condition inhomogeneous $f(\boldsymbol{x_0})$. So both terms do combine to the final result $u(\boldsymbol{x})$ of the Partial Differential Equation in particular weighted integrals with Green's function.

Hence, if the Green's function as defined in (1.4) can be found, then the inhomogeneous Poisson's equation with inhomogeneous Dirichlet boundary condition of section (1.1) could be solved. So the problem is transformed from solving the Poisson's equation directly, to finding a particular function called Green's function, which needs to satisfy the constraints in the definition of (1.4).

If one is interested in how the Green's functions for the Neumann boundary condition are defined, then one could look at chapter A in the Appendix.

2

INFINITE 3-DIMENSIONAL SPACE GREEN'S FUNCTIONS

In the previous chapter, a representation of the Green's function for the Poisson's equation with Dirichlet boundary conditions was obtained. In reality, these expressions can be complicated to find, because of the generality of the volume D in which the Green's function needs to be determined. This general volume D could be a difficult shape with a difficult (even piecewise) boundary ∂D. For a better understanding of what Green's functions $G(\boldsymbol{x}, \boldsymbol{x_0})$ are and subsequently how the points $\boldsymbol{x}$ and $\boldsymbol{x_0}$ affect each other, a solution of Green's function in an infinite 3-dimensional space will be given in this chapter.

2.1. INFINITE SPACE POISSON'S EQUATION

In chapter 1 the Poisson's equation was discussed for a general volume $D \subseteq \mathbb{R}^3$. In this chapter the problem is going to be extended to an infinitely large domain. Therefore, the volume D is given by $D = \mathbb{R}^3$. Now, there is still one problem, what happens at the boundaries of an infinite space volume? The boundaries are now at ∞ so how does one deal with this? Recall that the problem defined at (1.1) with $D = \mathbb{R}^3$ is given by:

$$\Delta u(\boldsymbol{x}) = \frac{\partial^2 u(\boldsymbol{x})}{\partial x^2} + \frac{\partial^2 u(\boldsymbol{x})}{\partial y^2} + \frac{\partial^2 u(\boldsymbol{x})}{\partial z^2} = Q(\boldsymbol{x}) \quad \text{or} \quad \boldsymbol{x} \in \mathbb{R}^3, \tag{2.1}$$

with the Dirichlet boundary condition:

$$u(\boldsymbol{x}) = f(\boldsymbol{x}) \quad \text{for} \quad \boldsymbol{x} \in \partial\mathbb{R}^3. \tag{2.2}$$

For this infinite large domain, as mentioned before, the boundaries are at ∞, so how does one deal with this? For answering this question, the origin of a lot of practical Poisson's equation in this report is going to be used. In this report, the solution of the Poisson's equation will represent a physical quantity and from physical quantities, it is known that these need to represent reality i.e. at ∞, not every function can describe this physical quantity, there need to be some constraints.

In the case of a Poisson's equation, this physical quantity is -most of the time- portrayed by a potential that is coupled by a gradient to an underlying conservative force. So to find this potential a path integral is taken over the force and this path integral is arbitrary to some constant. Therefore, the potential at ∞ is some constant and this constant can arbitrarily be chosen. However, most of the time, this constant is taken to be 0 out of simplicity. So if the potential is given by u, then it needs to follow that $\lim_{|\boldsymbol{x}|\to\infty} u = 0$. The gradient

of this potential ∇u is coupled to the field of the underlying conservative force. It is expected that at ∞ the force can not have any significant influence, therefore it is expected that $\lim_{|\boldsymbol{x}|\to\infty} \nabla u = 0$. To summarize, when the Poisson's equation in an infinite space for a physical quantity is given, then, in this report, the following boundary conditions are prescribed:

$$\lim_{|\boldsymbol{x}|\to\infty} u(\boldsymbol{x}) = 0 \quad \text{and} \quad \lim_{|\boldsymbol{x}|\to\infty} \nabla u(\boldsymbol{x}) = 0, \tag{2.3}$$

which states that the energy (the potential) at ∞ is chosen to be zero (Dirichlet) and that the flux (the force field) at ∞ needs to be 0 (Neumann). These boundary conditions will be used to solve the infinite space Poisson's equation.

2.2. INFINITE SPACE 3-DIMENSIONAL GREEN'S FUNCTIONS

Now let us look at the Green's functions on this infinite domain, and what properties these functions need to obey when having the boundary conditions of the last section in mind. Remember that the Poisson's equation that needs to be solved is given by:

$$\Delta u(\boldsymbol{x}) = Q(\boldsymbol{x}) \quad \text{for} \quad \boldsymbol{x} \in \mathbb{R}^3, \tag{2.4}$$

with the boundary conditions:

$$\lim_{|\boldsymbol{x}|\to\infty} u(\boldsymbol{x}) = 0 \quad \text{and} \quad \lim_{|\boldsymbol{x}|\to\infty} \nabla u(\boldsymbol{x}) = 0. \tag{2.5}$$

In the same manner as in chapter 1, Green's function will be defined to represent a three dimensional delta function in the following way:

$$\Delta G(\boldsymbol{x}, \boldsymbol{x_0}) = \delta(\boldsymbol{x} - \boldsymbol{x_0}) \quad \text{for all} \quad \boldsymbol{x}, \boldsymbol{x_0} \in \mathbb{R}^3. \tag{2.6}$$

The above equation for Green's function can be interpreted as a concentrated source at $\boldsymbol{x} = \boldsymbol{x_0}$ in a 3-dimensional space that has no boundaries. Therefore, intuitively, the solution should be symmetric around the source point $\boldsymbol{x} = \boldsymbol{x_0}$, because the delta function is also symmetric around this source point. [1]. When having this symmetric property in mind, it is useful to define the parameter ρ as the spatial distance from the source point $\boldsymbol{x_0}$ to a point $\boldsymbol{x}$ in space. Mathematically written, this parameter is defined in the following way:

$$\begin{aligned} &\boldsymbol{\rho} = \boldsymbol{x} - \boldsymbol{x_0}, \\ &\rho = |\boldsymbol{\rho}| = |\boldsymbol{x} - \boldsymbol{x_0}| = \sqrt{(x - x_0)^2 + (y - y_0)^2 + (z - z_0)^2}. \end{aligned} \tag{2.7}$$

The assumption is made, because of the symmetric property, that the Green's function $G(\boldsymbol{x}, \boldsymbol{x_0})$ only depends on the distance to the source given by ρ:

$$G(\boldsymbol{x}, \boldsymbol{x_0}) = G(\rho) = G(|\boldsymbol{x} - \boldsymbol{x_0}|). \tag{2.8}$$

For $\boldsymbol{x} \neq \boldsymbol{x_0}$ or $\rho \neq 0$, from the definition of Green's function (2.6), it is known that $\delta(\boldsymbol{x} - \boldsymbol{x_0}) = 0$, so in this region the following expression must hold:

$$\Delta G(\boldsymbol{x}, \boldsymbol{x_0}) = 0. \tag{2.9}$$

For the 3-dimensional case the solution must be spherically symmetric. If the Δ operator is written in spherical coordinates (r, θ, φ) [2], then the expression shown in (2.10) follows:

$$\Delta G = \frac{1}{\rho^2}\frac{\partial}{\partial \rho}\left(\rho^2 \frac{\partial f}{\partial \rho}\right) + \frac{1}{r^2 \sin(\theta)}\frac{\partial}{\partial \theta}\left(\sin(\theta)\frac{\partial G}{\partial \theta}\right) + \frac{1}{r^2 \sin(\theta)^2}\frac{\partial^2 G}{\partial \varphi^2}. \tag{2.10}$$

[1] The vector field that is created from this source is said to be an isotropic vector field. This means that for any spherical neighbourhood centered at the point source, the magnitude of the vector determined by any point on the sphere is equivalent (Misner et al. (1973)).

[2] In this definition of the spherical coordinates, r is the radial distance, θ is the polar angle and φ is the azimuthal angle. These spherical coordinates will also be defined in section (3.2) in chapter 3.

When having in mind that the solution needs to be spherically symmetric, then the following terms $\frac{\partial}{\partial\theta}$ and $\frac{\partial}{\partial\varphi}$ need to be neglected. After letting these terms vanish in the expression of (2.10), the following equation that needs to be solved arises:

$$\Delta G = \frac{1}{\rho^2}\frac{\partial}{\partial\rho}\left(\rho^2\frac{\partial G}{\partial\rho}\right) = 0. \tag{2.11}$$

This is an ordinary differential equation of second order, and the solution can easily be obtained by integrating twice over ρ:

$$G(\rho) = \frac{c_1}{\rho} + c_2, \tag{2.12}$$

where c_1 and c_2 are to be determined constants in $\mathbb{R}$. The singularity condition of the Poisson's equation for the Green's function (2.6) can be used to find one of these constants. To find this constant let us integrate equation (2.9) around a small sphere D with radius ρ:

$$\begin{aligned}\int_D \Delta G\, dV &= \int_D \delta(\boldsymbol{x}-\boldsymbol{x_0})\, dV = 1\\ &= \int_D \nabla\cdot(\nabla G)\, dV = \int_{\partial D} \nabla G\cdot\hat{\boldsymbol{n}}\, dS = \int_{\partial D}\frac{\partial G}{\partial\rho}\, dS,\end{aligned} \tag{2.13}$$

where the divergence theorem of Gauss (1.3) has been used in the second line and the spherical shell is denoted by ∂D. When using the expression of (2.13) and using the fact that the radius ρ is constant on the boundary, then one could find:

$$4\pi\rho^2\frac{\partial G}{\partial\rho} = 1. \tag{2.14}$$

In this result, the fact was used that the area of a sphere with radius ρ is given by $4\pi\rho^2$. When differentiating Green's function of expression (2.12) to ρ, then the constant c_1 can be found:

$$4\pi\rho^2\left(\frac{-c_1}{\rho^2}\right) = 1 \quad\rightarrow\quad c_1 = \frac{-1}{4\pi}. \tag{2.15}$$

The constant of c_2 is arbitrary, indicating that the infinite space Green's function for Poisson's equation is determined to be within an arbitrary additive constant. In the boundary conditions that were proposed for $u(\boldsymbol{x})$ the assumption was made that there needs to be no energy at ∞ i.e. the potential needs to be 0 at ∞. In order to do so, Green's function also needs to go to 0 if $G(\rho\rightarrow\infty)$, hence $c_2 = 0$. The infinite space 3-dimensional Green's function is thus given by the following equation:

$$G(\boldsymbol{x},\boldsymbol{x_0}) = \frac{-1}{4\pi|\boldsymbol{x}-\boldsymbol{x_0}|} = \frac{-1}{4\pi\sqrt{(x-x_0)^2+(y-y_0)^2+(z-z_0)^2}}. \tag{2.16}$$

2.3. SOLUTION AND DECAY CONDITION OF THE INFINITE SPACE POISSON'S EQUATION

In chapter 1 an important integral expression -for finding the solution of $u(\boldsymbol{x})$- was created, this integral expression was given in (1.2) and is also repeated below:

$$\int_D u\,\Delta G - G\,\Delta u\, dV = \int_{\partial D}(u\,\nabla G - G\,\nabla u)\cdot\hat{\boldsymbol{n}}\, dS. \tag{2.17}$$

In the integral at the right-hand side of the equal sign, an integration is done over the entire boundary ∂D. The infinite space $\mathbb{R}^3$ has no boundaries, so how can a solution still be constructed? To solve this problem, large spheres D are considered. In these large spheres the limit of the radius ρ is going to approach ∞ for an infinite space. For a sensible solution the contribution of this second integral needs to vanish for this infinitely large ρ, which results in:

$$\lim_{\rho\to\infty}\int_{\partial D}(u\nabla G - G\nabla u)\cdot\hat{\boldsymbol{n}}\,dS = 0. \tag{2.18}$$

In the same way as in chapter 1, when using the Delta function and the symmetric property of the Green function, the solution of $u(\boldsymbol{x})$ is found to be:

$$u(\boldsymbol{x}) = \int_D Q(\boldsymbol{x_0})G(\boldsymbol{x},\boldsymbol{x_0})dV_0, \tag{2.19}$$

where now $G(\boldsymbol{x},\boldsymbol{x_0})$ is given by the solution of the Green's function in an infinite space that can be found in (2.16). Now the condition for which the condition (2.18) is satisfied, still needs to be found. For this purpose, notice that the outward surface unit vector $\hat{\boldsymbol{n}}$ for a sphere is given by $\hat{\boldsymbol{\rho}}$, such that $\nabla\cdot\hat{n} = \frac{\partial}{\partial\rho}$, and also notice that after interchanging integration and taking the limit in (2.18), the following result for the integrand must hold:

$$\lim_{\rho\to\infty}\rho^2\left(u\frac{\partial G}{\partial\rho} - G\frac{\partial u}{\partial\rho}\right) = 0. \tag{2.20}$$

In equation (2.16) the Green's function for an infinite space was already calculated, so after substituting this in the expression above, then the following equation could be found:

$$\lim_{\rho\to\infty}\left(u + \rho\frac{\partial u}{\partial\rho}\right) = 0, \tag{2.21}$$

which is satisfied because the boundary conditions was chosen to be of physical relevance and therefore needed to satisfy the expressions in (2.3). The general solution u of Poisson's equation with the above condition tend to satisfy the relationship: $u \sim \frac{1}{\rho}$. Notice the familiarity here with the case of gravitational or even coulomb effects where the forces are decaying as $\sim \frac{1}{\rho^2}$ and the potentials are decaying as $\sim \frac{1}{\rho}$ in infinite space. There do exist other solutions u to Poisson's equation in infinite space (Haberman (2003)), but these other solutions tend to not satisfy the decaying condition of (2.21) and are therefore not useful in our analysis of a physical quantity.

3

GREEN'S FUNCTION FOR SPHERICAL COORDINATES

In this chapter, Green's functions for the characteristic shape of a sphere with volume D will be determined using an approach that is called the method of images. This determination of the Green's functions will be done using the infinite space Green's functions of chapter 2 in collaboration with the method of images (Morse and Feshbach (1954)), which will be described in the first section. In the second section, spherical coordinates will be introduced, and in the third section, the Green's function of a spherical volume will be found for given homogeneous Dirichlet conditions on the spherical surface shell.

3.1. METHOD OF IMAGES

In the previous chapter, the volume D was said to be infinite and on this infinite space, the Green's function was found using appropriate boundary conditions at ∞. In this section, the problem of the bounded domains will again be visited, but, this time, the infinite space Green's function of chapter 2 will be used in evaluating this case. In the same manner as with the first definition of the Green's function in chapter 1, the Poisson's Equation (1.1) that needs to be solved is given by:

$$\Delta G(\boldsymbol{x}, \boldsymbol{x_0}) = \delta(\boldsymbol{x} - \boldsymbol{x_0}) \quad \text{for} \quad \boldsymbol{x}, \boldsymbol{x_0} \in D, \tag{3.1}$$

with a homogeneous Dirichlet boundary condition on ∂D. In contrast to chapter 2 the volume D is again bounded as in chapter 1. Notice that in chapter 2 a solution of the Green's function was given for the case of a 3-dimensional infinite space, this solution can be interpreted as a particular solution to the bounded problem. With a particular solution it is meant that it solves the inhomogeneous condition in (3.1), but it does not solve the homogeneous Dirichlet boundary condition. This particular solution G_p, which was evaluated in expression (2.16), is given by:

$$G_p(\boldsymbol{x}, \boldsymbol{x_0}) = \frac{-1}{4\pi|\boldsymbol{x} - \boldsymbol{x_0}|}. \tag{3.2}$$

The problem is that this particular solution solves (3.1) but it does not solve the homogeneous Dirichlet boundary condition on ∂D. For also solving the boundary condition, let us consider the Green's function to become an addition of the particular solution with a homogeneous solution $w(\boldsymbol{x}, \boldsymbol{x_0})$:

$$G(\boldsymbol{x}, \boldsymbol{x_0}) = G_p(\boldsymbol{x}, \boldsymbol{x_0}) + w(\boldsymbol{x}, \boldsymbol{x_0}), \tag{3.3}$$

where the function $w(\boldsymbol{x}, \boldsymbol{x_0})$ represents the effect on the boundary. Because $w(\boldsymbol{x}, \boldsymbol{x_0})$ represents the effect on the boundary, and G_p already solves equation (3.1), $w(\boldsymbol{x}, \boldsymbol{x_0})$ needs to satisfy:

$$\Delta w(\boldsymbol{x}, \boldsymbol{x_0}) = 0 \quad \text{for} \quad \boldsymbol{x} \in D, \tag{3.4}$$

subject to some non-homogeneous boundary conditions on ∂D. To make this more clear an example will be illustrated in the following paragraph.

Let us consider the case where there is a Poisson's equation that has an inhomogeneous Dirichlet boundary condition. Then for the Green's function the following homogeneous boundary condition follows:

$$G(\boldsymbol{x}, \boldsymbol{x_0}) = 0 \quad \text{on} \quad \partial D.$$

To solve for this boundary condition the function $w(\boldsymbol{x}, \boldsymbol{x_0})$, which represents the effects on the boundary must have the following inhomogeneous boundary condition: $w(\boldsymbol{x}, \boldsymbol{x_0}) = \frac{1}{4\pi|\boldsymbol{x}-\boldsymbol{x_0}|}$ on ∂D, because then this expression (3.3) solves the Poisson's equation. To solve for the function $w(\boldsymbol{x}, \boldsymbol{x_0})$ a solution needs to be given for the Laplace equation with a non-homogeneous boundary condition for which, if the geometry allows it, separation of variables or a Laplace transform can be used. Thereafter, if the solution of $G_p(\boldsymbol{x}, \boldsymbol{x_0})$ and $w(\boldsymbol{x}, \boldsymbol{x_0})$ are combined, the solution of the Green's function and thereby the solution of the underlying Poisson's equation is found.

Notice that the expression of $w(\boldsymbol{x}, \boldsymbol{x_0})$ in (3.4) does not have a singularity at $\boldsymbol{x} = \boldsymbol{x_0}$ in contrast to the infinite space Green's function. Hence, the Green's function for a bounded domain also has a singularity at $\boldsymbol{x} = \boldsymbol{x_0}$, because the singularity of the infinite space Green function does not get compensated by $w(\boldsymbol{x}, \boldsymbol{x_0})$. This conclusion can be explained using the physical interpretation of the Green's function, as the response at a point $\boldsymbol{x}$ due to a source at $\boldsymbol{x_0}$, and that a response at a point nearby the source should, in general, not depend significantly on any boundaries.

The manner in which a function $w(\boldsymbol{x}, \boldsymbol{x_0})$ is constructed for dealing with the effects on the boundaries -which can only be done for certain geometries- is often called *The Method of Images* (Morse and Feshbach (1954)).

3.2. DEFINING THE SPHERICAL COORDINATES

The goal of this section is to transform a point $\boldsymbol{x} \in \mathbb{R}^3$ in Cartesian coordinates x, y and z to spherical coordinates r, θ and φ. Figure (3.1) is plotted to illustrate the way in which the spherical parameters r, φ and θ will be defined.

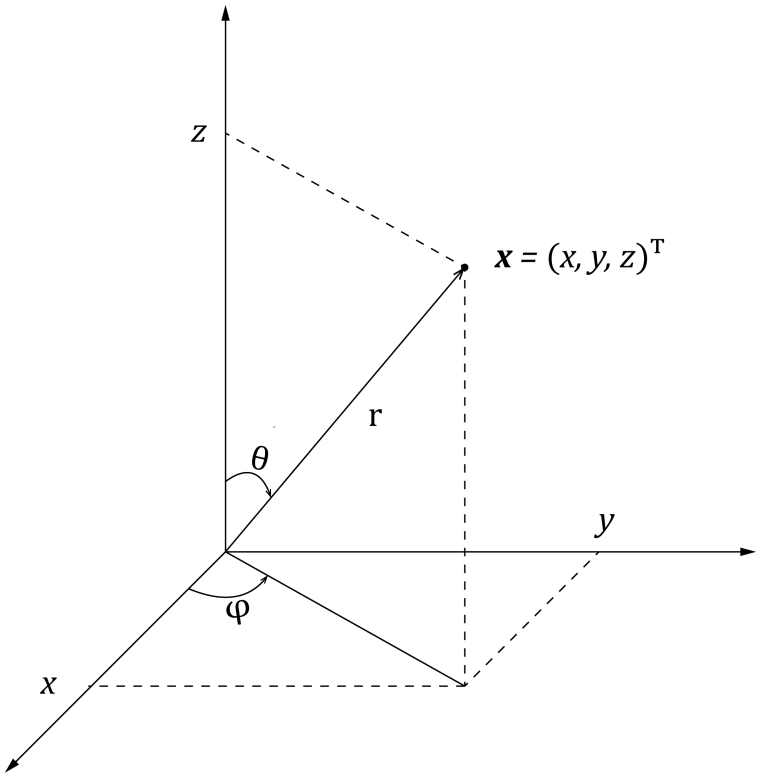

Figure 3.1: In this figure, the way in which the spherical coordinates are going to be defined are shown. The parameter r is the distance to the origin, the parameter φ is the angle to the x-axis in the xy-plane and the parameter θ is the angle to the z-axis. The r parameter is called the radial distance, the θ parameter is called the polar angle and the φ parameter is called the azimuthal angle.

In this figure the parameter r is the distance to the origin, φ is the azimuthal angle in the xy-plane to the x-axis and θ is the polar angle to the z-axis. First one can see r as the hypotenuse of a triangle with angle θ. Then the z-coordinate becomes $r\ \cos\theta$ and the line in the xy-plane becomes $r\ \sin\theta$. This line in the xy-plane is a hypotenuse of a triangle with angle φ. So then one could see that $x = r\ \sin\theta\ \cos\varphi$ and $y = r\ \sin\theta\ \sin\varphi$. In summary the result is:

$$\begin{aligned} x &= r\ \sin\theta\ \cos\varphi, \\ y &= r\ \sin\theta\ \sin\varphi, \\ z &= r\ \cos\theta. \end{aligned} \tag{3.5}$$

For a bijective coordination transformation -with exception of the poles- between the Cartesian- and spherical coordinates, the domain of the spherical coordinates needs to be $r > 0$, $0 < \varphi \leq 2\pi$ and $0 \leq \theta \leq \pi$. In chapter 1 an integral expression was found for calculating the solution to the Poisson's equation with a Dirichlet boundary condition. When the volume D in this expression is given by a sphere, it is useful and easier to integrate over spherical coordinates instead of Cartesian coordinates. A volume part in Cartesian and spherical coordinates is given by:

$$dV = dx\ dy\ dz = \frac{\partial(x,y,z)}{\partial(r,\theta,\varphi)}\ dr\ d\theta\ d\varphi, \tag{3.6}$$

where the Jacobian $\frac{\partial(x,y,z)}{\partial(r,\theta,\varphi)}$ for a transformation from Cartesian to spherical coordinates is

evaluated to be:

$$\begin{aligned}\frac{\partial(x,y,z)}{\partial(r,\theta,\varphi)} &= \begin{vmatrix} \partial x/\partial r & \partial x/\partial\theta & \partial x/\partial\varphi \\ \partial y/\partial r & \partial y/\partial\theta & \partial y/\partial\varphi \\ \partial z/\partial r & \partial z/\partial\theta & \partial z/\partial\varphi \end{vmatrix} \\ &= \begin{vmatrix} \sin\theta\,\cos\varphi & r\,\cos\theta\,\cos\varphi & -r\,\sin\theta\,\sin\varphi \\ \sin\theta\,\sin\varphi & r\,\cos\theta\,\sin\varphi & r\,\sin\theta\,\cos\varphi \\ \cos\theta & -r\,\sin\theta & 0 \end{vmatrix} \\ &= r^2\,\sin\theta. \end{aligned} \tag{3.7}$$

A spherical shell is created for a constant parameter r, let us call this parameter for which this shell follows a. Hence, dS is the surface for this a. The outgoing surface vector is given by $\hat{\boldsymbol{n}} = \hat{\boldsymbol{r}}$, and therefore for spherical coordinates it follows that for a surface part of this sphere:

$$dS = dS_r = \left|\frac{\partial \boldsymbol{x}}{\partial\theta} \times \frac{\partial \boldsymbol{x}}{\partial\varphi}\right| d\theta\, d\varphi = a^2\,\sin\theta\, d\theta\, d\varphi. \tag{3.8}$$

3.3. METHOD OF IMAGES FOR GREEN'S FUNCTION INSIDE A SPHERE

In this section, the Method of Images will be used to find the Green's function inside a spherical volume. Now consider a spherical volume D with radius a, in this section the Green's function on this sphere is the main objective to be found, in doing this, the method of images outlined in the first section is going to be used. The Poisson's equation that will be solved was given at the equation in (1.1), where now the choice is made that the volume D represents a sphere. In case of a sphere the following statements are equivalent $\boldsymbol{x} \in D \iff r = |\boldsymbol{x}| \leq a$ and $\boldsymbol{x} \in \partial D \iff r = |\boldsymbol{x}| = a$. For clarification the Poisson's equation that needs to be solved is copied below:

$$\Delta u(\boldsymbol{x}) = Q(\boldsymbol{x}) \quad \text{for} \quad |\boldsymbol{x}| \leq a, \tag{3.9}$$

with the Dirichlet boundary condition:

$$u(\boldsymbol{x}) = f(\boldsymbol{x}) \quad \text{for} \quad |\boldsymbol{x}| = a. \tag{3.10}$$

This problem transforms in solving for the following Green's function:

$$\Delta G(\boldsymbol{x}, \boldsymbol{x_0}) = \delta(\boldsymbol{x} - \boldsymbol{x_0}) \quad \text{for} \quad |\boldsymbol{x}| \leq a, \tag{3.11}$$

with homogeneous Dirichlet boundary condition:

$$G(\boldsymbol{x}, \boldsymbol{x_0}) = 0 \quad \text{for} \quad |\boldsymbol{x}| = a. \tag{3.12}$$

To solve this problem an image point $\boldsymbol{x_0^*}$ is constructed, and on this image point a function $w(\boldsymbol{x}, \boldsymbol{x_0})$ will be defined for dealing with the effects on the boundary. Let us first consider the infinite space Green's function given in (2.18) corresponding to a positive source at $\boldsymbol{x_0}$. Now, because the infinite space Green's function does not satisfy the boundary condition, a negative image source $\boldsymbol{x_0^*}$ outside the sphere will be made. This results in the following expression:

$$\Delta G(\boldsymbol{x}, \boldsymbol{x_0}) = \delta(\boldsymbol{x} - \boldsymbol{x_0}) - c\delta(\boldsymbol{x} - \boldsymbol{x_0^*}). \tag{3.13}$$

In this expression c is a real constant that represents the weight of the second function. Notice that because the image source $\boldsymbol{x_0^*}$ is outside the sphere, equation (3.11) is still satisfied

inside the sphere. Let us translate the expression of (3.13) using the infinite space Green's function:

$$G(\boldsymbol{x},\boldsymbol{x_0}) = -\frac{1}{4\pi|\boldsymbol{x}-\boldsymbol{x_0}|} + \frac{c}{4\pi\left|\boldsymbol{x}-\boldsymbol{x_0^*}\right|}. \tag{3.14}$$

The problem that needs to be addressed is "what is the position of $\boldsymbol{x_0^*}$?" and "what is the value of the weight c such that the boundary condition of (3.12) is satisfied?". For this purpose one could try if the following assumption leads to a sensible solution. The assumption that will be made is that for the cancellation of the Green's functions on the boundary (3.12), the point $\boldsymbol{x_0^*}$ needs to be on the same line from the origin of the sphere as $\boldsymbol{x_0}$, or in mathematical terms:

$$\boldsymbol{x_0^*} = k\,\boldsymbol{x_0}, \tag{3.15}$$

in which k is a real positive constant such that $\boldsymbol{x_0^*}$ is outside the sphere, hence $k > \frac{a}{|\boldsymbol{x_0}|}$. For a better understanding of the situation that is present, the following figure in (3.2) is constructed.

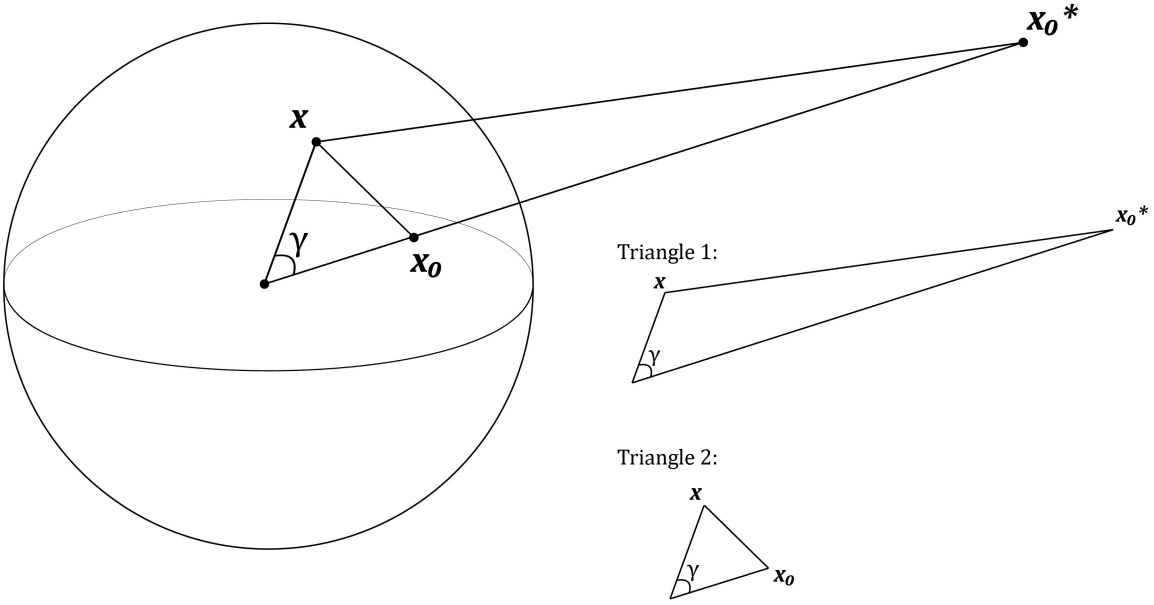

Figure 3.2: In this figure, a representation for determining the Green's function inside a sphere, using the method of images, is shown. In this representation $\boldsymbol{x}$ is the position where the field would liked to be found, $\boldsymbol{x_0}$ is the position of the source term, and $\boldsymbol{x_0^*}$ is the position of the image term. Next to the sphere, two triangles with the same angle γ to the midpoint of the sphere are highlighted to give a better understanding of the representation of the cosine rule used in this section.

In this figure, the points $\boldsymbol{x}$ and $\boldsymbol{x_0}$, wherefore the response needs to be determined, are chosen randomly in the sphere and the image source $\boldsymbol{x_0^*}$ is chosen to be on the same line from the origin as $\boldsymbol{x_0}$. The angle γ in the figure is defined as the angle between the point $\boldsymbol{x}$ and the point $\boldsymbol{x_0}$ seen from the mid-point of the sphere. Notice that because of the line assumption in (3.15) this angle γ is also the angle between $\boldsymbol{x}$ and $\boldsymbol{x_0^*}$. Therefore, the two triangles highlighted in the figure next to the sphere, can be constructed. If on both triangles the cosine rule is being used, then the following two expressions follow:

$$\text{Triangle 1:} \quad \left|\boldsymbol{x}-\boldsymbol{x_0^*}\right|^2 = |\boldsymbol{x}|^2 + \left|\boldsymbol{x_0^*}\right|^2 - 2\,|\boldsymbol{x}|\,\left|\boldsymbol{x_0^*}\right|\,\cos\gamma, \tag{3.16}$$

$$\text{Triangle 2:} \quad |\boldsymbol{x}-\boldsymbol{x_0}|^2 = |\boldsymbol{x}|^2 + |\boldsymbol{x_0}|^2 - 2\,|\boldsymbol{x}|\,|\boldsymbol{x_0}|\,\cos\gamma. \tag{3.17}$$

The boundary condition in (3.12) concludes that the Green's function of (3.14) needs to be 0 for $|\boldsymbol{x}| = a$. From now on -in the following expressions- the assumption is made that $|\boldsymbol{x}| = a$.

From this assumption the Green's function on the boundary becomes:

$$-\frac{1}{4\pi|\boldsymbol{x}-\boldsymbol{x_0}|}+\frac{c}{4\pi\left|\boldsymbol{x}-\boldsymbol{x_0^*}\right|}=0 \quad \Longleftrightarrow \quad c|\boldsymbol{x}-\boldsymbol{x_0}|=\left|\boldsymbol{x}-\boldsymbol{x_0^*}\right|. \tag{3.18}$$

When the expression shown in the right-hand of (3.18) is squared, and the expressions with the cosine rule for the triangles (3.16) are used, then it follows that:

$$c^2\left(a^2+|\boldsymbol{x_0}|^2-2\,a\,|\boldsymbol{x_0}|\,\cos\gamma\right)=a^2+\left|\boldsymbol{x_0^*}\right|^2-2\,a\,\left|\boldsymbol{x_0^*}\right|\cos\gamma. \tag{3.19}$$

The expression above needs to be valid for all different angles γ, therefore requiring γ and k to satisfy the following two equations:

$$c^2\left(a^2+|\boldsymbol{x_0}|^2\right)=a^2+\left|\boldsymbol{x_0^*}\right|, \tag{3.20}$$

$$2\,c^2\,a\,|\boldsymbol{x_0}|\cos\gamma=2\,a\,\left|\boldsymbol{x_0^*}\right|\cos\gamma. \tag{3.21}$$

When using the line assumption of (3.15), one could see that $\left|\boldsymbol{x_0^*}\right| = k|\boldsymbol{x_0}|$. When filling this in at the expression of (3.21), then it follows that for the weight c the following relation needs to be satisfied:

$$c^2=k. \tag{3.22}$$

Using this result in the expression of (3.20) and writing this expression as a second degree polynomial in k gives:

$$k^2-\left(1+\left(\frac{a}{|\boldsymbol{x_0}|}\right)^2\right)\,k+\left(\frac{a}{|\boldsymbol{x_0}|}\right)^2=0. \tag{3.23}$$

This second degree polynomial has 2, easily seen, real roots, namely:

$$k=1 \quad \text{and} \quad k=\left(\frac{a}{|\boldsymbol{x_0}|}\right)^2. \tag{3.24}$$

The first root is a rather obvious one, this can be seen by filling in the value of $k=1$ into the line segment (3.15), this results in placing the image source $\boldsymbol{x_0^*}$ on top of the normal source $\boldsymbol{x_0}$. Of course, a positive and negative source placed on top of each other, also cancel each other out, but this trivial solution is not a correct one. This is because $\boldsymbol{x_0^*}$ needed to be outside the sphere to solve for the Poisson's equation, which it now certainly is not. Hence, the first root needs to be disregarded.

The second root $k=\left(\frac{a}{|\boldsymbol{x_0}|}\right)^2$ is valid, because $|\boldsymbol{x_0}^*| = k|\boldsymbol{x_0}| = \frac{a^2}{|\boldsymbol{x_0}|} > a$, so $\boldsymbol{x_0^*}$ is outside the sphere. Now, the weighting factor c given in the equation in (3.22) becomes $c=\sqrt{k}=\frac{a}{|\boldsymbol{x_0}|}$.

In other words the parameters to solve the problem of the Green's function to be 0 at the boundary of a sphere have been found. Hence, the Green function (3.14) for a sphere with a homogeneous Dirichlet boundary condition is:

$$G(\boldsymbol{x},\boldsymbol{x_0})=-\frac{1}{4\pi|\boldsymbol{x}-\boldsymbol{x_0}|}+\frac{a/|\boldsymbol{x_0}|}{4\pi\left|\boldsymbol{x}-a^2\boldsymbol{x_0}/|\boldsymbol{x_0}|^2\right|}. \tag{3.25}$$

This function is still written in terms of the vectors $\boldsymbol{x}$ and $\boldsymbol{x_0}$. In the case of a spherical volume, it is useful to write Green's function in spherical coordinates, for this purpose the vectors in spherical coordinates (defined in the previous section (3.2)) are:

$$\boldsymbol{x}=\left(r\,\sin\theta\,\cos\varphi,\,r\,\sin\theta\,\sin\varphi,\,r\,\cos\theta\right)^T, \tag{3.26}$$

$$\boldsymbol{x_0}=\left(r_0\,\sin\theta_0\,\cos\varphi_0,\,r_0\,\sin\theta_0\,\sin\varphi_0,\,r_0\,\cos\theta_0\right)^T. \tag{3.27}$$

When using the cosine rule again on the absolute values in the expression of (3.25), and after bringing back the same angle γ between the vectors $\boldsymbol{x}$ and $\boldsymbol{x_0}$ as in figure (3.2), then one could derive the following expressions:

$$|\boldsymbol{x}-\boldsymbol{x_0}| = \sqrt{r^2+r_0^2-2rr_0\cos\gamma}, \tag{3.28}$$

$$\left|\boldsymbol{x}-a^2\boldsymbol{x_0}/|\boldsymbol{x_0}|^2\right| = \sqrt{r^2+a^4/r_0^2-2a^2r/r_0\cos\gamma}. \tag{3.29}$$

In figure (3.2), the angle γ was defined as the angle between the vectors $\boldsymbol{x}$ and $\boldsymbol{x_0}$, and therefore in spherical coordinates, the cosine of this angle, is given by:

$$\begin{aligned}\cos\gamma &= \frac{\boldsymbol{x}\cdot\boldsymbol{x_0}}{|\boldsymbol{x}|\,|\boldsymbol{x_0}|}\\ &= \sin\theta\sin\theta_0\cos\varphi\cos\varphi_0+\sin\theta\sin\theta_0\sin\varphi\sin\varphi_0+\cos\theta\cos\theta_0\\ &= \cos\theta\cos\theta_0+\sin\theta\sin\theta_0\cos\left(\varphi-\varphi_0\right).\end{aligned} \tag{3.30}$$

Substituting the previous two obtained results in the expression given in (3.25) results in the following Green's function of a spherical volume in spherical coordinates:

$$G(r,\theta,\varphi,r_0,\theta_0,\varphi_0) = \frac{-1}{4\pi}\left[\frac{1}{\sqrt{r^2+r_0^2-2rr_0\cos\gamma}}-\frac{1}{\sqrt{r^2r0^2/a^2+a^2-2rr0\cos\gamma}}\right]. \tag{3.31}$$

In section (1.4) -for solving the Poisson's equation- the derivative of the Green's function to the outward boundary unit vector $\hat{\boldsymbol{n_0}}$ on the boundary ∂D was also an expression that needs to be evaluated. For a sphere it is easy to see that the outward unit vector on the boundary $\hat{\boldsymbol{n_0}}$ is the same as $\hat{\boldsymbol{r_0}}$, so when using the expression of the Green's function from (3.31) and taking the derivative, then it can be seen that:

$$\begin{aligned}\frac{\partial G}{\partial n_0} &= \frac{\partial G(r,\theta,\varphi,r_0,\theta_0,\varphi_0)}{\partial r_0}\\ &= \frac{1}{4\pi}\left[\frac{r_0-r\cos\gamma}{\left(r^2+r_0^2-2rr_0\cos\gamma\right)^{3/2}}-\frac{r_0r^2/a^2-r\cos\gamma}{\left(r^2r_0^2/a^2+a^2-2rr_0\cos\gamma\right)^{3/2}}\right].\end{aligned} \tag{3.32}$$

In the integral expression for the Poisson's equation this expression needs to be given on the boundary of the volume, and for our sphere this is at $r_0=a$, evaluating this gives:

$$\frac{\partial G}{\partial r_0}\Big|_{r_0=a} = \frac{1}{4\pi}\frac{a^2-r^2}{a\left(r^2+a^2-2ra\cos\gamma\right)^{3/2}}. \tag{3.33}$$

At this moment all expressions have been found to solve (if the source $Q(r_0,\theta_0,\varphi_0)$ and the boundary condition $f(r_0,\theta_0,\varphi_0)$ are given) the Poisson's equation in (4.3). Or in other words a general solution through the means of Green's functions has been found to solve all Poisson's equations with Dirichlet boundary condition on a sphere.

If in the integral expression for Dirichlet problems (1.11) the above equations are substituted and the change has been made to spherical coordinates i.e. $dV_0 = r_0^2\,\sin\theta_0\,dr_0d\theta_0d\varphi_0$ and $dS_0 = a^2\,\sin\theta_0\,d\theta_0d\varphi_0$, then the solution $u(\boldsymbol{x})$ of the Poisson's equation with source term $Q(\boldsymbol{x})$ and Dirichlet boundary condition $f(\boldsymbol{x})$ for a sphere can be found through the

following expression:

$$\begin{aligned} u(\boldsymbol{x}) &= \int_D G(\boldsymbol{x},\boldsymbol{x_0})Q(\boldsymbol{x_0})dV_0 \\ &\quad + \int_{\partial D} \frac{\partial G(\boldsymbol{x},\boldsymbol{x_0})}{\partial n_0} f(\boldsymbol{x_0})dS_0 \qquad (3.34) \\ &= \int_0^{2\pi}\int_0^{\pi}\int_0^{a} G(r,\theta,\varphi;r_0,\theta_0,\varphi_0)\, Q(r_0,\theta_0,\varphi_0)\, r_0^2 \sin\theta_0\, dr_0 d\theta_0 d\varphi_0 \\ &\quad + \int_0^{2\pi}\int_0^{\pi} \frac{\partial G(r,\theta,\varphi;r_0,\theta_0,\varphi_0)}{\partial r_0}\Big|_{r_0=a} f(a,\theta_0,\varphi_0)\, a^2 \sin\theta_0\, d\theta_0 d\varphi_0. \qquad (3.35) \end{aligned}$$

Although the expression looks pretty messy, some appreciation needs to be given to the fact that a generic and closed expression has been found for solving all Poisson's equations with a Dirichlet boundary condition on a sphere. This expression is going to be very useful in the physical counterpart of this report, where Gauss's law of gravitation on a planet (where the planet is assumed to be spherical) gives rise to a Poisson's equation on a sphere, and therefore with this expression an immediate manner, to solve for the solution inside the sphere, which is given by the gravitational potential, is presented.

3.4. GREEN'S FUNCTION OUTSIDE A SPHERE

For continuity reasons that will be explained in chapter 4, it is also needed to find the Green's function outside a sphere i.e. on the volume $D^c = \mathbb{R}^3 \setminus D$. For this purpose it is useful to use the same figure as for the inside case (3.2), only for the outside case the point in which the response needs to be found $\boldsymbol{x}$ needs to be outside the sphere and the response term $\boldsymbol{x_0}$ also needs to be outside the sphere. The latter can easily be done through interchanging the response point of the inside case $\boldsymbol{x_0}$ with the image point of the inside case $\boldsymbol{x_0^*}$. Notice that in an exact same manner, as was done with the inside case, two triangles could be constructed for these new points and the cosine rule could be applied to them again. Hence, the Green's function for the outside case will be exactly the same as for the inside case, only with points $\boldsymbol{x}$ and $\boldsymbol{x_0}$ outside the sphere and $\boldsymbol{x_0^*}$ inside the sphere. So the Green's function outside the sphere is given by:

$$\hat{G}(r,\theta,\varphi,r_0,\theta_0,\varphi_0) = \frac{-1}{4\pi}\left[\frac{1}{\sqrt{r^2+r_0^2-2rr_0\cos\gamma}} - \frac{1}{\sqrt{r^2r0^2/a^2+a^2-2rr0\cos\gamma}}\right]. \qquad (3.36)$$

The Green's function outside the sphere $\hat{G}(r,\theta,\varphi,r_0,\theta_0,\varphi_0)$ is given a hat on top of it for making the distinction to the Green's function inside the sphere. In this case, it was not needed because they are the same. However, there is one difference, the normal vector on the boundary ∂D has a negative orientation i.e. the direction of this vector goes in the sphere instead of out the sphere, therefore the outward normal derivative of the Green's function outside the sphere $\frac{\hat{G}(r,\theta,\varphi,r_0,\theta_0,\varphi_0)}{r_0}$ switches sign with the case of the Green's function inside the sphere $\frac{G(r,\theta,\varphi,r_0,\theta_0,\varphi_0)}{r_0}$, and is now given by:

$$\frac{\partial \hat{G}}{\partial r_0}\Big|_{r_0=a} = -\frac{\partial G}{\partial r_0}\Big|_{r_0=a} = -\frac{1}{4\pi}\frac{a^2-r^2}{a\left(r^2+a^2-2ra\cos\gamma\right)^{3/2}} = \frac{1}{4\pi}\frac{r^2-a^2}{a\left(r^2+a^2-2ra\cos\gamma\right)^{3/2}}. \qquad (3.37)$$

At this moment it is also possible, when substituting the results above, to find the solution outside this sphere, using the following expression:

$$\begin{aligned}\hat{u}(\boldsymbol{x}) = &\int_0^{2\pi}\int_0^{\pi}\int_0^{a} \hat{G}(r,\theta,\varphi,r_0,\theta_0,\varphi_0)\,\hat{Q}(r_0,\theta_0,\varphi_0)\,r_0^2\sin\theta_0\,dr_0 d\theta_0 d\varphi_0 \\ &+\int_0^{2\pi}\int_0^{\pi} \frac{\partial \hat{G}}{\partial r_0}\Big|_{r_0=a}\hat{f}(a,\theta_0,\varphi_0)\,a^2\sin\theta_0\,d\theta_0 d\varphi_0. \end{aligned} \tag{3.38}$$

In the above expression $\hat{u}(\boldsymbol{x})$ is the solution to the Poisson's equation with source term $\hat{Q}(r_0,\theta_0,\varphi_0)$ and Dirichlet boundary condition $\hat{f}(a,\theta,\varphi)$ on the volume D^c.

The solution of the Green's function in- and outside a sphere with a Neumann boundary condition can be found in the Appendix A.

Part II: Physical Problem

4

Solving Poisson's Law for Gravity and Physical Constraints

In this chapter, Poisson's law for gravity, which is given by a Poisson's equation, will be solved for the gravitational potential of a self-gravitating and rotating planet. Before the gravitational potential will be solved, Poisson's law for gravity is derived from Newton's law for gravity in the first section. In the second section, the appropriate boundary conditions for a rotating object are discussed, and they will be evaluated in the case of a self-gravitating and rotating planet. In the last section, the expression of the gravitational potential is deduced with appropriate conditions in which this expression is valid.

4.1. Poisson's Law for Gravity

In this section Poisson's law for gravity will be derived from Newton's law for gravity. Newton's law for gravity states that the force $\boldsymbol{F_{21}}$ on object 2 with point mass m_2 at position $\boldsymbol{r}_2$ exerted by object 1 with point mass m_1 at position $\boldsymbol{r}_1$, separated by a distance $|\boldsymbol{r_{12}}| = |\boldsymbol{r_2} - \boldsymbol{r_1}|$, is given by:

$$\boldsymbol{F_{21}} = \mathscr{G}\frac{m_1 m_2}{|\boldsymbol{r_{12}}|^2}\hat{\boldsymbol{r}}_{12}. \tag{4.1}$$

In this equation $\mathscr{G}$ is the universal gravitational constant, which has the approximate value of $6.67408 \cdot 10^{-11}$ $\mathrm{m^3\ kg^{-1}\ s^{-2}}$. The gravitational field is a vector field that describes the gravitational force that is exerted on an object in a point in space per unit mass. This field is better known as the gravitational acceleration at that particular point. Now consider object 2 to be an object which is located in the gravitational field of another object 1. Let us define object 1 as being a heavy object such as a planet, take for example the Earth, this is done to study the gravitational field in which object 2 can move. When using Newton's second law on the force on object 2, $\boldsymbol{F_{21}} = m_2\ \boldsymbol{a} = m_2\ \boldsymbol{g}(\boldsymbol{r_2})$, in combination with the expression (4.1), then the gravitational acceleration at the position of object 2 is given to be:

$$\boldsymbol{g}(\boldsymbol{r_2}) = -\mathscr{G}\frac{m_1}{|\boldsymbol{r_2} - \boldsymbol{r_1}|^2}\hat{\boldsymbol{r}}_{12} = -\mathscr{G}\frac{m_1(\boldsymbol{r_2} - \boldsymbol{r_1})}{|\boldsymbol{r_2} - \boldsymbol{r_1}|^3}. \tag{4.2}$$

This equation is valid for a given point mass at position 1. Now suppose that the gravitational acceleration is affected by an object 1, which is not a point mass, but a distributed mass with density distribution $\rho(\boldsymbol{r_1})$ and corresponding volume D. Then the gravitational acceleration at point 2 is given by the superposition of all point masses in this distributed

mass, therefore the following integral expression for the gravitational field follows:

$$\boldsymbol{g}(\boldsymbol{r_2}) = -\mathcal{G}\int_D \rho(\boldsymbol{r_1})\frac{\boldsymbol{r_2}-\boldsymbol{r_1}}{|\boldsymbol{r_2}-\boldsymbol{r_1}|^3}d^3\boldsymbol{r_1}. \tag{4.3}$$

When using the fact that $\nabla\left(\frac{\boldsymbol{r}}{|\boldsymbol{r}|}\right) = 4\pi\delta(\boldsymbol{r})$, which is proved in Abramowitz and Stegun (1948), and taking the divergence of expression (4.3), the following result can be found: [1]

$$\nabla\boldsymbol{g}(\boldsymbol{r_2}) = -\mathcal{G}\int_D \rho(\boldsymbol{r_1})4\pi\delta(\boldsymbol{r_2}-\boldsymbol{r_1})d^3\boldsymbol{r_1} = -4\pi G\rho(\boldsymbol{r_2}). \tag{4.4}$$

This equation is known as the divergent form of Gauss's law of gravitation. When using a general coordinate $\boldsymbol{x}$ instead of $\boldsymbol{r_2}$ the gravitational acceleration field, created by an object, could be found at every point. Let us summarize this result in the following theorem:

Theorem 4.1 (Gauss's Law for Gravity)**.** *Let $D \subseteq \mathbb{R}^3$ be a closed and bounded volume with mass density distribution $\rho(\boldsymbol{x})$ at position $\boldsymbol{x}$, then the gravitational acceleration $\boldsymbol{g}(\boldsymbol{x})$ at this point $\boldsymbol{x}$ satisfies the following expression:*

$$\nabla\boldsymbol{g}(\boldsymbol{x}) = -4\pi\mathcal{G}\rho(\boldsymbol{x}).$$

In this expression $\mathcal{G}$ is the universal gravitational constant of Newton.

From the fact that the gravitational force is conservative, i.e. $\nabla \times \boldsymbol{F} = 0$, it can be deduced that the gravitational acceleration $\boldsymbol{g} = \frac{\boldsymbol{F}}{m}$ also needs to be a conservative quantity, hence a scalar gravitational potential field $\phi(\boldsymbol{x})$ exists such that:

$$\boldsymbol{g}(\boldsymbol{x}) = -\nabla\phi(\boldsymbol{x}). \tag{4.5}$$

When combining this equation for the gravitational potential together with Gauss's law for gravity given in (4.1), then the following result that is called Poisson's law for gravity, can be found:

Theorem 4.2 (Poisson's Law for Gravity)**.** *Let $D \subseteq \mathbb{R}^3$ be a closed and bounded volume with mass density distribution $\rho(\boldsymbol{x})$ at position $\boldsymbol{x}$, then the gravitational potential $\phi(\boldsymbol{x})$ at position $\boldsymbol{x}$ satisfies the following expression:*

$$\Delta\phi(\boldsymbol{x}) = 4\pi\mathcal{G}\rho(\boldsymbol{x}).$$

In this expression $\mathcal{G}$ is the universal gravitational constant of Newton.

Notice that the Poisson's law for gravity is exactly a Poisson's equation that was examined in the mathematical construction part of this report. At the construction part this Poisson's equation was defined in expression (1.1), therefore the mathematical frame work which was constructed in Part I of this report can be used to solve Poisson's law for gravity for a certain volume D.

In the study of self-gravitating planets, there is another force, that besides gravity, acts on the planet, this force results from the rotation of the planet and is called the centrifugal force. This force will be examined in the following section.

[1] In this expression the order of integration and differentiation i.e. taking the divergence ∇, are interchanged. This is valid because the integrand -when taking a well-behaved mass distribution $\rho(\boldsymbol{r_1})$- and the divergence of the integrand are all continuous functions in a well-behaved volume D. (Leibniz Integral Rule) (Carothers (2003))

4.2. THE CENTRIFUGAL POTENTIAL

In the next section the boundary condition for a self-gravitating and rotating planet will be explored. However, before this can be done, the centrifugal potential must be known, therefore in this section the centrifugal potential for a sphere will be examined. The centrifugal force has been defined in, for example McComb (1999), and is given by:

$$\boldsymbol{F_c}(\boldsymbol{x}) = -m\boldsymbol{\omega} \times (\boldsymbol{\omega} \times \boldsymbol{x}). \tag{4.6}$$

In this equation $\boldsymbol{F_c}(\boldsymbol{x})$ is the centrifugal force at position $\boldsymbol{x}$, m is the mass of the particle and $\boldsymbol{\omega}$ is the angular velocity in the direction of the axis of rotation. In the same way as with the gravitational force, the centrifugal force is also conservative $\nabla \times \boldsymbol{F_c} = \boldsymbol{0}$, because of this conservative property, the negative gradient of the centrifugal potential $-\nabla\phi_c$ can be defined as the centrifugal force per unit mass:

$$\boldsymbol{a_c} = \frac{\boldsymbol{F_c}}{m} = -\nabla\phi_c. \tag{4.7}$$

In this expression $\boldsymbol{a_c}$ is the centrifugal acceleration. When using Cartesian coordinates and defining the z-axis to be in the direction of the rotation axis, then it follows that the rotation vector is given by $\boldsymbol{\omega} = (0,0,\omega)^T$. Now let $\boldsymbol{x}$ be a random vector in Cartesian coordinates, then the vector can be given by $\boldsymbol{x} = (x,y,z)^T$. Combining the expressions of (4.6) and (4.7) gives:

$$\nabla\phi_c = \left(\frac{\partial\phi_c}{\partial x}\,,\,\frac{\partial\phi_c}{\partial y}\,,\,\frac{\partial\phi_c}{\partial y}\right)^T = \boldsymbol{\omega} \times (\boldsymbol{\omega} \times \boldsymbol{x}) = -\omega^2\,(x\,,\,y\,,\,0)^T. \tag{4.8}$$

Solving for these 3 partial differential equations and combining them gives the following formulae for the centrifugal potential:

$$\phi_c(\boldsymbol{x}) = -\frac{1}{2}\,\omega^2\,(x^2+y^2) + C\, = -\frac{1}{2}\,\omega^2\,(x^2+y^2). \tag{4.9}$$

As with the gravitational potential the centrifugal potential is arbitrary to some constant C. For simplicity it is taken that $C = 0$. If spherical coordinates, as defined in section (3.2), are used, then the centrifugal potential is given by:

$$\phi_c(r,\theta,\varphi) = -\frac{1}{2}\,\omega^2\,r^2\,\sin^2\theta. \tag{4.10}$$

4.3. PHYSICAL CONDITIONS

Suppose that a certain self-gravitating and rotating planet is given and let us think about what conditions the potentials on this body must obey. First of all, the gravitational potential that this body generates must be continuous in- and outside the body of this object, if this was not the case the gravitational acceleration could become ∞, which means that gravity could become infinitely large. Another simple condition is that the gravitational acceleration generated by this body must also be continuous in- and outside the body. The last condition that needs to be satisfied is that the Earth is assumed to be a geoid, in other words, a surface of constant geopotential, why this is the case will be elaborated more on later in this section. Thus, in solving the Poisson's equation for gravitation for a rotating and self-gravitating planet the following 3 conditions need to be satisfied, namely:

1. The gravitational potential needs to be continuous across the surface of the planet.
2. The normal derivative of the gravitational potential needs to be continuous across the surface of the planet.

3. The surface of the Planet is an equipotential surface (geoid).

The third condition comes from the fact that the planet has been spinning for such a long time that it is expected that the planet is in an equilibrium state. This condition will become more clear with the help of figure (4.1).

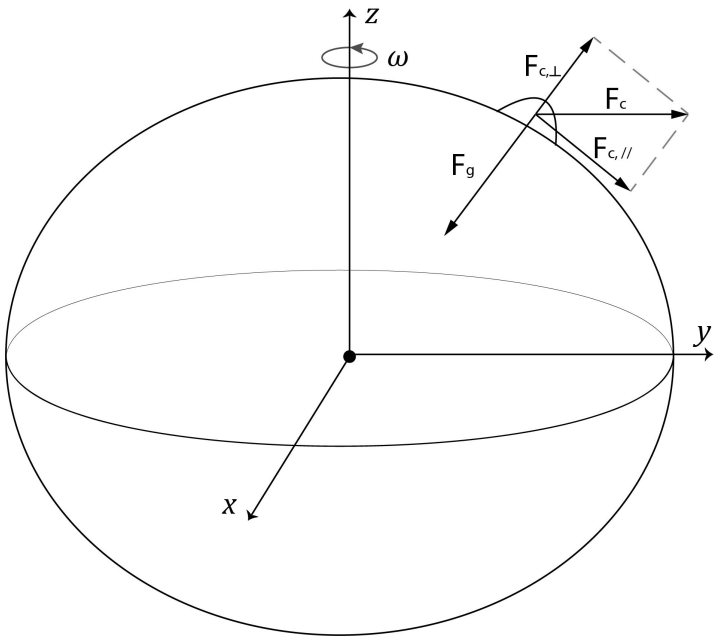

Figure 4.1: In this figure, a schematic representation of the forces that act on a pile of sand on a self-gravitating and rotating planet are shown to demonstrate how a geoid is formed. The centrifugal force is given by F_c and the gravitational force is given by F_g. The centrifugal force has been decomposed in a perpendicular component $F_c, \perp$ that, together with the not-drawn normal force, counters the gravitational force and a parallel component $F_c, \parallel$ that flattens out the pile of sand on the surface of this planet.

In figure (4.1) a schematic representation of a self-gravitating and rotating planet is shown. This planet rotates around the z-axis with rotation speed ω. On the surface of this planet lays a pile of sand, and on this pile of sand, the applied forces are drawn. These applied forces are the gravitational force F_g and the centrifugal force F_c. The centrifugal force has been divided into one component parallel to the surface of the body $F_c, \parallel$, and one component perpendicular to the surface of this body $F_c, \perp$. Notice that this perpendicular centrifugal force, together with a not drawn normal force, counteracts the gravitational force for having equilibrium in the direction of the outward surface vector. The parallel force of the centrifugal force will displace the pile of sand over the surface of the body until another shape of the body emerges. The displacement of this sand gives rise to a redistribution of the mass in the direction of the outward surface vector. Mass is the origin of the gravitational field and therefore after this redistribution a change in the gravitational field is present. This redistribution of mass and gravitational field will go on until a situation is presented in which the gravitational force and centrifugal force will cancel each other.

This state, in which at all points the gravitational and centrifugal forces cancel each other on the surface is called a geoid. For a perfect geoid, the whole of the planet needs to be made out of sand or some other loose material as water, then one would get a spheroid (Chandrasekhar (1969)). However, the Earth is not a perfect spheroid because of tidal motions and non-loose materials as mountains, but these disturbances are relatively small compared to the Earth's radius. Therefore, in this report, planets that are being portrayed by a geoid, are going to be studied. This geoid with volume D has an equipotential surface, that is to say, that the geopotential (sum of gravitational- and centrifugal potential) needs

to be constant on the surface ∂D:

$$\phi(\boldsymbol{x}) + \phi_c(\boldsymbol{x}) = \text{constant} \quad \text{for} \quad \boldsymbol{x} \in \partial D. \tag{4.11}$$

When evaluating this in spherical coordinates, then this leads to the following condition:

$$\phi(R,\theta,\varphi) + \phi_c(R,\theta,\varphi) = \text{constant}, \tag{4.12}$$

in which R is the radius of the body.

4.4. POISSON'S EQUATION FOR THE GRAVITATIONAL POTENTIAL

In theorem (4.2) it was found that for the gravitational potential $\phi(\boldsymbol{x})$ inside a mass distribution D with density $\rho(\boldsymbol{x})$, Poisson's law of gravitation needs to be satisfied:

$$\Delta\phi(\boldsymbol{x}) = 4\pi\mathcal{G}\rho(\boldsymbol{x}). \tag{4.13}$$

When the assumption is made that this mass distribution has been spinning for long enough and has so been evaluated into a geoid, then the following boundary condition also needs to be satisfied as given in expression (4.11):

$$\phi(\boldsymbol{x}) + \phi_c(\boldsymbol{x}) = \text{constant} \quad \text{for} \quad \boldsymbol{x} \in \partial D. \tag{4.14}$$

Let $-K$ be the constant parameter in the expression above, this constant parameter K is called the geopotential surface constant. If the centrifugal potential is moved to the right sight of the equation, then it can be seen that (4.13) together with (4.14) is just a Poisson's equation with a nonhomogeneous Dirichlet boundary condition. To make this more clear, let in the definition of the Poisson's equation in Chapter 1 at (1.1) the source be given by $Q(\boldsymbol{x}) = 4\pi\mathcal{G}\rho(\boldsymbol{x})$ and the Dirichlet boundary condition be given by $f(\boldsymbol{x}) = -K - \phi_c(\boldsymbol{x})$, then the following situation in theorem (4.3) arises.

Theorem 4.3 (Gravitational Potential for a Self-Gravitating and Rotating Planet)**.** *Let D be the volume of a self-gravitating and rotating planet with (smooth) boundary ∂D and mass density distribution $\rho(\boldsymbol{x})$. The gravitational potential $\phi(\boldsymbol{x})$ on this planet needs to satisfy:*

$$\begin{aligned} \Delta\phi(\boldsymbol{x}) &= 4\pi\mathcal{G}\rho(\boldsymbol{x}) \quad \textit{for} \quad \boldsymbol{x} \in D, \\ \phi(\boldsymbol{x}) &= -K - \phi_c(\boldsymbol{x}) \quad \textit{for} \quad \boldsymbol{x} \in \partial D. \end{aligned}$$

This Poisson's equation was written in terms of the Green's function in the mathematical construction part of the report. Notice that at the mathematical construction part it was found that if the Green's function $G(\boldsymbol{x},\boldsymbol{x_0})$ satisfied:

$$\begin{aligned} \Delta G(\boldsymbol{x},\boldsymbol{x_0}) &= \delta(\boldsymbol{x}-\boldsymbol{x_0}) \quad \text{for} \quad \boldsymbol{x} \in D, \\ G(\boldsymbol{x},\boldsymbol{x0}) &= 0 \quad \text{for} \quad \boldsymbol{x} \in \partial D. \end{aligned}$$

Then the solution of the gravitational potential can be written as (1.11):

$$\phi(\boldsymbol{x}) = 4\pi\mathcal{G}\int_D G(\boldsymbol{x},\boldsymbol{x_0})\rho(\boldsymbol{x_0})\,dV_0 + \int_{\partial D}\left[(-K-\phi_c(\boldsymbol{x_0}))\frac{\partial G(\boldsymbol{x},\boldsymbol{x_0})}{\partial n_0}\right]_{\boldsymbol{x_0}\in\partial D} dS_0. \tag{4.15}$$

Notice that, as an example, in Chapter 3 the Green function was found when the volume D was a sphere. The powerful result is that with the expression of (4.15) it is now possible to solve all different gravitational profiles when any density distribution $\rho(\boldsymbol{x})$ is given on this sphere.

4.5. GRAVITATIONAL POTENTIAL AND CONTINUITY CONDITIONS

The physical conditions of section (4.3) are related to the gravitational potential on the surface of the planet. For evaluating the continuity of the gravitational field and the derivative of the gravitational field, it is needed to also have the field on the outside of this planet, or in other words, in empty space.

In the mathematical construction part in Chapter 1, at expression (1.11), the following solution had been found for the Poisson's equation inside the volume D:

$$u(\boldsymbol{x}) = \int_D G(\boldsymbol{x},\boldsymbol{x_0})Q(\boldsymbol{x_0})dV_0 + \int_{\partial D}\left[f(\boldsymbol{x_0})\frac{\partial G(\boldsymbol{x},\boldsymbol{x_0})}{\partial n_0}\right]_{x_0\in\partial D} dS_0. \tag{4.16}$$

Now let us give a look at the volume outside D given by $D^c = \mathbb{R}^3 \setminus D$. Every parameter which plays a role outside the volume D is given a hat $\hat{\cdot}$ on top of the parameter, for making a distinction with the parameters inside the volume D. For example, $\hat{G}(\boldsymbol{x},\boldsymbol{x_0})$ is the Green's function in the volume $D^c = \mathbb{R}^3 \setminus D$. Notice that the volume D^c is an infinite space, hence the Green's function $\hat{G}(\boldsymbol{x},\boldsymbol{x_0})$ needs to obey the decay condition described in chapter 2. In the volume D^c the solution is, in the same manner as with D, given by:

$$\hat{u}(\boldsymbol{x}) = \int_{D^c} \hat{G}(\boldsymbol{x},\boldsymbol{x_0})\hat{Q}(\boldsymbol{x_0})dV_0 + \int_{\partial D^c}\left[\hat{f}(\boldsymbol{x_0})\frac{\partial \hat{G}(\boldsymbol{x},\boldsymbol{x_0})}{\partial \hat{n}_0}\right]_{x_0\in\partial D^c} dS_0. \tag{4.17}$$

So the total solution of the problem for the total volume $\mathbb{R}^3$ is given by:

$$u(\boldsymbol{x}) = \begin{cases} \int_D G(\boldsymbol{x},\boldsymbol{x_0})Q(\boldsymbol{x_0})dV_0 + \int_{\partial D}\left[f(\boldsymbol{x_0})\frac{\partial G(\boldsymbol{x},\boldsymbol{x_0})}{\partial n_0}\right]_{x_0\in\partial D} dS_0 & \text{if } \boldsymbol{x}\in D, \\ \int_{D^c} \hat{G}(\boldsymbol{x},\boldsymbol{x_0})\hat{Q}(\boldsymbol{x_0})dV_0 + \int_{\partial D^c}\left[\hat{f}(\boldsymbol{x_0})\frac{\partial \hat{G}(\boldsymbol{x},\boldsymbol{x_0})}{\partial \hat{n}_0}\right]_{x_0\in\partial D^c} dS_0 & \text{if } \boldsymbol{x}\in D^c. \end{cases} \tag{4.18}$$

The main goal of this section is to show how the physical conditions displayed in section (4.3) translate to conditions on these expressions in- and outside the volume. Before this can be done, some intermediate results are needed to be mentioned. First of all, ∂D and ∂D^c have same the same surface, the only difference is that ∂D has positive orientation, i.e. the surface enclosed is on the left hand side, and ∂D^c has negative orientation i.e. the surface enclosed is on the right hand side. This results in the fact that the normal surface vector of ∂D^c given by $\hat{\boldsymbol{n}}_0$ is only different in sign from the normal surface vector of ∂D given by $\boldsymbol{n}_0$. Hence, in the integral expression of D^c one can immediately conclude that:

$$\frac{\partial \hat{G}(\boldsymbol{x},\boldsymbol{x_0})}{\partial \hat{n}_0} = \frac{\partial \hat{G}(\boldsymbol{x},\boldsymbol{x_0})}{\partial(-n_0)} = -\frac{\hat{G}(\boldsymbol{x},\boldsymbol{x_0})}{\partial n_0}. \tag{4.19}$$

When using the above expression (4.19) and the fact that ∂D and ∂D^c are the same boundary, then the following result for the total solution follows:

$$u(\boldsymbol{x}) = \begin{cases} \int_D G(\boldsymbol{x},\boldsymbol{x_0})Q(\boldsymbol{x_0})dV_0 + \int_{\partial D}\left[f(\boldsymbol{x_0})\frac{\partial G(\boldsymbol{x},\boldsymbol{x_0})}{\partial n_0}\right]_{x_0\in\partial D} dS_0 & \text{if } \boldsymbol{x}\in D, \\ \int_{D^c} \hat{G}(\boldsymbol{x},\boldsymbol{x_0})\hat{Q}(\boldsymbol{x_0})dV_0 - \int_{\partial D}\left[\hat{f}(\boldsymbol{x_0})\frac{\partial \hat{G}(\boldsymbol{x},\boldsymbol{x_0})}{\partial n_0}\right]_{x_0\in\partial D} dS_0 & \text{if } \boldsymbol{x}\in D^c. \end{cases} \tag{4.20}$$

Let us write the total solution $u(\boldsymbol{x})$ for the case which needs to be evaluated, namely the case of the gravitational potential for a self-gravitating and rotating planet. Therefore, $u(\boldsymbol{x}) = \phi(\boldsymbol{x})$ and D represents the volume of this planet (which can be spherical, oblate spheroidal or even something completely different [2]). From Poisson's law for gravity, given in (4.2), it immediately follows that $Q(\boldsymbol{x_0})$ is given by $4\pi G\rho(\boldsymbol{x_0})$ and $\hat{Q}(\boldsymbol{x_0})$ is given by 0.

[2] At this moment, no knowledge of physical solutions to the planet have been evaluated, and therefore the volume could still be of any sort.

The latter result may come as a surprise and needs some extra explanation. This result follows from the following important assumption, that throughout the rest of the physical section, is going to be made:

- The assumption is made that the atmosphere of the planet, with the special case of the Earth, is absent and is therefore neglected in further calculations.

Because the atmosphere of the planet is absent it immediately follows that $\hat{\rho}(\boldsymbol{x_0}) = 0$, and hence $\hat{Q}(\boldsymbol{x_0}) = 0$.

The reader may have some discomfort with the assumption of neglecting the planet's atmosphere. The first argument is that many planets do not even have an atmosphere and for the planets that have an atmosphere, the atmosphere has a minor effect on gravity.

Because in chapter 5 the Earth will be studied, an evaluation of some parameters of the Earth's atmosphere compared to the Earth itself will be given. The mass of the atmosphere m_{atm}, according to the American National Center for Atmospheric Research and displayed in Trenberth and Smith (2005), is estimated to be between the values of $1.2\ 10^{15}$ kg and $1.5\ 10^{15}$ kg. This wide range is a result of the fact that the amount of moisture stored in the atmosphere of the Earth is different throughout an annual cycle, wherein northern summer, when temperatures are the highest, the most amount of moisture is stored in the atmosphere.

For the comparison of these masses, the maximum of the mass of the Earth's atmosphere is taken i.e. $m_{\text{atm}} = 1.5\ 10^{15}$ kg, when comparing this to the mass of the Earth, listed in the List of Constants, $M_e = 5.9722\ 10^{24}$ kg, then it follows that:

$$\frac{m_{\text{atm}}}{M_e} = 2.5\ 10^{-10} = 0.00000000025 = 0.000000025\%. \tag{4.21}$$

Since mass is the origin of the gravitational field, through Gauss's law of gravity given in (4.1), the conclusion can be made that the atmosphere has a minor effect on the overall gravity profile of the Earth.

Besides the mass of the atmosphere, one could also be interested in the radius of the atmosphere compared to the radius of the Earth, most of the mass (> 95 %) of the atmosphere can be found under a radius of $r_{\text{atm}} = 30$ km (Trenberth and Smith (2005)). When comparing the radius of the atmosphere to the radius of the Earth, it follows that :

$$\frac{r_{\text{atm}}}{R_e} = 4.7\ 10^{-3} = 0.0047 = 0.47\%, \tag{4.22}$$

which states that the atmosphere of the Earth is just a thin layer compared to the Earth itself.

The combination of the small mass (4.21) and the small radius (4.22) of the atmosphere compared to the Earth results in the conclusion that the atmosphere of the Earth will not contribute significantly to the gravitational potential, and is therefore neglected for simplicity.

The main result of this report is namely to look at the wide range of the gravitational potential of the Earth, although if one is specifically interested in how the gravitational potential changes in the atmosphere, then it is useful to model the atmosphere. The modeling of the atmosphere can easily be done by changing the volume D of the Earth to also contain the atmosphere, and then add the atmosphere in a piece-wise manner to the density of the Earth. Another way to add the density of the atmosphere can be done by not changing the volume D, but by modeling the density through $\hat{Q}$ using Poisson's law for gravity.

Now let us further look at the problem of the gravitational potential, the result of $\hat{Q}(\boldsymbol{x_0})$ has now been explained. Recall that ∂D and ∂D^c represent the same boundaries only with different orientation, the third physical condition in (4.3) said that:

- The surface of the Earth is an equipotential surface (geoid).

In (4.11) this condition was translated to the fact that:

$$\phi(\boldsymbol{x}) = -K - \phi_c(\boldsymbol{x}) \quad \text{for} \quad \boldsymbol{x} \in \partial D,$$

in which K was the geopotential constant. Notice that this is exactly the boundary condition of the gravitational potential of the Earth for both volumes D and D^c, hence:

$$f(\boldsymbol{x_0}) = -K - \phi_c(\boldsymbol{x_0}) = \hat{f}(\boldsymbol{x_0}) \quad \text{for} \quad \boldsymbol{x_0} \in \partial D.$$

These results for $Q(\boldsymbol{x})$, $\hat{Q}(\boldsymbol{x})$, $f(\boldsymbol{x_0})$ and $\hat{f}(\boldsymbol{x_0})$ gives the following expression for the gravitational potential in- and outside of the Earth:

$$\phi(\boldsymbol{x}) = \begin{cases} 4\pi\mathcal{G}\int_D G(\boldsymbol{x},\boldsymbol{x_0})\rho(\boldsymbol{x_0})dV_0 + \int_{\partial D}\left[(-K-\phi_c(\boldsymbol{x_0}))\frac{\partial G(\boldsymbol{x},\boldsymbol{x_0})}{\partial n_0}\right]_{x_0\in\partial D} dS_0 & \text{if } \boldsymbol{x}\in D, \\ -\int_{\partial D}\left[(-K-\phi_c(\boldsymbol{x_0}))\frac{\partial \hat{G}(\boldsymbol{x},\boldsymbol{x_0})}{\partial n_0}\right]_{x_0\in\partial D} dS_0 & \text{if } \boldsymbol{x}\in D^c. \end{cases} \tag{4.23}$$

Now after the third condition is satisfied, let us give a look to the results that would follow from the first and second physical conditions. The first condition is repeated in the following sentence:

- The gravitational potential needs to be continuous across the surface of the Earth.

This conditions leads to the following equation:

$$4\pi\mathcal{G}\int_D G(\boldsymbol{x},\boldsymbol{x_0})\rho(\boldsymbol{x_0})dV_0 + \int_{\partial D}\left[(-K-\phi_c(\boldsymbol{x_0}))\frac{\partial G(\boldsymbol{x},\boldsymbol{x_0})}{\partial n_0}\right]_{\boldsymbol{x_0}\in\partial D} dS_0 \tag{4.24}$$

$$= -\int_{\partial D}\left[(-K-\phi_c(\boldsymbol{x_0}))\frac{\partial \hat{G}(\boldsymbol{x},\boldsymbol{x_0})}{\partial n_0}\right]_{\boldsymbol{x_0}\in\partial D} dS_0 \quad \text{for} \quad \boldsymbol{x}\in\partial D. \tag{4.25}$$

From the definition of the Green's function for a Dirichlet boundary condition given in (4.3) it immediately follows that $G(\boldsymbol{x}\in\partial D,\boldsymbol{x_0}) = 0$, so the equation, after pairing the integrals over ∂D, becomes:

$$\int_{\partial D}\left[(-K-\phi_c(\boldsymbol{x_0}))\left\{\frac{\partial G(\boldsymbol{x},\boldsymbol{x_0})}{\partial n_0} + \frac{\partial \hat{G}(\boldsymbol{x},\boldsymbol{x_0})}{\partial n_0}\right\}\right]_{x_0\in\partial D} dS_0 = 0 \quad \text{for} \quad \boldsymbol{x}\in\partial D. \tag{4.26}$$

In chapter 3 the normal derivative of the Green's function inside $\frac{\partial G(\boldsymbol{x},\boldsymbol{x_0})}{\partial n_0}$ and outside $\frac{\partial G(\boldsymbol{x},\boldsymbol{x_0})}{\partial n_0}$ a sphere with radius a were evaluated. For this sphere the statement $\boldsymbol{x_0}\in D$ is equivalent in spherical coordinates $(r_0,\,\theta_0,\,\varphi_0)$ with $r_0 = a$. And the outward unit vector $\hat{\boldsymbol{n_0}}$ for a sphere is given by $\hat{\boldsymbol{r_0}}$. From expression (3.33) and (3.37) it immediately follows that for a spherical volume:

$$\frac{\partial G}{\partial r_0}\Big|_{r_0=a} = -\frac{\partial \hat{G}}{\partial r_0}\Big|_{r_0=a} \implies \int_{\partial D}\left[(-K-\phi_c(\boldsymbol{x_0}))\left\{\frac{\partial G(\boldsymbol{x},\boldsymbol{x_0})}{\partial n_0} + \frac{\partial \hat{G}(\boldsymbol{x},\boldsymbol{x_0})}{\partial n_0}\right\}\right]_{x_0\in\partial D} dS_0 = 0. \tag{4.27}$$

So, for the sake of an example, when D portrays a sphere (4.26), then the gravitational potential is automatically continuous over the surface of the planet.

At this moment condition 1 and 3 have been evaluated, so let us take a look at condition 2:

- The normal derivative of the gravitational potential needs to be continuous across the surface of the Earth.

If the normal derivative is given by $\frac{\partial}{\partial n}$, applying these to the gravitational potential in- and outside the Earth (4.24), then the following expression emerges:

$$\begin{aligned}&\frac{\partial}{\partial n}\left\{4\pi\mathcal{G}\int_D G(\boldsymbol{x},\boldsymbol{x_0})\rho(\boldsymbol{x_0})dV_0+\int_{\partial D}\left[(-K-\phi_c(\boldsymbol{x_0}))\frac{\partial G(\boldsymbol{x},\boldsymbol{x_0})}{\partial n_0}\right]_{x_0\in\partial D}dS_0\right\}\\&=\frac{\partial}{\partial n}\left\{-\int_{\partial D}\left[(-K-\phi_c(\boldsymbol{x_0}))\frac{\partial \hat{G}(\boldsymbol{x},\boldsymbol{x_0})}{\partial n_0}\right]_{x_0\in\partial D}dS_0\right\}\quad\text{for}\quad \boldsymbol{x}\in\partial D.\end{aligned}\tag{4.28}$$

Interchanging the order of integration and differentiation in the volume integral and pairing the surface integrals gives:

$$\begin{aligned}&4\pi\mathcal{G}\int_D\frac{\partial G(\boldsymbol{x},\boldsymbol{x_0})}{\partial n}\Big|_{\boldsymbol{x}\in\partial D}\rho(\boldsymbol{x_0})dV_0\\&+\frac{\partial}{\partial n}\left(\int_{\partial D}\left[(-K-\phi_c(\boldsymbol{x_0}))\left\{\frac{\partial G(\boldsymbol{x},\boldsymbol{x_0})}{\partial n_0}+\frac{\partial \hat{G}(\boldsymbol{x},\boldsymbol{x_0})}{\partial n_0}\right\}\right]_{\boldsymbol{x_0}\in\partial D}dS_0\right)\Big|_{\boldsymbol{x}\in\partial D}=0.\end{aligned}\tag{4.29}$$

In case of a sphere it was seen through (3.33) and (3.37) that the boundary integral vanishes, yet over the volume integral nothing can be said.

Let us now for clarification summarize all the results in a single theorem.

Theorem 4.4 (Gravitational Potential of a self-gravitating and rotating planet)**.** *The gravitational potential $\phi(\boldsymbol{x})$ of a self-gravitating rotating planet of volume D with mass density $\rho(\boldsymbol{x})$ that has been rotating for long enough such that it is in equilibrium (geoid) needs to satisfy:*

$$\phi(\boldsymbol{x})=\begin{cases}4\pi\mathcal{G}\int_D G(\boldsymbol{x},\boldsymbol{x_0})\rho(\boldsymbol{x_0})dV_0+\int_{\partial D}\left[(-K-\phi_c(\boldsymbol{x_0}))\frac{\partial G(\boldsymbol{x},\boldsymbol{x_0})}{\partial n_0}\right]_{x_0\in\partial D}dS_0 & \text{if } \boldsymbol{x}\in D,\\ -\int_{\partial D}\left[(-K-\phi_c(\boldsymbol{x_0}))\frac{\partial \hat{G}(\boldsymbol{x},\boldsymbol{x_0})}{\partial n_0}\right]_{x_0\in\partial D}dS_0 & \text{if } \boldsymbol{x}\in D^c.\end{cases}$$

In these equations, $\mathcal{G}$ is the universal gravitational constant, D^c is given by $\mathbb{R}^3\setminus D$, K is the geopotential constant of this planet, $\phi_c(\boldsymbol{x})$ the centrifugal force, $G(\boldsymbol{x},\boldsymbol{x_0})$ is the appropriate Green's function on the volume D and $\hat{G}(\boldsymbol{x},\boldsymbol{x_0})$ is the appropriate Green's function on the volume D^c. Out of physical relevance it is known that across the boundary ∂D of the planet the gravitational potential and the normal derivative of the gravitational potential need to be continuous, this is equivalent of obeying the following conditions shown in expression (4.26) and expression (4.29).

This last theorem sums up all the important results of this whole chapter so far. It is good to summarize what results are obtained for not losing eye of the progress that has been made so far. So for a general self-gravitating rotating body of volume D, it was deduced that the gravitational potential needed to satisfy the Poisson's equation for gravity. This Poisson's equation could be pretty hard to solve for a general volume D and the mass density $\rho(\boldsymbol{x})$ could be of any form, therefore the problem was deduced to a problem in which a particular function $G(\boldsymbol{x},\boldsymbol{x_0})$ called the Green's function needed to be found, which did not depend on this mass density. When this Green function has been found in- and outside the volume D, then, when obeying the conditions the whole gravitational potential field in- and outside of the volume for any mass density $\rho(\boldsymbol{x})$ could be calculated using the theorem in (4.4).

A major part to notice in theorem (4.4) is that the gravitational outside the volume D is completely generated by the integral over the boundary of D, and is not directly dependent on the volume integral over the density of this volume D. The important thing to notice from this is the similarity of this theory of gravity with classical electrodynamics. In classical electrodynamics it is known that the charge density inside a body does not directly affect the field outside this body, this field is completely generated through the surface charge distribution and/or dipole-layer distribution. These topics are, for example, treated in the book *Classical Electrodynamics* from Jackson (2007).

However, there are certain differences between gravity and electrodynamics, the main difference is the fact that in electrodynamics negative sources do exist, and in the case of gravity, they do not exist. Positive sources in electrodynamics are positive charges and negative sources are negative charges. In the case of gravity, positive sources are matter, but negative sources do not exist, there is no thing as negative matter. [3] Because of this, it is also strange to talk about things as dipoles made out of matter.

In the construction of the expression for the gravitational potential, the method of images was used, and in the method of images a negative source -which is negative matter- was placed outside the volume D for constructing the gravitational potential inside this volume D. And in the case of making the expression of the gravitational potential outside D, this negative source was placed inside D. Therefore, in both cases, the negative source is portrayed in the area where the gravitational potential was not being studied and is therefore also not of a major problem, it is just used as a mathematical tool.

Even in electrodynamics -where negative sources do exist- this is also often used as a mathematical tool. To portray the situation of a positive charge and a conducting surface, the situation is sketched as being similar to a positive charge and a negative charge mirrored through this conducting surface. Thereafter, you solve the problem in the domain of the situation of the positive charge and negative charge, and the solution is given in the whole of space. When transforming this back to the situation of the conducting surface, only in the side of space where the positive charge is located seen from the conducting surface, does the solution of the positive and negative source make sense. On the other side of this conducting surface, the solution is not given by the positive and negative charge, this would not make any sense. But, you only wanted to find the field between the positive source and conducting surface anyways, so it is not that big of a problem. So the construction of the positive- and negative source is also used as a mathematical tool to solve for a particular area where the negative source is not located.

In the construction of the Green's functions in- and outside a sphere, the negative charge was exactly located in the other area than the solution was liked to be found. So when the solution was liked to be found in the sphere, the negative source was out the sphere, and in the case, the solution was liked to be found out the sphere, the negative source was in the sphere. So, indeed, this negative matter was being used as a mathematical tool.

4.6. GRAVITATIONAL ACCELERATION

When the gravitational potential is found, one could be curious what kind of gravitational field this gravitational potential establishes. Therefore, the acceleration of gravitation $\boldsymbol{g}(\boldsymbol{x})$ is needed, which was stated in the first section in expression (4.5) to be coupled to the

[3] The reason why there is no negative matter results from the weak energy condition. The weak energy condition states that for particles moving along valid trajectories, the distribution of mass-energy will always be positive at every point in spacetime. This condition is only physical and has no mathematical background, in mathematics negative matter is not a problem. In general relativity there are mathematical solutions - which are being used as mathematical tools- that have negative energy densities, for example, the Alcubierre Metric (Lobo and Visser (2004)).

gravitational potential $\phi(\boldsymbol{x})$ by:

$$\boldsymbol{g}(\boldsymbol{x}) = -\nabla\phi(\boldsymbol{x}). \tag{4.30}$$

So after finding the gravitational potential via theorem (4.4) and taking the gradient of this expression the gravitational acceleration can be found.

However, the integrals of theorem (4.4) are often difficult to solve because of the singularity of the Green's function, the maybe difficult mass density $\rho(\boldsymbol{x})$ and the maybe difficult volume D. Even for the spherical case most of these integrals can not be solved analytically, therefore most of the time a numerical integration is needed.

The problem that arises is that it is not possible to take the gradient of this numerical gravitational potential without using a curve fitting tool or interpolation, this problem can be omitted when interchanging the gradient and integral of theorem (4.4). Notice that the gradient is a gradient to the $\boldsymbol{x}$ parameter and has nothing to do with the $\boldsymbol{x_0}$ parameter, to address this point extra clearly the gradient will be notated by: $\nabla = \nabla_{\boldsymbol{x}}$. The only parameter in theorem (4.4) which has anything to do with the $\boldsymbol{x}$ is the Green's function, the other functions will pass like constants to this operator. So the gravitational acceleration could be calculated by:

$$\boldsymbol{g}(\boldsymbol{x}) = \begin{cases} 4\pi\mathscr{G}\int_D(\nabla_{\boldsymbol{x}}\, G(\boldsymbol{x},\boldsymbol{x_0}))\rho(\boldsymbol{x_0})\, dV_0 + \\ \int_{\partial D}\left((-K-\phi_c(\boldsymbol{x_0}\in\partial D)\right)\, \nabla_{\boldsymbol{x}}\frac{\partial(G(\boldsymbol{x},\boldsymbol{x_0}))}{\partial n_0}\Big|_{x_0\in\partial D}\, dS_0 & \text{if } \boldsymbol{x}\in D, \\ \\ -\int_{\partial D}\left((-K-\phi_c(\boldsymbol{x_0}\in\partial D)\right)\, \nabla_{\boldsymbol{x}}\frac{\partial(\hat{G}(\boldsymbol{x},\boldsymbol{x_0}))}{\partial n_0}\Big|_{x_0\in\partial D}\, dS_0 & \text{if } \boldsymbol{x}\in D^c. \end{cases} \tag{4.31}$$

Notice that in this expression $(\nabla_{\boldsymbol{x}}G(\boldsymbol{x},\boldsymbol{x_0}))$, $\nabla_{\boldsymbol{x}}\frac{\partial(G(\boldsymbol{x},\boldsymbol{x_0}))}{\partial n_0}\Big|_{x_0\in\partial D}$ and $\nabla_{\boldsymbol{x}}\frac{\partial(\hat{G}(\boldsymbol{x},\boldsymbol{x_0}))}{\partial n_0}\Big|_{x_0\in\partial D}$ are vectors and that all integration needs to be done over all of the elements of these vectors separately. And also notice that $\nabla_{\boldsymbol{x}}$ has nothing to do with dV_0 and dS_0, which are coupled to $\boldsymbol{x_0}$, therefore do not think of this expression as being an integral as in the divergence theorem (1.3).

5

Results of the Gravitational Field for a Spherical Earth

In this chapter, the gravitational potential and gravitational acceleration will be solved for a spherical Earth using different models for the mass density distribution of the Earth. The three models which will be evaluated are the homogeneous density model, linear density model, and the PREM density model (Dziewonski and Anderson (1981)). Where the latter one is a density model that keeps track of all the different layers of the Earth. This layered model of the Earth will be explained in the section where the PREM model firstly occurs. Before these models are evaluated, a look will be given to the expressions of the gravitational potential and gravitational acceleration for a spherical Earth, where the latter can be used to check if the model satisfies the famous 9.81 m s^{-2} on the Earth's surface.

5.1. The Gravitational Potential and Acceleration

Before looking at the results of the gravitational potential and acceleration of the Earth, let us recapitulate what expressions are necessary to calculate these quantities and let us also recapitulate how these expressions need to be interpreted in case of the Earth. In the first subsection the result for the gravitational potential is shown and in the second subsection the result for the gravitational acceleration is shown.

5.1.1. Gravitational Potential for a Spherical Earth

The gravitational potential for a general self-gravitating planet was given by the theorem in (4.4). In the case of a spherical volume the outward unit surface vector is given by $\boldsymbol{\hat{n}_0} = \boldsymbol{\hat{r}_0}$ and the condition $\boldsymbol{x_0} \in \partial D$ corresponds in spherical coordinates with $r_0 = R$, in which R is the radius of the Earth. Using the infinitesimal volume element of spherical coordinates (3.6) and the infinitesimal surface element of spherical coordinates (3.8), it follows that $dV_0 = dx_0\, dy_0\, dz_0 = {r_0}^2 \sin\theta_0\, dr_0\, d\theta_0\, d\varphi_0$ and $dS_0 = a^2\, \sin\theta_0\, d\theta_0\, d\varphi_0$. In section (3.2) the Green's function in spherical coordinates (r,θ,φ) inside a sphere was calculated to be (3.31):

$$G(r,\theta,\varphi,r_0,\theta_0,\varphi_0) = \frac{-1}{4\pi}\left[\frac{1}{\sqrt{r^2+r_0^2-2rr_0\cos\gamma}} - \frac{1}{\sqrt{r^2r0^2/a^2+a^2-2rr0\cos\gamma}}\right]. \tag{5.1}$$

And the derivative to the outward normal vector, on the boundary i.e. $r_0 = R$, respectively in- and outside the sphere were given to be:

$$\frac{\partial G}{\partial r_0}\Big|_{r_0=R} = \frac{1}{4\pi}\frac{R^2 - r^2}{a\left(r^2 + R^2 - 2rR\cos\gamma\right)^{3/2}}, \qquad \frac{\partial \hat{G}}{\partial r_0}\Big|_{r_0=R} = \frac{1}{4\pi}\frac{r^2 - R^2}{R\left(r^2 + R^2 - 2rR\cos\gamma\right)^{3/2}}. \tag{5.2}$$

In these expressions $\cos\gamma$ was given by:

$$\cos\gamma = \cos\theta\cos\theta_0 + \sin\theta\sin\theta_0\cos\left(\varphi - \varphi_0\right). \tag{5.3}$$

Substituting all these expressions in the expression of the gravitational potential (4.4) gives rise to the following expression of the gravitational potential in spherical coordinates:

$$\phi(r,\theta,\varphi) = \begin{cases} 4\pi\mathcal{G}\int_0^{2\pi}\int_0^{\pi}\int_0^{R} G(r,\theta,\varphi,r_0,\theta_0,\varphi_0)\,\rho(r_0,\theta_0,\varphi_0)\,{r_0}^2\sin\theta_0\,dr_0 d\theta_0 d\varphi_0 \\ +\int_0^{2\pi}\int_0^{\pi}(-K-\phi_c(R,\theta_0,\varphi_0))\,\frac{\partial G}{\partial r_0}\Big|_{r_0=R} R^2\,\sin\theta_0\,d\theta_0\,d\varphi_0 & \text{if } |\boldsymbol{x}| \le R, \\ \\ -\int_0^{2\pi}\int_0^{\pi}(-K-\phi_c(R,\theta_0,\varphi_0))\,\frac{\partial \hat{G}}{\partial r_0}\Big|_{r_0=R} R^2\,\sin\theta_0\,d\theta_0\,d\varphi_0 & \text{if } |\boldsymbol{x}| > R. \end{cases} \tag{5.4}$$

The centrifugal force in spherical coordinates was derived in expression (4.10) and is given by:

$$\phi_c(r,\theta,\varphi) = -\frac{1}{2}\omega^2 r^2\sin^2(\theta).$$

At this moment if the mass density $\rho(\boldsymbol{x})$ is given then it is possible -using the above expressions- to solve for the gravitational potential of the Earth.

5.1.2. GRAVITATIONAL ACCELERATION FOR A SPHERICAL EARTH

The gravitational acceleration was given in chapter 4 in the following expression (4.31). If the same procedure is followed as with the gravitational potential above i.e. showing that D represents Earth as a sphere with radius R and mass density $\rho(\boldsymbol{x})$, recalling the spherical Green's functions of chapter 3 and transforming the integral into spherical integrals, then the following expression for the gravitational acceleration in- and outside the Earth follows:

$$\boldsymbol{g}(\boldsymbol{x}) = \begin{cases} 4\pi\mathcal{G}\int_0^{2\pi}\int_0^{\pi}\int_0^{R} \nabla_{(r,\theta,\varphi)}G(r,\theta,\varphi,r_0,\theta_0,\varphi_0)\,\rho(r_0,\theta_0,\varphi_0)\,{r_0}^2\sin\theta_0\,dr_0 d\theta_0 d\varphi_0 \\ +\int_0^{2\pi}\int_0^{\pi}(-K-\phi_c(R,\theta_0,\varphi_0))\,\nabla_{(r,\theta,\varphi)}\left(\frac{\partial G}{\partial r_0}\Big|_{r_0=R}\right) R^2\,\sin\theta_0\,d\theta_0\,d\varphi_0 & \text{if } |\boldsymbol{x}| \le R, \\ \\ -\int_0^{2\pi}\int_0^{\pi}(-K-\phi_c(R,\theta_0,\varphi_0))\,\nabla_{(r,\theta,\varphi)}\left(\frac{\partial \hat{G}}{\partial r_0}\Big|_{r_0=R}\right) R^2\,\sin\theta_0\,d\theta_0\,d\varphi_0 & \text{if } |\boldsymbol{x}| > R. \end{cases} \tag{5.5}$$

In these expressions, the Green's functions are the same as in the case of the gravitational potential and $\nabla_{(r,\theta,\varphi)}$ represents the gradient in spherical coordinates. Again notice that the gradient has nothing to with the variables of integration and that it makes the integrand into a vector, in which over all the components of the vector the integration needs to be done.

MAXIMA IN GRAVITATIONAL ACCELERATION

To gain some understanding of how the gravitational acceleration profiles will behave and why some maxima may occur, a simplified evaluation of the radial parameter of the gravitational acceleration g_r can be useful. First of all, the assumption is made that the density

distribution ρ only depends on the radial distance r, such that the density is given by $\rho(r)$. Beginning with Poisson's law for gravity (1.1) and using the fact that the gravitational acceleration is the gradient of the potential, it follows that:

$$\nabla \boldsymbol{g}(r) = -4\pi \mathcal{G} \rho(r). \tag{5.6}$$

Taking a volume integral over spherical volume D over both sides and using the divergence theorem (1.3), then one can find for the radial part of the gravitational acceleration:

$$g_r(r) = -\frac{\mathcal{G} M_{\text{enc}}}{r^2}. \tag{5.7}$$

In this expression M_{enc} is the enclosed mass of a sphere with radius r. So the gravitational acceleration profile depends on how fast the enclosed mass is increasing with increasing r in relation to r^2. Using the expression of the enclosed mass in spherical coordinates ($M_{\text{enc}} = \int_D \rho(r) dV = 4\pi \int_0^r \bar{r}^2 \rho(\bar{r}) d\bar{r}$) and getting the $1/r^2$ inside this expression, then it follows that:

$$g_r(r) = -4\pi \mathcal{G} \int_0^r \frac{\bar{r}^2}{r^2} \, \rho(\bar{r}) \, d\bar{r}. \tag{5.8}$$

From this expression, it can easily be deduced that if $\rho(r)$ is a polynomial of degree n, then $g_r(r)$ will be a polynomial of degree $n+1$. Therefore it can be the case that inside the Earth some maxima may occur for the gravitational acceleration because the enclosed mass increases faster with radial distance r for densities $\rho \sim r$ then $1/r^2$ decreases.

5.2. HOMOGENEOUS MASS DENSITY MODEL

The model that will be examined first is the most simple one. In this model a homogeneous mass density $\rho_h(\boldsymbol{x})$ will be proposed. The parameters of Earth that are going to be used can be found in the List of Constants after the introduction. Notice that in case of a sphere the volume is just $V = \frac{4}{3}\pi R^3$, such that the homogeneous density becomes:

$$\rho_h(\boldsymbol{x}) = \frac{M_E}{V} = \frac{M_E}{\frac{4}{3}\pi R^3} \approx 5513 \text{ kg m}^{-3}. \tag{5.9}$$

Notice that this density is approximately 5 times as dense as water but less dense than pure iron. Filling this homogeneous density in (5.4) and using the numerical integration tool of Wolfram Mathematica 12.0 (notebook code can be found in the Appendix C) it is possible to construct the following plots of the gravitational potential.

5.2.1. GRAVITATIONAL POTENTIAL FOR HOMOGENEOUS MASS DENSITY

The gravitational potential in- and outside the sphere will first be plotted against the radial distance r, polar angle θ and the azimuthal angle φ in the three panel of plots shown in figure (5.1). In these particular plots the other two dependencies have been taken constant to look at the dependency of particular interest.

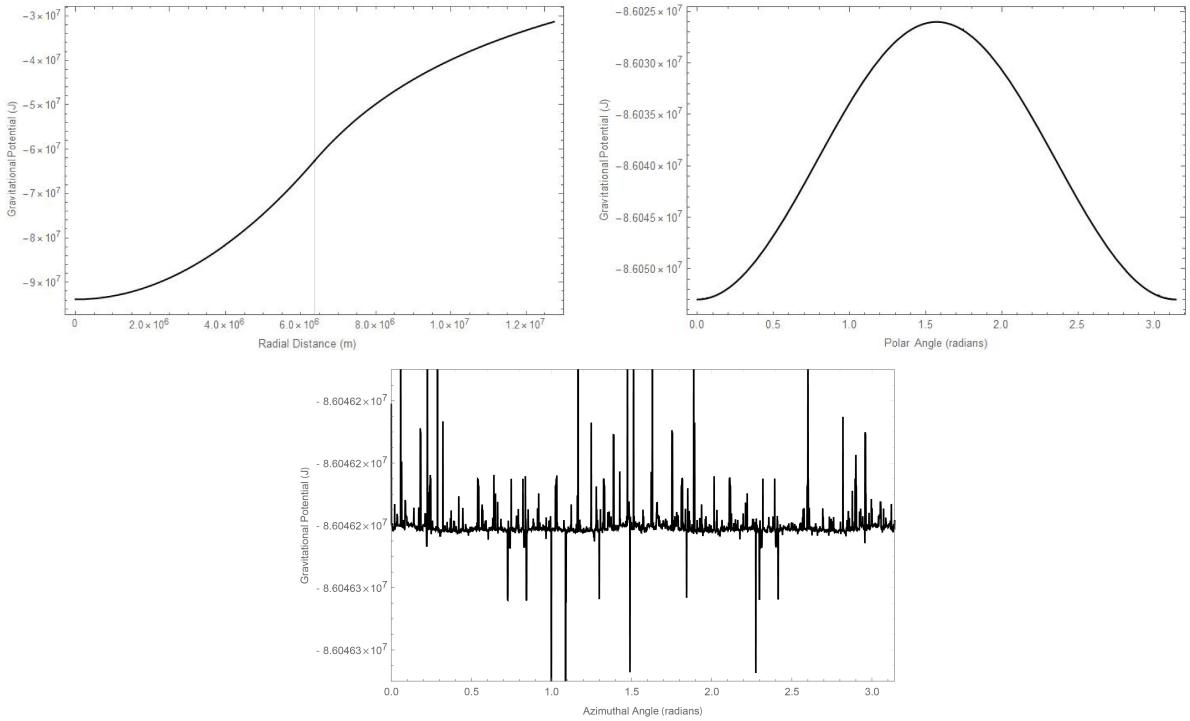

Figure 5.1: In this figure the gravitational potential $\phi(r,\theta,\varphi)$ for homogeneous density $\rho_h(r)$ has been plotted against one of it's dependencies r, θ or φ, where the other dependencies have been taken constant. The gravitational potential $\phi(r,\ \theta=\pi/4,\ \varphi=\pi/6)$ is plotted against the radial distance r in the left-hand corner, $\phi(r=R/2,\ \theta,\ \varphi=\pi/6)$ is plotted against the polar angle θ in the right-hand corner and $\phi(r=R/2,\ \theta=\pi/4,\ \varphi)$ is plotted against the azimuthal angle φ in the plot below.

In figure (5.1) in the upper left-hand corner the gravitational potential $\phi(r,\ \theta=\pi/4,\ \varphi=\pi/6)$ has been plotted against the radial distance r, in figure (5.1) in the upper right-hand corner the gravitational potential $\phi(r=R/2,\ \theta,\ \varphi=\pi/6)$ has been plotted against the polar angle θ and in figure (5.1) below the gravitational potential $\phi(r=R/2,\ \theta=\pi/4,\ \varphi)$ has been plotted against the azimuthal angle φ. In the radial distance plot, a gridline has been added at the radial value of about 6.7×10^6 m, because this gridline represents the radius of the Earth R. Hence, everything to the left of this gridline is the gravitational potential inside the Earth and everything to the right of this gridline is the gravitational potential outside the Earth.

Notice that at the Gridline the gravitational potential in- and outside the Earth is continuous and also the derivative to the radial parameter appears continuous to the naked eye. But this is not ab initio clear and is elaborated on at the section of the acceleration of gravitation.

At the plot in the lower part of figure (5.1), it can be seen that the gravitational potential $\phi(r=R/2,\ \theta=\pi/4,\ \varphi)$ against the azimuthal angle φ looks unstable. When comparing the gravitational potential amplitude of this plot against the gravitational values of the other figures, it can easily be seen that these amplitudes are not of significant value, and the plot that is seen in this figure can be described to noise in the numerical integration tool of Wolfram Mathematica. Thus, the gravitational potential does not depend on the azimuthal angle φ, which is an intuitive result because our boundary condition and the density also did not depend on this azimuthal angle.

When looking at the plot in the upper right-hand corner of figure (5.1), it can be seen that the gravitational potential $\phi(r=R/2,\ \theta,\ \varphi=\pi/6)$ depends on θ in a way that looks like a negative sine wave. This result comes from the fact that the geopotential (sum of gravitational and centrifugal potential) needed to be constant on the surface of the Earth,

and because of the symmetrical density distribution in a homogeneous density, the result is that on every spherical shell with radius r the geopotential is constant. In other words, the geopotential only depends on the radial distance r and not on the angles θ and φ. Because the geopotential is spherically symmetric and the geopotential was given by the sum of gravitational- and centrifugal potential, it can not be the case that the gravitational potential is spherically symmetric. This comes from the fact that the centrifugal potential has a θ dependency that needs to be canceled by the gravitational potential for the result of constant geopotential. This θ dependency of the gravitational potential can be seen in the right-hand corner in figure (5.1), where the opposite $\sin^2(\theta)$ pattern of the centrifugal potential is shown.

5.2.2. GRAVITATIONAL ACCELERATION FOR HOMOGENEOUS MASS DENSITY

After this explanation of the gravitational potential, a look can be given to the radial parameter of the gravitational acceleration $g_r(r,\theta,\varphi)$ of the Earth. The radial parameter of the absolute value [1] of the gravitational acceleration for a homogeneous density distribution is given in figure (5.2). In the plot in the left-hand side of figure (5.2) the acceleration of gravitation in- and outside the Earth $g_r(r,\ \theta=\pi/4,\ \varphi=\pi/6)$ is plotted against the radial distance r. And in the plot in the right-hand side of figure (5.2) the acceleration of gravitation in- and outside the Earth $g_r(r=0.999R,\ \theta=\pi/4,\ \varphi=0)$ and $g_r(r=1.001R,\ \theta,\ \varphi=0)$ are plotted against the polar angle θ.

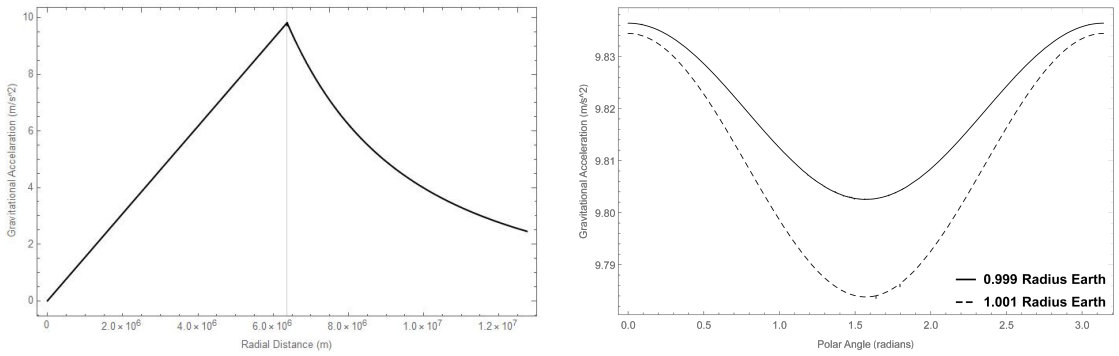

Figure 5.2: In this figure, the absolute value of the radial parameter of the gravitational acceleration $g_r(r,\theta,\varphi)$ for homogeneous density $\rho_h(r)$ is plotted against one of it's dependencies r and θ, where the other dependencies have been taken constant. The gravitational acceleration $g_r(r,\ \theta=\pi/4,\ \varphi=0)$ is plotted against the radial distance r in the left-hand corner, and $g_r(r=0.999\ R,\ \theta,\ \varphi=0)$ and $g_r(r=1.001\ R,\ \theta,\ \varphi=0)$ are plotted against the polar angle θ in the right-hand corner.

In the plot on the left-hand side of figure (5.2), in the same way as with the gravitational potential, a gridline has been added to account for the position of the radius of the Earth. At the radius of the Earth, the acceleration of gravitation takes on an approximate value of 9.81 m s $^{-2}$ on the equator, which is close to measurements of the gravitational acceleration at the surface of the Earth. In the inside of the Earth the acceleration of gravitation is displayed through a linear relation beginning in the origin. That this pattern originates from a homogeneous density profile can easily be seen through expression (5.8) outlined in the first section. After the radius of the Earth, the gravitational acceleration declines with $1/r$, and therefore the gravitational acceleration will converge to 0 far from the Earth (where the assumption is made that, of course, other planets, asteroids, stars, and other space matter are not present).

[1] Actually the plot needs to be mirrored through the x-axis and hereby every value of the gravitational acceleration needs to be negative. This is the case because when looking at the radial parameter r of our spherical model, then this radial parameter goes outwards into free space, but gravity and thereby the gravitational acceleration pulls inward such that the direction is reversed. However, the absolute value has been taken, because in real-world applications, this is the usual way of looking at results of the gravitational field.

In the plot on the right-hand side of figure (5.2), the radial parameter of the gravitational acceleration $g_r(r,\ \theta,\ \varphi)$ has been plotted against the polar angle. In the dashed line the gravitational acceleration was calculated in the Earth for 99.9% of the radius of the Earth and the normal line was calculated outside the Earth for 100.1% of the radius of the Earth.

The reason why these plots have been made so close to the surface of the Earth is to study the pattern in the acceleration of gravitation close to the Earth's surface. From this plot, it can be deduced that there is, indeed, a significant difference in the value of the acceleration of gravitation at the poles in comparison with the equator. These differences originate from centrifugal effects of a rotating planet.

It is difficult to come closer to the Earth's surface, then this 0.1 %. Because the Green's functions are discontinuous at the Earth's surface, and together with the numerical integration tool, this results in plots that are highly oscillatory for percentages closer than 0.1 %. Even in the plot shown for 0.1 %, it can be seen that at certain points some, but not significant, instability occurs.

This oscillatory behavior beginning at 0.1 % is true for the polar angle θ, however, for the radial parameter, the oscillatory behavior starts at, around, 0.01 %, as will be shown later. These differences result from the fact that the polar angle θ at the denominator of the Green's function is given through trigonometrical functions, instead of the radial parameter r, which is given through a polynomial function. This polynomial function is easier to handle for the numerical integration tool of Mathematica.

The question that still arises is the question if the normal derivative of the gravitational potential, condition (3) in (4.3), is satisfied. For this purpose, the plot in the left-hand corner of (5.1) is made for values of the radial parameter r close to the Earth's surface, and for different polar angles θ, given in figure (5.3).

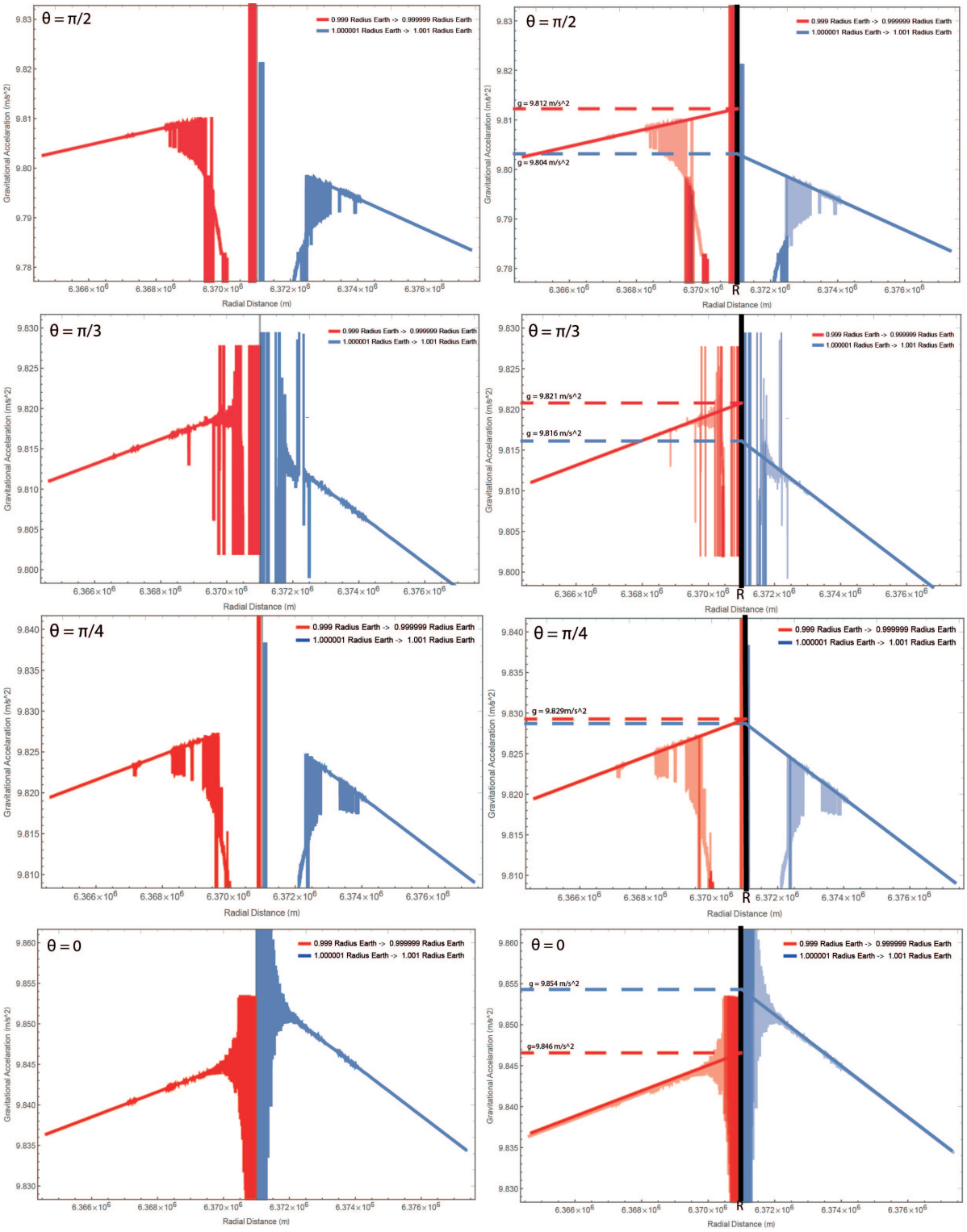

Figure 5.3: In the left-situated plots the acceleration of gravitation for homogeneous mass density, in red, inside the Earth, for 99.9 % to 99.9999 % of the Earth's radius, and the acceleration of gravitation, in blue, outside the Earth, for 100.0001 % to 100.1% of the Earth's radius, are plotted for different polar angles $\theta = \pi/2, \pi/3, \pi/4$ and 0 against the radial distance r. In the right-situated plots the stable regions of the left-situated plots have been extrapolated for approximating the values of the acceleration of gravitation at the surface of the Earth for these different different polar angles θ.

In figure (5.3), the acceleration of gravitation g_r is plotted inside the Earth, in red, for 99.9 % to 99.9999 % of the Earth's radius and outside the Earth, in blue, for 100.0001 % to 100.1% of the Earth's radius. Every plot is made for a different polar angle θ that is shown in the upper left-hand corner of each plot. In all the left-situated plots the evaluated plots are given, in these plots it can be seen that oscillation occurs when approaching the surface of the Earth. These oscillations occur because of the discontinuity of the Green's function on the surface of the Earth, in collaboration with the numerical integration tool of Wolfram Mathematica 12.0.

For these distances so close to the surface of the Earth, even the acceleration of gravitation g_r outside the Earth, which is given by a $1/r$ relation, can be approximated by a linear relation.

Extrapolation of these linear relations, at the places where the solution is stable, can be used to gain insight into the values of the acceleration of gravitation at the Earth's surface. These extrapolations with the corresponding values of the acceleration of gravitation g at the Earth's surface can be found in the plots in the right-situated plots. The original results from the left-situated plots have been made transparent at the right-situated plots, and the extrapolation lines have been made according to these transparent linear relations where no oscillation occurs.

The results of the acceleration of gravitation are showed to make a *quantitative* analysis about the (dis)continuity, and are therefore approximated, therefore do not take these as *qualitative* results.

Let us summarize all extrapolated values of the gravitational acceleration for different polar angles in- and outside the Earth in table (5.1).

Table 5.1: In this table, the extrapolated results of the plots in figure (5.3) are shown for accompanying polar angle $\theta = \pi/2\,, \pi/3/, \pi/4$ and 0. The extrapolated results from inside the Earth are given by $g_\uparrow$, the extrapolated results from outside the Earth are given by $g_\downarrow$, the differences from the inside $g_\uparrow$ compared to the outside $g_\downarrow$ are given by Δg and the percentages the insides $g_\uparrow$ are above the outsides $g_\downarrow$ are given by $\frac{\Delta g}{g_\downarrow} \times 100\%$.

Polar Angle θ	$\pi/2$	$\pi/3$	$\pi/4$	0
$g_\uparrow$ [m/ s^2]	9.812	9.821	9.829	9.846
$g_\downarrow$ [m/ s^2]	9.804	9.816	9.829	9.854
Δg [m/s^2]	0.008	0.005	0.000	-0.008
$\frac{\Delta g}{g_\downarrow} \times 100\%$	0.08%	0.05%	0.00%	-0.08%

In table (5.1), the extrapolated values of the acceleration of gravitation inside the Earth $g_\uparrow = \lim_{r\uparrow R} g(r)$, the acceleration of gravitation outside the Earth $g_\downarrow = \lim_{r\downarrow R} g(r)$, the difference $\Delta g = g_\uparrow - g_\downarrow$ and the percentage $g_\uparrow$ is above $g_\downarrow$ given by $\frac{\Delta g}{g_\downarrow} \times 100\%$ are displayed for the polar angles $\theta = \pi/2,\ \pi/3,\ \pi/4$ and 0.

The major result that immediately must be noticed -through the plots in figure (5.3) or the results in table (5.1)- is that the normal derivative of the gravitational potential is not continuous through the surface of the Earth. Therefore the third physical condition, denoted in (4.3), is not satisfied for a spherical Earth with homogeneous mass density distribution.

These theoretical discrepancies were expected because they result from centrifugal effects. It was not a priori clear however that these discrepancies should come in the form of significant observable effects, as compared to e.g. the numerical accuracy of the numerical

methods involved.

At the equator i.e. at $\theta = \pi/2$, the centrifugal effects are maximal, and the discrepancy also maximizes to 0.08%. Notice that at the north-pole i.e. at $\theta = 0$ the discrepancy is minimized to -0.08%. From Newtonian mechanics, it can directly be concluded that there exist net forces. Whereat the equator there is a force that wants to expand and at the pole there is a force that wants to contract. And at the polar angle $\theta = \pi/4$ the difference in the field is 0, and there is no net force present.

From these results, one can expect that the equator expands and the poles shrinks until geostatical equilibrium according to the physical conditions in (4.3) is obtained.

5.3. LINEAR MASS DENSITY

After inspecting the homogeneous mass density model it is possible to look at a more realistic density [2] that increases with increasing radius r. Let ρ_0 be the density at the center of the Earth and let ρ_1 be the density at the surface of the Earth. The linear density $\rho(r)$ in terms of the radial distance r is defined to be:

$$\rho_l(r) = \rho_0 - (\rho_0 - \rho_1)\frac{r}{R}. \tag{5.10}$$

Because the radius and mass of the Earth are known, it is only possible to have one degree of freedom in choosing ρ_0 and ρ_1, by:

$$M_E = \int_V \rho_l(\boldsymbol{x})\,dV = 4\pi\int_0^R r^2\rho_l(r)\,dr = \frac{4}{3}\pi R^3\left[\frac{1}{4}\rho_0 + \frac{3}{4}\rho_1\right] \implies \frac{1}{4}\rho_0 + \frac{3}{4}\rho_1 = \rho_h, \tag{5.11}$$

where ρ_h is the homogeneous density. In choosing the parameter of ρ_0 some insider knowledge, which will be made clear in the next section, is going to be used. This knowledge is that the center of the Earth is made out of a iron ball with density 13088.5 kg m^{-3}, this will declare the density of ρ_0 and ρ_1 to be:

$$\rho_0 = 13088.5 \text{ kg m}^{-3} \implies \rho_1 = \frac{4}{3}\left(\rho_h - \frac{1}{4}\rho_0\right) \approx 2993 \text{ kg m}^{-3}. \tag{5.12}$$

5.3.1. GRAVITATIONAL POTENTIAL FOR LINEAR MASS DENSITY

In the same way as with the homogeneous density distribution the gravitational potential $\phi(r,\theta,\varphi)$ can be plotted against the radial distance r, the polar angle θ and the azimuthal angle φ, wherein each plot the other dependencies have been taken constant. The results are shown in the following figure (5.4).

[2] The angular momentum of the Earth $\boldsymbol{L}$ is given by $\boldsymbol{L} = I\,\boldsymbol{\omega}$, in which I is the moment of inertia and $\boldsymbol{\omega}$ the angular rotation vector. The moment of inertia for a solid sphere with homogeneous mass density is given by $I = \frac{2}{5}mR^2$, where m is the total mass of the sphere and R the radius of the sphere. When using a homogeneous Earth with mass M_e and radius R for the moment of inertia together with the known rotation vector ω, then the calculated angular momentum would be lower then the angular momentum that has been measured for the Earth. Hence, for a more realistic model there must be more mass situated near the core of the Earth then mass situated at the surface.

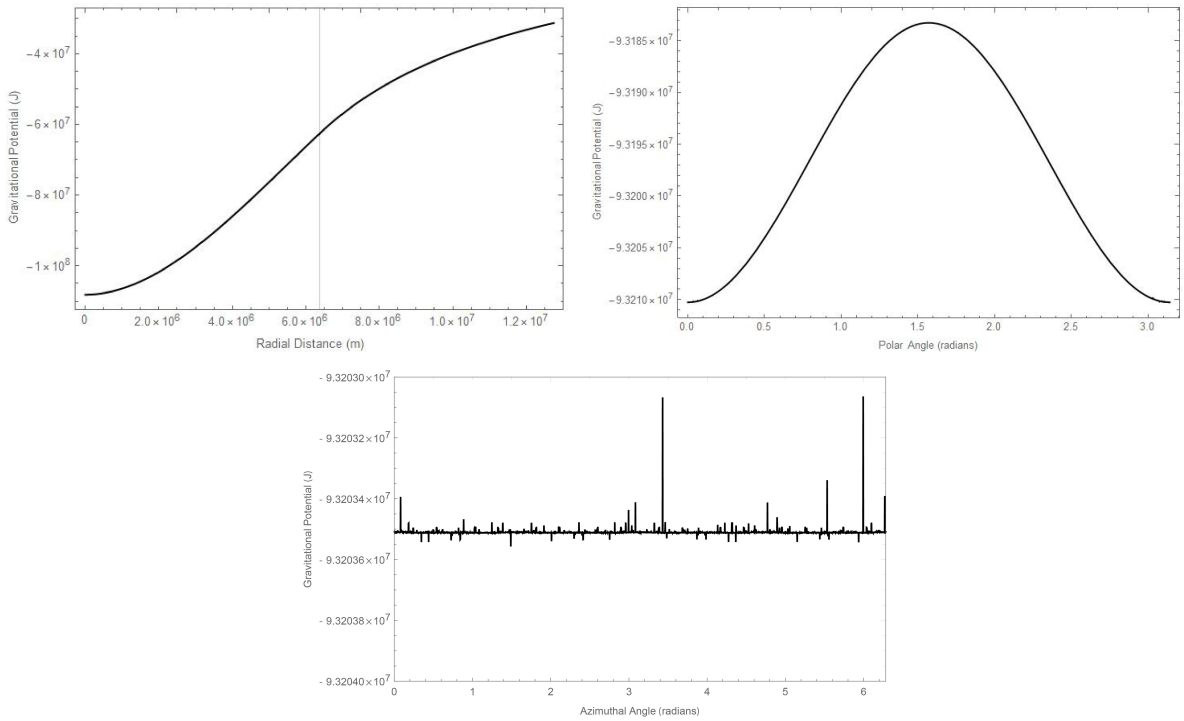

Figure 5.4: In this figure the gravitational potential $\phi(r,\theta,\varphi)$ for linear density $\rho_l(r)$ is plotted against one of it's dependencies r, θ or φ, where the other dependencies have been taken constant. The gravitational potential $\phi(r,\theta=\pi/4,\varphi=\pi/6)$ is plotted against the radial distance r in the left-hand corner, $\phi(r=R/2,\theta,\varphi=\pi/6)$ is plotted against the polar angle θ in the right-hand corner and $\phi(r,\theta=\pi/4,\varphi=\pi/6)$ is plotted against the azimuthal angle φ in the plot below.

In upper left-hand side of figure (5.4) the gravitational potential $\phi(r,\theta=\pi/4,\varphi=\pi/6)$ is plotted against the radial distance r, in the upper right-hand side of figure (5.4) the gravitational potential $\phi(r=R/2,\theta,\varphi=\pi/6)$ is plotted against the polar angle θ and in the plot below in figure (5.4) the gravitational potential $\phi(r=R/2,\theta=\pi/4,\varphi)$ is plotted against the azimuthal angle φ.

Notice that again, the gravitational potential is continuous and that the gravitational potential again has a polar angle dependency to counteract the centrifugal effects, and there is no relation concerning the azimuthal angle.

An important question that arises is if the discontinuity for the acceleration of gravitation for this more realistic linear mass density becomes better, worse, or stays the same. For this purpose, a look will again be given to the gravitational acceleration.

5.3.2. GRAVITATIONAL ACCELERATION FOR LINEAR MASS DENSITY

The main difference of the gravitational potential of the linear mass density and the homogeneous mass density is the fact that the gravitational potential of the linear model begins with a lower value then the gravitational potential of the homogeneous model, and the derivative of the linear gravitational potential model needs to change more drastically for obeying the continuity condition of the gravitational potential. This becomes more clear when looking at the acceleration of gravitation shown in figure (5.5).

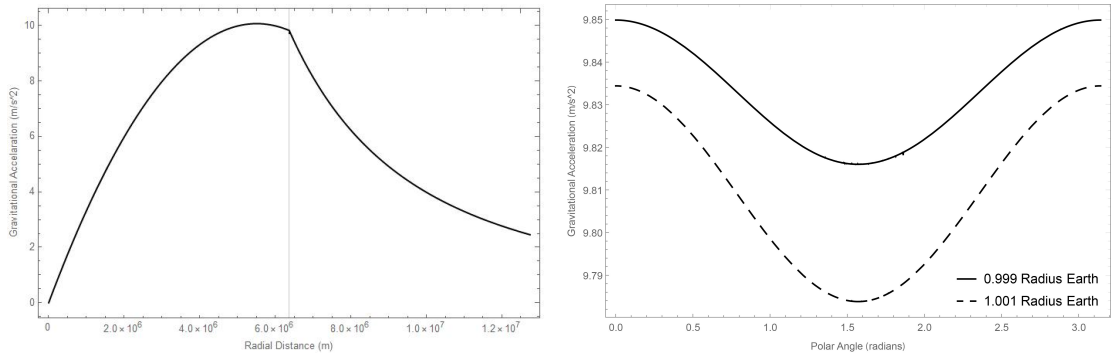

Figure 5.5: In this figure, the absolute value of the radial parameter of the gravitational acceleration $g_r(r,\theta,\varphi)$ for linear density $\rho_l(r)$ is plotted against one of it's dependencies r,θ, where the other dependencies have been taken constant. The gravitational acceleration $g_r(r,\ \theta=\pi/4,\ \varphi=0)$ is plotted against the radial distance r in the left-hand corner, and $g_r(r=0.999$ Radius Earth, $\theta,\ \varphi=0)$ and $g_r(r=1.001$ Radius Earth, $\theta,\ \varphi=0)$ are plotted against the polar angle θ in the right-hand corner.

In figure (5.5) the absolute value of the radial parameter of the gravitational acceleration $g_r(r,\ \theta=\pi/4,\ \varphi=0)$ is plotted against the radial distance r in the plot on the left-hand side, and $g_r(r=0.999R,\ \theta,\ \varphi=0)$ and $g_r(r=1.001\ R,\ \theta,\ \varphi=0)$ are plotted against the polar angle θ in the right-hand side.

In the plot of g_r against the radial distance r a local maximum of the gravitational acceleration inside the Earth occurs because the gravitational acceleration follows a parabolic curve. This parabolic curve comes from the fact that if ρ is a polynomial of degree n, then g_r will be a polynomial of degree $n+1$, this can be explained with the expression in (5.8). Also in this plot that it can be seen that the value at the Earth's surface again converges to 9.81 m s^{-2}.

Notice that in the polar angle plot, the gravitational acceleration of linear density is higher then the homogeneous gravitational acceleration was in figure (5.2). This is because in the radial distance plot it can be seen that the linear relation approaches the value at the surface from above instead of from beneath, which was the case for the homogeneous mass density.

The question that arises is if the continuity of the normal derivative of the gravitational potential, condition (3) in (4.3), is satisfied for linear mass density. For this purpose, the plot in the left-hand corner of figure (5.5) is made for values of the radial parameter r close to the Earth's surface, and for different polar angles θ, given in figure (5.6).

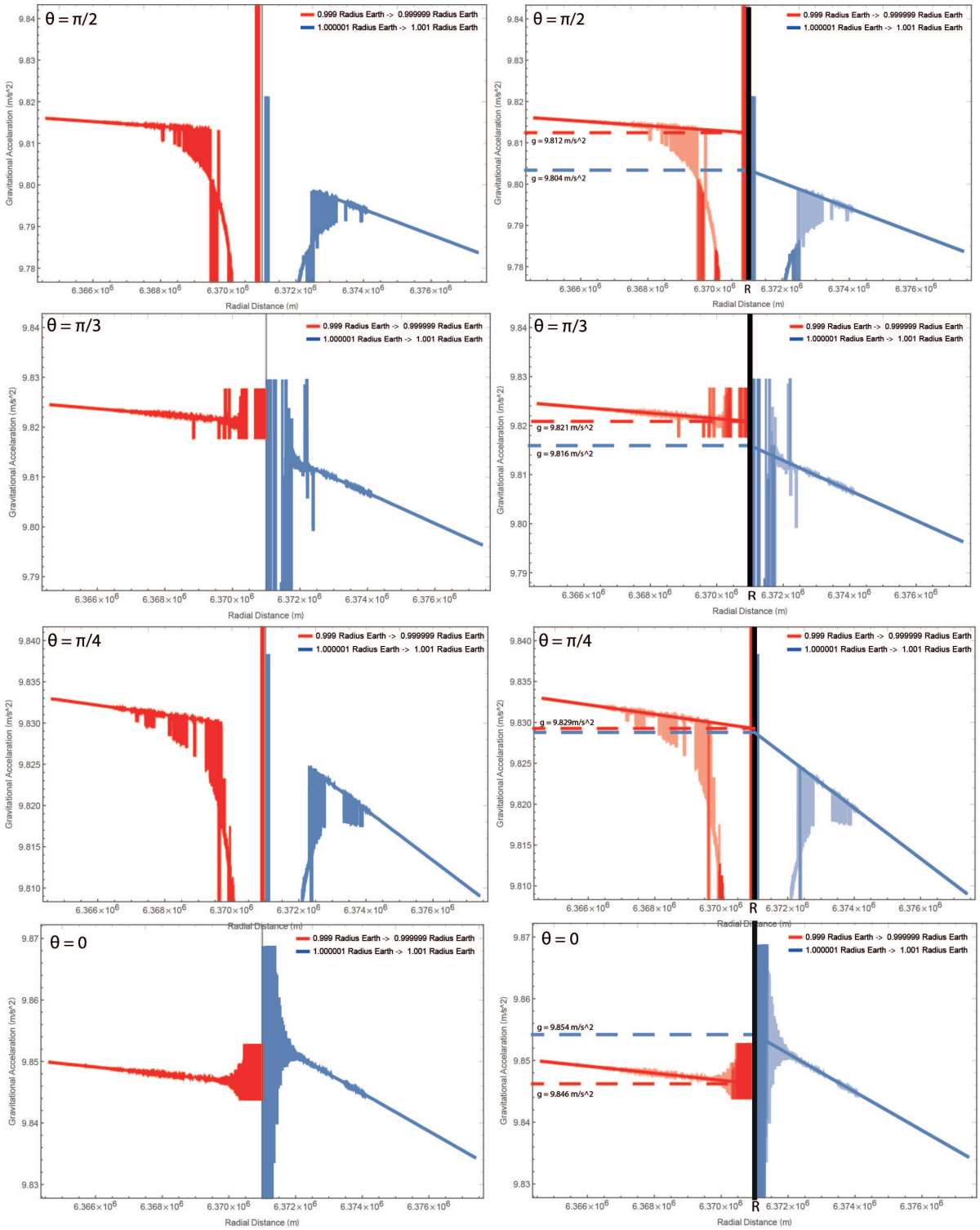

Figure 5.6: In the left-situated plots, the acceleration of gravitation for linear mass density, in red, inside the Earth, for 99.9 % to 99.9999 % of the Earth's radius, and the acceleration of gravitation, in blue, outside the Earth, for 100.0001 % to 100.1% of the Earth's radius, are plotted for different polar angles $\theta = \pi/2, \pi/3, \pi/4$ and 0 against the radial distance r. In the right-situated plots the stable regions of the left-situated plots have been extrapolated for approximating the values of the acceleration of gravitation at the surface of the Earth for these different polar angles θ.

In the left-situated plots, the red lines portray the acceleration of gravitation inside the Earth for values of 99.9 % to 99.9999 % of the Earth's radius, and the blue lines portray the acceleration of gravitation outside the Earth for values of 100.0001 % to 100.1% of the Earth's radius. The difference between the plots is the constant polar angle θ that takes on the values $\pi/2$, $\pi/3$, $\pi/4$ and 0.

In the right-situated plots, the regions where the plots are stable i.e. do not oscillate or deviate from a linear relation, are being extrapolated with the stable part of the solution. These extrapolations are displayed in the linear lines that are displayed over the now transparent original solutions. From these lines, the approximate value of the acceleration of gravitation at the Earth's surface can be extracted.

The results of the acceleration of gravitation are again showed to make a *quantitative* analysis of the (dis)continuity, and are therefore approximated, therefore do not take these as *qualitative* results.

Let us summarize all extrapolated values of the gravitational of acceleration for different polar angles in- and outside the Earth in table (5.2).

Table 5.2: In this table, the extrapolated results for linear mass density of the plots in figure (5.6) are shown for corresponding polar angles $\theta = \pi/2\ , \pi/3, \pi/4$ and 0. The extrapolated results from inside the Earth are given by $g_\uparrow$, the extrapolated results from outside the Earth are given by $g_\downarrow$, the differences from the inside $g_\uparrow$ compared to the outside $g_\downarrow$ are given by Δg and the percentages the insides $g_\uparrow$ are above the outsides $g_\downarrow$ are given by $\frac{\Delta g}{g_\downarrow} \times 100\%$.

Polar Angle θ	$\pi/2$	$\pi/3$	$\pi/4$	0
$g_\uparrow$ [m/ s^2]	9.812	9.821	9.829	9.846
$g_\downarrow$ [m/ s^2]	9.804	9.816	9.829	9.854
Δg [m/s^2]	0.008	0.005	0.000	-0.008
$\frac{\Delta g}{g_\downarrow} \times 100\%$	0.08%	0.05%	0.00%	-0.08%

In table (5.2), the extrapolated value, for linear mass density, of the acceleration of gravitation inside the Earth $g_\uparrow = \lim_{r\uparrow R} g(r)$, the acceleration of gravitation outside the Earth $g_\downarrow = \lim_{r\downarrow R} g(r)$, the difference $\Delta g = g_\uparrow - g_\downarrow$ and the percentage $g_\uparrow$ is above $g_\downarrow$ given by $\frac{\Delta g}{g_\downarrow} \times 100\%$ are displayed for the polar angles $\theta = \pi/2$, $\pi/3$, $\pi/4$ and 0.

In the same way as with the homogeneous mass density, notice that the acceleration of gravitation for linear mass density is also not continuous over the surface of the Earth, because of centrifugal effects. The centrifugal effect maximizes at the equator $\theta = \pi/2$ and minimizes at the pole $\theta = 0$. From Newtonian mechanics, it again follows that for the spherical Earth with linear mass density the pole wants to shrink and the equator wants to expand. At $\theta = \pi/4$ no difference in the field is present and there is no net force on this position.

The most remarkable thing is that the table of the linear mass density (5.2) is equivalent in values to the table of homogeneous mass density (5.1). Even though the linear plots in figure (5.6) approach the surface of the Earth from a completely different angle than the plots in figure (5.3), they both approach the same limit at the surface of the Earth. The linear mass density, which portrays a more realistic density distribution of the Earth, is therefore not more realistic for a general self-gravitating and rotating planet then the homogeneous mass density model is. The discontinuities stay the same.

To study this effect more, a look will be given to the most realistic density distribution that exists for the interior of our Earth, named the PREM density model.

5.4. PREM MASS DENSITY MODEL

The abbreviation PREM stands for the Preliminary Earth Reference model and this model is a 1-dimensional model of the Earth that uses the fact that our Earth is built up from multiple layers. These different layers with their accompanying density were found using the measurement of seismic waves inside the Earth, these measurements have been evaluated in Dziewonski and Anderson (1981). In the first subsection, a deeper understanding of this model and the results will be given and in the following subsections the gravitational potential and acceleration that result form this model are presented.

5.4.1. INTRODUCING THE PREM MASS DENSITY MODEL

The preliminary Earth reference model uses the approach of measuring the period of standing waves and free oscillations, which depend upon the variation of elastic constant and density with depth. These standing waves and free oscillations are a result of large earthquakes, which will oscillate our elastic Earth. After the occurrence of such a large earthquake, these oscillations could be continuing oscillating for hours or even days. These seismic waves, which have a very long wavelength, are reinforced at specific periods and therefore will result in certain standing waves inside the Earth. These standing waves sample the underlying elastic constants and densities. The preliminary Earth reference model measures these standing waves through their wave velocities and uses inversion to best fit the underlying densities that produce these free oscillations (Dziewonski and Anderson (1981)).

In modeling these free oscillations the preliminary Earth reference model assumes that the Earth is spherical and only uses the depth as a parameter of density. These large earthquakes that produce these huge seismic waves are not a regular thing on Earth, and the measurement of these seismic waves is still a contemporary active process. When a large earthquake occurs many different stations on different sides of the Earth immediately start measuring these wave velocities, and therefore the measurements of the Earth's interior are still an active process today, and refinements in the PREM model to the densities are still being made. However, most of the refinements are only being made in the high-gradient regions of the lowermost mantle and in the inner core. Because in the other regions no significant changes are detected (Hinze et al. (2018)).

Before stating the densities which are subsequent from the PREM model, it is useful to recapitulate how the interior of the Earth is constructed. In the following figure (5.7) from Sharp (2014), the interior of the Earth is portrayed.

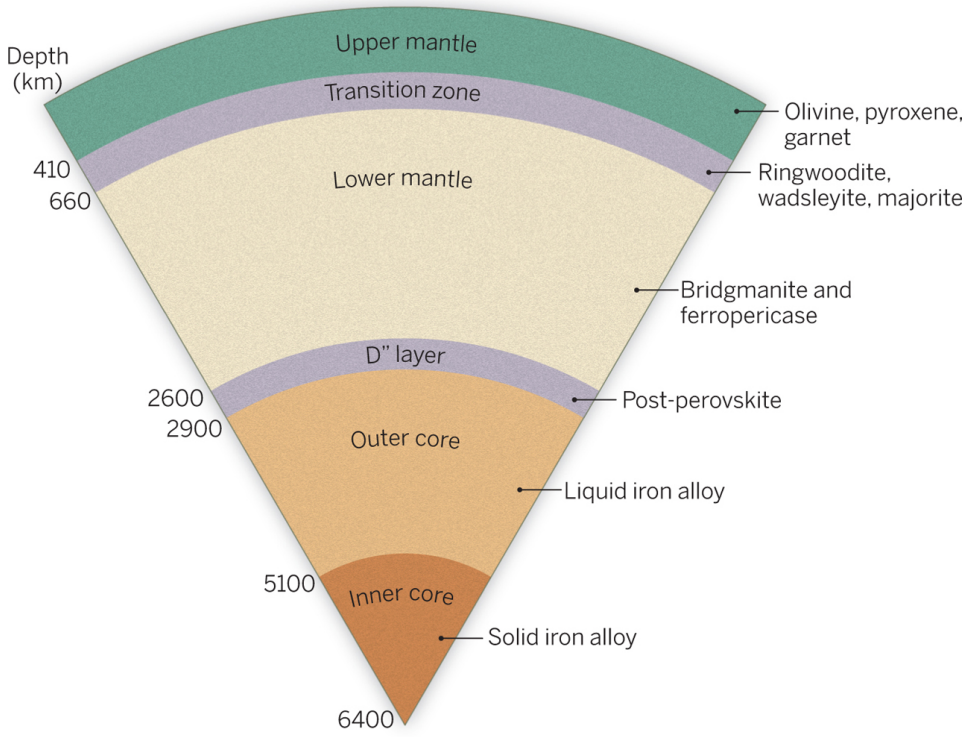

Figure 5.7: In this figure, the interior of the Earth is displayed for gaining a better understanding of the different layers which play a role in the interior of the Earth. In the middle of each layer, the categorization of this particular layer is presented, so the deepest layer is the inner core and the most upper layer is the upper mantle. On the left-hand side of each layer, the appropriate depth can be found, and on the right-hand side, the composition of each layer can be found. This figure originates from- and all credit is due to Sharp (2014).

In figure (5.7) all the different layers, which play a role in the interior of the Earth, are being categorized. The categorization of each layer can be found in the middle of this particular layer. So in the center of the Earth, the solid inner core is found, then a liquid outer core embodies this inner core. Thereafter the high-gradient zone displayed by the "D"-layer is found, this layer is the layer where most uncertainty still arises in the inner-core model, as mentioned in the PREM description. After this "D"-layer the lower mantle, transition zone, and upper mantle are found, the transition zone is a gradually changing density area for coupling the lower and upper mantle. And in the end, the Earth's crust is found that is complete oblivion in this picture because it has neglect-able depth in comparison with the other layers. On the left-hand side of each layer, the appropriate depth of this particular layer can be found, and at the right-hand side of each layer, the appropriate compositions of this particular layer can be found.

5.4.2. PREM MASS DENSITY

Now, after a better understanding of the interior of the Earth has been established, it is possible to denote the appropriate densities for each layer that are measured by the PREM model. The densities of the PREM model for different radial distances r that correspond to

different layers of the Earth are shown in the following expression:

$$\rho_{\text{PREM}}(r) = \begin{cases} \rho_{\text{InnerCore}}(r) = 13088.5 - 8838.1(r/R)^2, & \text{if} \quad 0 \le r < 1.2215 \times 10^6 \\ \rho_{\text{OuterCore}}(r) = 12581.5 - 1263.8(r/R) - \\ 3642.6(r/R)^2 - 5528.1(r/R)^3, & \text{if} \quad 1.2215 \times 10^6 \le r < 3.48 \times 10^6 \\ \rho_{\text{LowerMantle}}(r) = 7956.5 - 6476.1(r/R) + \\ 5528.3(r/R)^2 - 3080.7(r/R)^3, & \text{if} \quad 3.48 \times 10^6 \le r < 5.701 \times 10^6 \\ \rho_{\text{TransitionZone1}}(r) = 5319.7 - 1483.6(r/R), & \text{if} \quad 5.701 \times 10^6 \le r < 5.771 \times 10^6 \\ \rho_{\text{TransitionZone2}}(r) = 11249.4 - 8029.8(r/R), & \text{if} \quad 5.771 \times 10^6 \le r < 5.971 \times 10^6 \\ \rho_{\text{TransitionZone3}}(r) = 7108.9 - 3804.5(r/R), & \text{if} \quad 5.971 \times 10^6 \le r < 6.151 \times 10^6 \\ \rho_{\text{UpperMantle}}(r) = 2691.0 + 692.4(r/R) & \text{if} \quad 6.151 \times 10^6 \le r < 6.3466 \times 10^6 \\ \rho_{\text{crust1}}(r) = 2900, & \text{if} \quad 6.3466 \times 10^6 \le r < 6.3560 \times 10^6 \\ \rho_{\text{crust2}}(r) = 2900, & \text{if} \quad 6.3560 \times 10^6 \le r < 6.3680 \times 10^6 \\ \rho_{\text{ocean}}(r) = 1020 & \text{if} \quad 6.3680 \times 10^6 \le r < 6.3710 \times 10^6 \end{cases}$$

In this expression all densities ρ are displayed in kg m $^{-3}$, all radial distances r are displayed in m and R is the radius of the Earth in m. Notice that this piece-wise defined density is spherically symmetric, because it is only depends on the parameter r, and also notice that all dependencies on this parameter r are polynomial. At the Earth's surface, the assumption has been made -out of simplicity- that the surface is completely covered with ocean water. Let us plot the PREM density against the radial distance r for gaining a better understanding of the polynomial distribution in- and between each layer. The plot is given in the following figure (5.8).

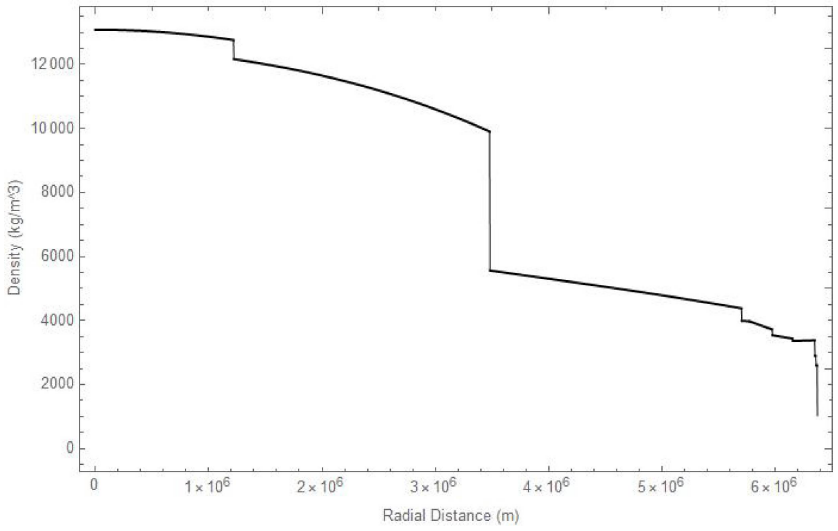

Figure 5.8: In this figure the PREM mass density distribution $\rho_{\text{PREM}}(r)$ is plotted against the radial distance r. At every discontinuity in this model a vertical line has been plotted between the discontinuities for making the figure easier to read.

In the plot above, the density distribution of the PREM model against the radial distance r can be seen. As outlined in the introduction of this model, this density distribution is only related to the radial distance r and assumes that the Earth is spherical. This spherical PREM density distribution can be used to solve for the gravitational potential and acceleration of a spherical Earth.

5.4.3. GRAVITATIONAL POTENTIAL FOR PREM MASS DENSITY

In the same manner as with the homogeneous and linear density distributions, the gravitational potential $\phi(r,\theta,\varphi)$ can again be solved and be plotted against the radial distance r, the polar angle θ and the azimuthal angle φ, where in each plot the other dependencies have been taken constant. The results are shown in figure (5.9).

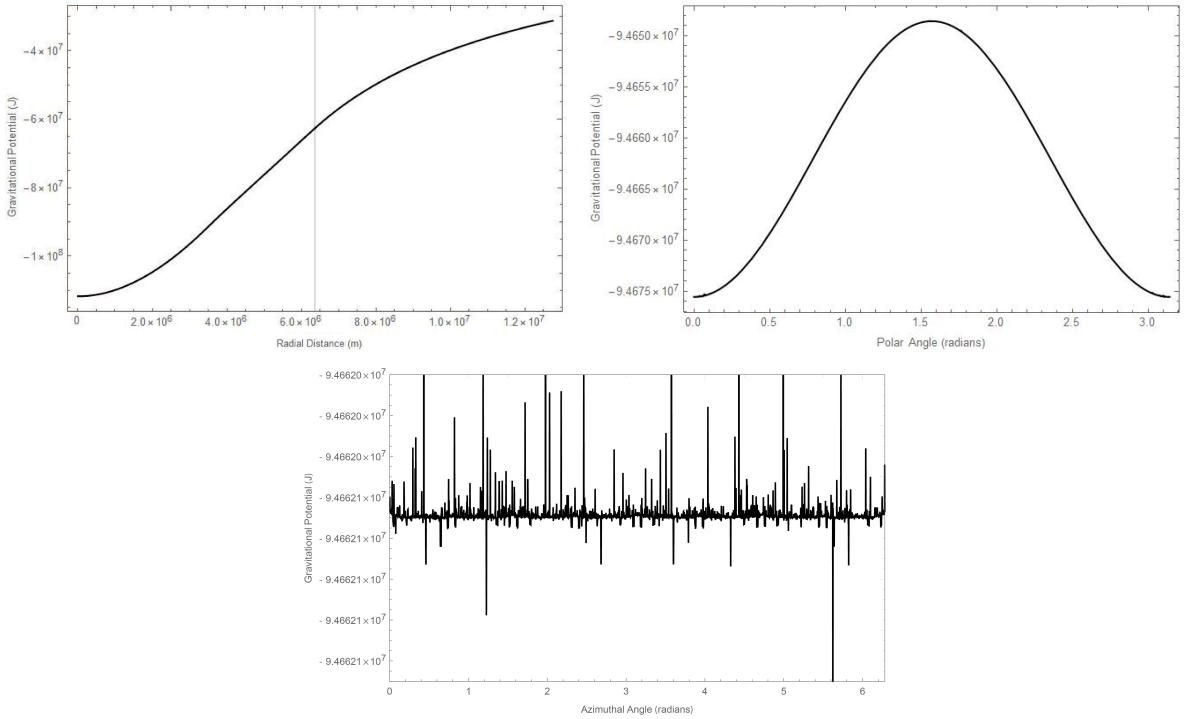

Figure 5.9: In this figure the gravitational potential $\phi(r,\theta,\varphi)$ for PREM density $\rho_{\text{PREM}}(r)$ is plotted against one of it's dependencies r, θ or φ, where the other dependencies have been taken constant. The gravitational potential $\phi(r,\theta=\pi/4,\varphi=\pi/6)$ is plotted against the radial distance r in the upper left-hand corner, $\phi(r=R/2,\theta,\varphi=\pi/6)$ is plotted against the polar angle θ in the upper right-hand corner and $\phi(r=R/2,\theta=\pi/4,\varphi)$ is plotted against the azimuthal angle φ in the plot below.

In the plot in the upper left-hand corner of figure (5.9) the gravitational potential $\phi(r,\theta=\pi/4,\varphi=\pi/6)$ has been plotted against the radial distance r, in the plot in the upper right-hand corner of figure (5.9) the gravitational potential $\phi(r=R/2,\theta,\varphi=\pi/6)$ has been plotted against the polar angle θ and in the plot below of figure (5.9) the gravitational potential $\phi(r=R/2,\theta=\pi/4,\varphi)$ has been plotted against the azimuthal angle φ.

Notice that again, the gravitational potential is continuous through the surface of the Earth, given by the gridline in the upper left-hand plot. Moreover, the gravitational potential also has a polar angle dependency to counteract centrifugal effects, and there is no relation concerning the azimuthal angle.

5.4.4. GRAVITATIONAL ACCELERATION FOR PREM MASS DENSITY

After the gravitational potential has been inspected, it is also possible to look at the radial parameter of the gravitational acceleration. Because there was no relation of the gravitational potential $\phi(r,\theta,\varphi)$ to the azimuthal angle φ, the gravitational acceleration will also have no relationship to the azimuthal angle φ, and will therefore not be inspected.

The radial parameter of the acceleration of gravitation $g_r(r,\theta,\varphi)$ is plotted against the dependencies r and the polar angle θ in figure (5.10).

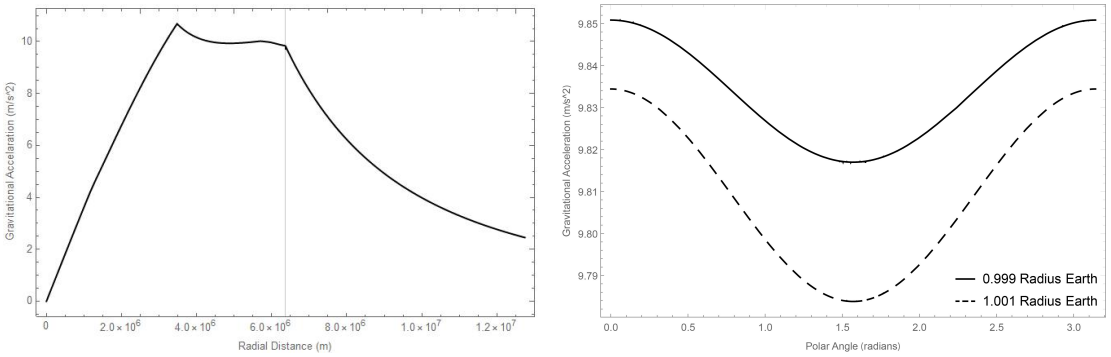

Figure 5.10: In this figure, the absolute value of the radial parameter of the gravitational acceleration $g_r(r,\theta,\varphi)$ for PREM density $\rho_{PREM}(r)$ is plotted against one of it's dependencies r and θ, where the other dependencies have been taken constant. The gravitational acceleration $g_r(r,\ \theta=\pi/4,\ \varphi=0)$ is plotted against the radial distance r in the left-hand corner, and $g_r(r=0.999$ Radius Earth, $\theta,\ \varphi=0)$ and $g_r(r=1.001$ Radius Earth, $\theta,\ \varphi=0)$ are plotted against the polar angle θ in the right-hand corner.

In figure (5.10) the absolute value of the radial parameter of the gravitational acceleration $g_r(r,\ \theta=\pi/4,\ \varphi=0)$ is plotted against the radial distance r in the plot on the left-hand side, and $g_r(r=0.999\ R,\ \theta,\ \varphi=0)$ and $g_r(r=1.001\ R,\ \theta,\ \varphi=0)$ are plotted against the polar angle θ in the right-hand side.

In the plot of g_r against the radial distance r local maxima and minima, of polynomial curves, of the gravitational acceleration inside the Earth occur. These polynomial curves are resulting from the fact that if ρ is a polynomial of degree n, then g_r will be a polynomial of degree $n+1$, this can be explained with the expression in (5.8). So the PREM density, which is a piece-wise function of polynomials, gives rise to these polynomial curves in g_r against the radial distance r, and these curves have local maxima and minima.

Notice that in the plot of g_r against the polar angle θ the gravitational acceleration of PREM density follows a trigonometrical function, such that the acceleration at the poles is the highest, and the acceleration at the equator is the lowest. These results can be attributed to centrifugal effects.

The PREM mass density model for portraying the interior of the Earth is the most realistic model that exists today, and, therefore, the gravitational acceleration in the plots in figure (5.10) must be very close to reality.

However, there are still some flaws in this model, namely the fact that the PREM model portrays Earth as a sphere and the PREM model does not account for local anomalies and generalizes Earth only on the radial distance r (more about this in the discussion).

In the case of the spherical Earth with homogeneous and linear mass density distributions, the result was that the third physical condition i.e. the normal derivative of the gravitational potential, was not continuous throughout the surface of the Earth. The PREM model also portrays the Earth through a sphere with a spherically symmetric mass distribution, therefore, the question arises if this "realistic" model has any theoretical discrepancies according to the third physical condition.

For this purpose, the plot in the left-hand corner of figure (5.10) is made for values of the radial parameter r close to the Earth's surface, and for different polar angles θ, given in figure (5.11).

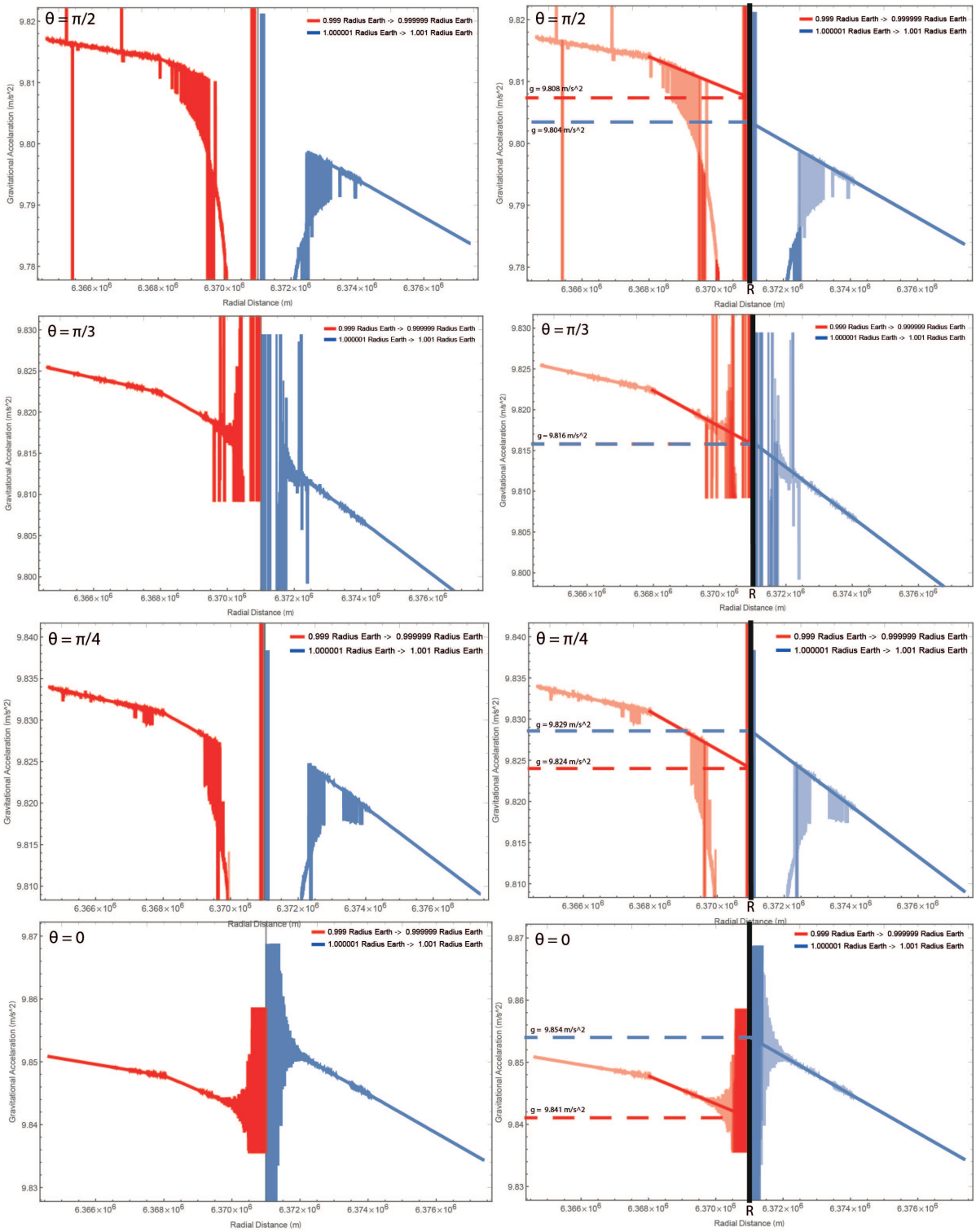

Figure 5.11: In the left-situated plots, the acceleration of gravitation for PREM mass density, in red, inside the Earth, for 99.9 % to 99.9999 % of the Earth's radius, and the acceleration of gravitation, in blue, outside the Earth, for 100.0001 % to 100.1% of the Earth's radius, are plotted for different polar angles $\theta = \pi/2, \pi/3, \pi/4$ and 0 against the radial distance r. In the right-situated plots the stable regions of the left-situated plots have been extrapolated for approximating the values of the acceleration of gravitation at the surface of the Earth for these different polar angles θ.

In the left-situated plots of figure (5.11), the red lines portray the acceleration of gravitation inside the Earth for values of 99.9 % to 99.9999 % of the Earth's radius, and the blue lines portray the acceleration of gravitation outside the Earth for values of 100.0001 % to 100.1% of the Earth's radius. The difference between the plots is the constant polar angle θ that takes on the values $\pi/2$, $\pi/3$, $\pi/4$ and 0.

In the right-situated plots of figure (5.11), the regions where the plots are stable i.e. do not oscillate or deviate from a linear relation, are being extrapolated with the stable part of the solution. These extrapolations are displayed in the linear lines that are displayed over the now transparent original solutions. From these lines, the approximate value of the acceleration of gravitation at the Earth's surface can be extracted.

Notice that, in comparison with the homogeneous case in figure (5.3) and linear case in figure (5.6), the PREM figure (5.11) has two linear red lines close to the Earth's surface that make a nod with each other. These lines are not a result of numerical integration but are a result of the transition of the Earth's crust to the ocean at the radial distance of $r = 6.368 \times 10^6$ m. This transition is portrayed in the PREM density in section (5.4.2). Therefore, when extrapolating, the line most close to the surface, which corresponds to the ocean, is used.

Let us summarize all extrapolated values of the gravitational of acceleration for different polar angles in- and outside the Earth in table (5.3).

Table 5.3: In this table, the extrapolated results, for PREM mass density, of the plots in figure (5.11) are shown for corresponding polar angles $\theta = \pi/2\,, \pi/3/, \pi/4$ and 0. The extrapolated results from inside the Earth are given by $g_\uparrow$, the extrapolated results from outside the Earth are given by $g_\downarrow$, the differences from the inside $g_\uparrow$ compared to the outside $g_\downarrow$ are given by Δg and the percentages the insides $g_\uparrow$ are above the outsides $g_\downarrow$ are given by $\frac{\Delta g}{g_\downarrow} \times 100\%$.

Polar Angle θ	$\pi/2$	$\pi/3$	$\pi/4$	0
$g_\uparrow$ [m/ s^2]	9.808	9.816	9.824	9.841
$g_\downarrow$ [m/ s^2]	9.804	9.816	9.829	9.854
Δg [m/s^2]	0.004	0.000	-0.005	-0.013
$\frac{\Delta g}{g_\downarrow} \times 100\%$	0.04%	0.00%	-0.05%	-0.13%

From figure (5.11) and the results in table (5.3) the immediate conclusion can be made that the acceleration of gravitation is not continuous over the surface of the Earth. These theoretical discrepancies do differ from the discrepancies in the table of homogeneous- and linear mass density. For the PREM model, the deviation at the pole is bigger then the deviation at the equator and an equilibrium occurs at $\pi/3$.

It is interesting to see that even the PREM model, which is the best contemporary model for the interior of the Earth, does not satisfy the underlying laws of physics for self-gravitating and rotating planets. This fact was -in all means- not a priori clear.

The main assumption of the PREM model, to have a spherical Earth with spherically symmetric mass distribution, does not portray the underlying reality of our Earth. And -this is one of the main results- correction to these models must be made for the sake of describing reality as accurately as possible. Ultimately, this is what theoretical physics is all about. Means in the pursuit of corrections to the PREM model are presented in the discussion and recommendations.

5.5. COMPARISON OF THE DIFFERENT MODELS

In the previous sections all the models were plotted separately, but for gaining some insight in the relative values in the radial distance of these models. Let us plot the gravitational potentials $\phi(r, \theta = \pi/4, \varphi = \pi/6)$ for homogeneous density, linear density and PREM density against the radial distance r together in one plot. This plot is shown in figure (5.12).

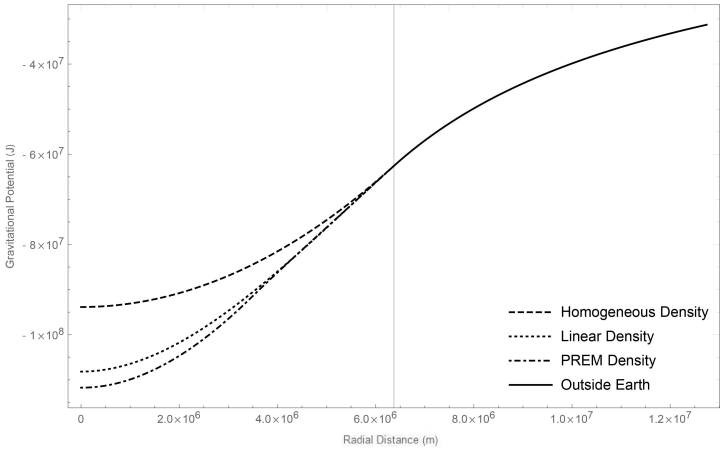

Figure 5.12: In this figure the gravitational potentials $\phi(r, \theta = \pi/4, \varphi = \pi/6)$ of the homogeneous, linear, and PREM models are plotted together against the radial distance r. In the legend, in the bottom right-hand corner of the figure, it can be found that the dashed line corresponds to the homogeneous density, the dotted line corresponds to the linear density, the dot-dashed line corresponds to the PREM density and the normal line to the gravitational potential outside the Earth.

In the legend in the bottom right-hand corner of the plot in figure (5.12), it can be seen which gravitational potential corresponds to which line in the plot. So, the dashed line corresponds to the homogeneous density, the dotted line corresponds to the linear density, the dot-dashed line corresponds to the PREM density and the normal line corresponds to the outside of the Earth. The vertical gridline in the plot represents the radius of the Earth. Notice that at this gridline all gravitational potentials are continuous.

Let us also look at the comparison of the radial parameter of the gravitational acceleration $g_r(r, \theta = \pi/4, \varphi = \pi/6)$ against the radial distance r in figure (5.13).

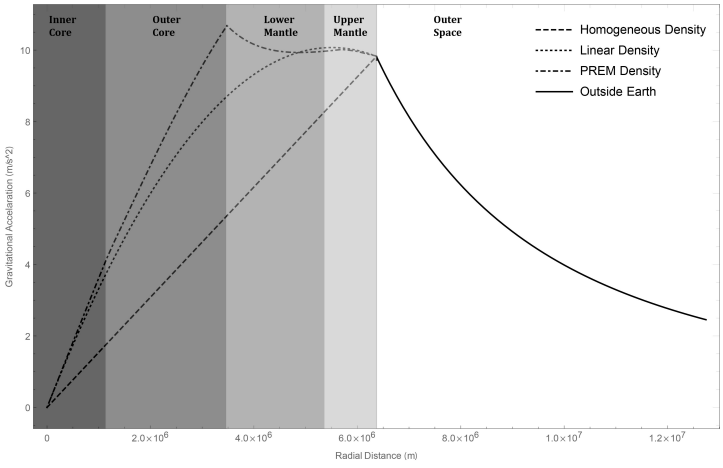

Figure 5.13: In this figure the gravitational acceleration $g_r(r, \theta = \pi/4, \varphi = \pi/6)$ of the homogeneous, linear, and PREM models are plotted together against the radial distance r. In the legend in the upper right-hand corner of the figure can be found that the dashed line corresponds to the homogeneous density, the dotted line corresponds to the linear density, the dot-dashed line corresponds to the PREM density and the normal line to the gravitational potential outside the Earth. Color bars have been added in this plot for categorizing the different layers in the Earth's composition.

In the top right-hand corner of the plot in figure (5.13), a legend has been added to

denote which line corresponds to which model, such that the dashed line is the homogeneous model, the dotted line is the linear model and the dot-dashed line is the PREM model. Also in this plot, the different regions of the interior of the Earth given by the Inner Core, Outer Core, Lower Mantle, and Upper mantle are portrayed by color bars in different shades of gray. The biggest gravitational acceleration for the PREM model occurs just outside of the outer core because in the inner and outer core the enclosed mass increases massively through the high densities.

5.5.1. MAIN RESULT OF THE MODELS

The result that can be made is that the spherical Earth with homogeneous-, linear- or, even, PREM mass density model does not correspond with the underlying laws of physics for self-gravitating and rotating planets in equilibrium. That this result arises for this formalism with Green's function was not a priori clear. These spherical models with spherical mass distribution do satisfy the geoid condition, which is forced as boundary condition through the Green's functions, and do also satisfy the continuity of the gravitational potential, however, they do not satisfy the continuity of the acceleration of gravitation.

The conclusion is made that this method is indeed capable of detecting, and even quantifying, the incompatibility of spherically symmetric mass distribution with the fundamental laws of physics for self-gravitating and rotating planets. This opens a way to computing corrections to spherically symmetric mass distributions, such as the PREM model. Based on this method, a further way forward to this end is suggested in the discussion and recommendations.

6

Discussion and Recommendations

Before starting the discussion I want to mention that the results in this report are the start of a new self-consistent model that may arise and that this report is an introduction to this new model. There are a lot of discussion points and suggestions for further research that I would like to address in this chapter. I will personally investigate this given points in the future out of curiosity, however, I needed to end this report right here because it is part of my Bachelor End Thesis that has a limited amount of time. I will address the discussion and recommendation points one by one in the sections below, and if the reader has any suggestions or comments, then do not hesitate to contact me, because all information is welcome in the study of better understanding our underlying world in the part of physics.

Green's Functions and Eigenfunction Expansions

The first discussion point that one probably has in mind after reading is: "Why does one want to use the Green's functions in the first place when one could use separation of variables and could find an eigenfunction expansion?". When using separation of variables and thereafter find the eigenfunctions with the eigenvalues of the problem, then one would probably end up with an infinitely large series. The coefficients of this series are probably found by using the appropriate boundary conditions. The disadvantage of this series expression is the fact that it is an infinite series that converges slowly, therefore it is very difficult to gain general insights in the general behavior of the solution, its peculiarities near edges etcetera. Because of this, in many aspects of the problem, it is more desirable to have a closed function represent the solution, even if it is an integral expression build-up from closed functions. The theory of Green's functions provides such a closed solution for certain geometries (Morse and Feshbach (1954)).

However, once the closed solution is found, it is -most of the time- needed to calculate the final solution using numerical integration, and these integral expressions have a singular function so this also leads to slow convergence. In many textbooks, for example Jackson (2007), it is found that the infinite space Green's $G(\boldsymbol{x}, \boldsymbol{x_0})$ function can be translated to spherical harmonics $Y_{lm}(\theta, \varphi)$ in the following way:

$$G(\boldsymbol{x}, \boldsymbol{x_0}) = \frac{-1}{4\pi} \frac{1}{|\boldsymbol{x} - \boldsymbol{x_0}|} = \sum_{l=0}^{\infty} \sum_{m=-l}^{l} \frac{-1}{2l+1} \frac{r_<^l}{r_>^l} Y_{lm}^*(\theta_0, \varphi_0)\, Y_{lm}(\theta, \varphi). \tag{6.1}$$

With this expression, the similarity between the Green's function and the spherical harmonics, which often occur as eigenfunctions when studying spherical volumes, can be seen. Instead of thinking of the Green's functions as being a different method then the

eigenfunction expansion, it is better to think about the Green's functions as being complementary to eigenfunction expansions. The mathematical Green's functions provide a theoretical framework for thinking about point sources as the cause of a certain physical field. In some highly symmetrical geometries, such as circles and certain planes in two dimensions and spheres and certain planes in three dimensions, the Green's function can directly be constructed of the infinite space Green's function, such as with the sphere in chapter 3. These solutions, which are closed expressions i.e. are not formed by an infinite series, can be thought of as a major auto-didactic advantage.

Besides the argument of the closed solution, another argument containing the physical interpretation of the Green's function could be given. When one would like to obtain the field caused by a distributed source (in our theory this was the mass distribution $\rho(\boldsymbol{x})$), then one just calculates the effect of each elementary position and adds them all up. The Green's function $G(\boldsymbol{x}, \boldsymbol{x_0})$ can be physically interpreted to be the field at observer point $\boldsymbol{x}$ caused by a unit source at $\boldsymbol{x_0}$, so the field at the observer point $\boldsymbol{x}$ caused by the source distribution $\rho(\boldsymbol{x_0})$ is just the integral over $G(\boldsymbol{x}, \boldsymbol{x_0})$ over the whole range of sources $\boldsymbol{x_0}$ occupied by the source distribution $\rho(\boldsymbol{x_0})$.

Boundary conditions can be interpreted in an almost equivalent manner. The effects of the boundary on a position $\boldsymbol{x}$ are also found by an integral over all the Green's function (or it's derivative, this depends on the type of boundary condition) which are located at position $\boldsymbol{x_0}$ together with the source distribution of the boundary given by the appropriate boundary condition $f(\boldsymbol{x_0})$.

The sum of the source distribution and the boundary condition integrals then give the result of the field at position $\boldsymbol{x}$. The advantage is that this result with fields and potentials is more physically intuitive than the result with the infinite series, which depends on an infinite sum with somewhat strange coefficients to satisfy the boundary condition.

ASSUMPTION OF SPHERICAL EARTH

In the model of chapter 5, a look was given to the gravitational profiles of the Earth where the assumption was made that the Earth was spherical. However, the Earth is not a spherical object and is more closely related to an oblate spheroid (Chandrasekhar (1969)). This is easy to understand when thinking about the gravity force that points to the center of the Earth and the centrifugal force that points out to the axis of rotation. Because of the direction of the centrifugal force, the mass on the equator is pulled to the boundary of the Earth and the mass on the poles does not feel the centrifugal force pull at all, because the poles are at $\theta = 0$. Therefore, intuitively for a geoid to exist, the distance from the Earth's center to the equator must be larger than the distance to the poles. So the spherical assumption that has been made is physically not true i.e. it does not represent the underlying reality of our world.

This failure of the representation of reality can also be seen in the models, where the discontinuity of the gravitational acceleration arises. At first, we started with the boundary condition that geopotential constant K needed to be constant on the boundary. Besides this constant on the boundary, a look was given to spherically symmetric densities. For a spherically symmetric density, the geopotential constant K can only be constant for an oblate spheroidal surface. Our spherical model does not have this oblate spheroidal surface and therefore the gravitational acceleration was not continuous over the surface of the Earth. To fix this discontinuity, two different recommendations for further research will be presented in the following subsections. The first one is to keep the spherical model and change the density distribution to minimize the error. The second one is to disregard the

spherical model and generate an oblate spheroidal model. After these recommendations, the general strength of the model that was built will be presented for suggesting the density distributions via the perceptible boundary.

Recommendation of changing the density distribution

The first recommendation is to keep our spherical model, and thereby our spherical Green's functions, and try to minimize the discontinuity of the gravitational acceleration by changing the density. The first merit of this approach is that one keeps the spherical Green's functions, which have been calculated using the method of images. In the book *Methods of Theoretical Physics* (Morse and Feshbach (1954)), it is outlined that the method of images can only be used for planes and circles in a 2-dimensional space and for planes and spheres in a 3-dimensional space, and not for any other volume in these dimensions. Therefore, the closed Green's functions of the spherical case are being preserved.

To counteract the discontinuities of the gravitational acceleration, it is possible to change the density distribution. The PREM density distribution did only depend on the radial distance, and one could try to deform this distribution such that discontinuity on the surface of the Earth minimizes. The reader may be uncomfortable with deforming this density distribution of the Earth because one deforms a quantity that was measured with instruments. However, the reader must know that the PREM density model *assumed* that "the Earth is spherical" and "the density distribution is spherically symmetric", whereas in this work it was shown that both of these assumptions can not hold for a rotating planet. The only reason that the PREM model has no dependency on the polar angle θ is because of the lack of information that was measured in Dziewonski and Anderson (1981). Therefore, one could try to come up with a density distribution that depends on θ and minimizes the effect in the discontinuity of the gravitational acceleration. For doing this, one could expand the PREM density distribution with a series of spherically harmonic functions. These spherically harmonic functions form an orthogonal base for the polar angle θ and the azimuthal angle φ. With this series expansion the number of coefficients needed with their amplitude to minimize the discontinuity in the gravitational acceleration could be evaluated.

Recommendation of further Research with the oblate Spheroid

Instead of changing the density distribution, one could also let go of the assumption that the Earth is spherical. The theory outlined in chapters 1,2 and 4 is still valid for different volumes, and transforming the gravitational potential expression in (4.4) to oblate spheroidal coordinates and finding the Green's function can give a model that is (more) physically valid. The latter case in the previous sentence, finding the Green's function for an oblate spheroid, is a more difficult problem. If one uses the same technique with the method of images as with the spherical object, then one would find a weighting factor that will depend on the azimuthal angle ν of oblate spheroidal coordinates, and taking the laplacian of this expression will result, via the product rule for derivatives, into an extra function besides the required delta function outside this volume. Hence, the method of images is not satisfied.

An introduction to the oblate spheroidal coordinates and the failure of the method of images is evaluated in part (B) of the Appendix. One could use the method of images as a beginning point and thereafter use eigenfunction expansions to counteract the error to find the Green's function. In the pursuit of the Green's function for an oblate spheroid, a lot of other mathematical concepts show up as infinite Series and spherical harmonics.

ADVANTAGE OF THE MODEL USING THE PERCEPTIBLE BOUNDARY

Take the assumption that it is indeed possible to construct the Green's functions within an oblate spheroidal volume which obeys the homogeneous Dirichlet boundary condition on the surface of this spheroid. Hence, it is possible, using the Green's functions formalism, to construct the gravitational field for a rotating planet, where:

a) The surface is a spheroidal equipotential surface (geoid)

b) An arbitrary mass density profile $\rho(\boldsymbol{x_0})$ is given.

This is possible because the formalism of the Green's function facilitates this solution to an arbitrary density profile, it is just a mathematical tool that evaluates integrals. Through item (a) it is forced that the surface of the planet is a geopotential surface, which is an *essential* condition for geostatical equilibrium.

However, this is in fact -on itself- not a *sufficient* condition for this equilibrium, because besides geostatical equilibrium, the acceleration of gravitation also needs to be continuous across the surface of the planet. This is not satisfied a priori.

Therefore, a third condition (c) could be facilitated, which can be used to determine if a certain mass density distribution is compatible with the relevant laws of physics.

The shape of a planet is directly observable. This shape could *directly* be perceived with the usage of satellites and geodesy. This is in contrast with the gigantic interior of the planet that could only be measured *indirectly*.

The major advantage of the formalism with the Green's functions provides a method to directly use the perceptibility of the surface of the planet to solve for the interior of this planet. The general strategy becomes the following:

1. Measure the shape of the surface of the planet. Thereafter, model this shape with, for example, an oblate spheroid.

2. Prescribe that this spheroid must be a geoid, through the means of taking the surface to be an equipotential surface. Now, it is possible with the formalism of the Green's functions to solve for the accompanying gravitational field.

3. Adjust the density distribution $\rho(\boldsymbol{x_0})$ in such a way that the acceleration of gravitation becomes continuous through the surface of the Earth for all geographical positions i.e. for every latitude and longitude.

Item (3) could be done through the already mentioned means of developing this distribution into spherically harmonic functions, and then evaluating the number of coefficients needed with accompanying amplitude, such that the discontinuity in the acceleration of gravitation is minimized.

The result is that through the planet's *perceptible* surface in collaboration with the formalism of Green's functions, something can be concluded about the compatible density distribution in the *interior* of this planet.

POSSIBLE APPLICATIONS AND MERITS OF THE METHOD

In this thesis, the methods of Green's functions have been studied and documented, especially that of Green's functions that obey boundary conditions at the surface of a planet. In particular, it was studied and documented how this method can be applied to build a model for calculating the gravitational field using the shape and the internal mass distribution of a self-gravitating and rotating planet.

All things considered, it is possible to conclude that an important application of this method may be in the formulation of ab-initio self-consistent models in geophysics. With ab-initio it is meant that the models will be based on simple, well-known, first principles, such as the fundamental laws of Newtonian Mechanics and Newtonian Gravitation. And with self-consistent, it is meant that the model is strictly mathematically consistent with those fundamental physical laws.

Ultimately, self-consistent models should not only answer questions like "What would be the shape and internal mass distribution of a self-gravitating and rotating planet in equilibrium?". They should also show us, in some sense, why, the shape and mass are as they are. It has to be admitted that questions of why belong to metaphysics, rather than physics. Yet, questions of this type have always been appealing to scholars and researchers (Aristotle (1956)). [1]

Forming a self-consistent, mathematical and physical model seems to be as close as one could come to addressing such questions. Furthermore, when it comes to developing a well-founded understanding of important phenomena such as the dynamics of the Earth's magnetic field (Buffett (2010)), which in its turn will depend on the virtually inaccessible ingredients and processes in the interior of the Earth, self-consistent mathematical-physical modelling is among the best tools that we have at our disposal.

It is the author's wish that someday the work presented in the present thesis may contribute to a well-founded understanding of our and other planet's internal dynamics, that is, understanding in the sense meant here.

[1] The year 1956 is the year of the English translation by Warrington et al. The original in Greek is from ca 350 B.C.E.

7

Conclusion

In this report, a mathematical-physical self-consistent model for solving Poisson's law of gravitation, for self-gravitating and rotating planets, through the use of Green's functions that obey boundary conditions on the surface of this planet, has been formalized.

For a geostatical equilibrium of this self-gravitating and rotating planet, the gravitational potential and the acceleration of gravitation need to be continuous over the surface of this planet. Moreover, the surface of this planet needs to be an equipotential surface (geoid).

Forcing this latter condition through the formalism of Green's functions on a spherical Earth with a homogeneous density, a linear spherically symmetric density, or PREM density, then it was evaluated that the gravitational potential is continuous. However, discontinuities occur in the acceleration of gravitation across the surface of the Earth, in the range of 0.01%-0.13%.

These theoretical discrepancies are a symptom of incompatibility with the laws of physics for geostatical equilibrium, and it is certainly significant as compared to the numerical accuracy of the solution.

The conclusion is made that this method is indeed capable of detecting, and even quantifying, the incompatibility of spherically symmetric mass distribution with the fundamental laws of physics for spherical self-gravitating and rotating planets. This opens a way to computing corrections to spherically symmetric mass distributions, such as the PREM model.

For further research, it is recommended to generate the PREM model through a series of spherical harmonics and changing the volume of the planet to an oblate spheroidal body.

Acknowledgements

I would like to express a lot of appreciation to my supervisor Ramses van der Toorn, who helped me continually and convincingly with knowledge and logical reasoning at the moments where I was stuck in the chaos of circular reasoning. Without his guidance and persistent help, this thesis would not have been possible.

I also would like to thank my other supervisor Dr. ir. D.J. Verschuur for the enthusiastic discussion we had over the gravity profiles of the Earth, and for his engagement in mastering this subject. Moreover, I would like to thank him for final checking my thesis.

I would like to thank my committee members, Dr. ir. W.G.M. Groenevelt and Dr. B. Rieger, for the time and engagement they are willing to spend in studying this thesis and attending the final presentation.

I thank the university and all its engaging teachers for all the wisdom and knowledge that I have attained in my bachelor programs and my work as a teaching assistant. I would like

to thank my friends- which I had the privilege to meet in Delft -, they did help me become a more responsible and professional being in the journey from adolescence to adultery.

Appendices

A

NEUMANN BOUNDARY CONDITION

In this chapter of the appendix the Green's function for a Poisson's equation with Neumann boundary condition is considered.

A.1. POISSON'S EQUATION FOR NEUMANN BOUNDARY CONDITION

The Poisson's equation is defined in definition (1.1) and was given by:

Definition A.1 (Poisson's Equation)**.** Let $D \subset \mathbb{R}^3$ be a volume, $u(\boldsymbol{x}) : D \to \mathbb{R}$ be a twice continuously differentiable function and $Q(\boldsymbol{x}) : D \to \mathbb{R}$ be a function, often known as the source term. A Poisson's equation is a Partial Differential Equation on this volume D that for all $\boldsymbol{x} \in D$ satisfies:

$$\Delta u(\boldsymbol{x}) = Q(\boldsymbol{x}). \tag{A.1}$$

In the case that the source term is zero-valued i.e. $Q(\boldsymbol{x}) = 0$ for all $\boldsymbol{x} \in D$, then this particular Poisson's equation is also called a Laplace equation.

In the case of a Neumann boundary condition, a specific distribution of the normal derivative on the function $u(\boldsymbol{x})$, denoted by $\frac{\partial u(\boldsymbol{x})}{\partial n}$, is prescribed on the boundary of our volume D, denoted by ∂D.

Problem A.1. *Let $D \subseteq \mathbb{R}^3$ be a closed bounded set with piecewise smooth boundary ∂D, let $u : D \to \mathbb{R}$ be a twice continuously differentiable function, and let $Q : D \to \mathbb{R}$ be a function known as the source term. The problem that needs to be solved is the following Poisson's equation:*

$$\Delta u(\boldsymbol{x}) = \frac{\partial^2 u(\boldsymbol{x})}{\partial x^2} + \frac{\partial^2 u(\boldsymbol{x})}{\partial y^2} + \frac{\partial^2 u(\boldsymbol{x})}{\partial z^2} = Q(\boldsymbol{x}) \quad \textit{for} \quad \boldsymbol{x} \in D,$$

with the appropriate Neumann boundary condition:

$$\frac{\partial u(\boldsymbol{x})}{\partial n} = f(\boldsymbol{x}) \quad \textit{for} \quad \boldsymbol{x} \in \partial D.$$

Where $\frac{\partial u(\boldsymbol{x})}{\partial n}$ is the derivative to the outward unity surface vector $\hat{\boldsymbol{n}}$ on the boundary ∂D.

A.2. GREEN'S FUNCTION FOR NEUMANN BOUNDARY CONDITION

The main result of section (1.2) was the last integral expression (1.5):

$$\int_D u\,\Delta v - v\,\Delta u\,dV = \int_{\partial D} u\,\frac{\partial v}{\partial n} - v\,\frac{\partial u}{\partial n}\,dS. \tag{A.2}$$

The definition of Green's function for the Neumann problem is almost analog to that of the Dirichlet problem but only differs in the boundary condition.

The main difference is that in the case of a Dirichlet boundary condition the factor $v\,\frac{\partial u}{\partial n}$ needed to vanish, because there was no information about $\frac{\partial u}{\partial n}$ on ∂D. That is the reason why Green's function needed to have $v = G = 0$ on ∂D.

In the case of the Neumann boundary condition information of $\frac{\partial u}{\partial n}$ on ∂D is given, however, in this case, no information of u on ∂D is known. Therefore, now the term of $u\,\frac{\partial v}{\partial n}$ needs to vanish. In order to do so the boundary condition of Green's function is defined to become $\frac{\partial v}{\partial n} = \frac{\partial G}{\partial n} = 0$ on ∂D. This result is put formally in the next definition.

Definition A.2 (Green's function for Neumann boundary condition)**.** Let $D \subseteq \mathbb{R}^3$ be the same closed bounded subset with piecewise smooth boundary ∂D as given above. We define the Green's function $G : D \times D \to \mathbb{R}$, for the Neumann boundary condition, in the following manner:

$$\Delta G(\boldsymbol{x}, \boldsymbol{x_0}) = \delta(\boldsymbol{x} - \boldsymbol{x_0}) \quad \text{for} \quad \boldsymbol{x} \in D,$$
$$\frac{\partial G(\boldsymbol{x}, \boldsymbol{x_0})}{\partial n} = 0 \quad \text{for} \quad \boldsymbol{x} \in \partial D.$$

Let us define the functions u and v in the integral expression shown in (A.2) as:

$$u = u(\boldsymbol{x}) \quad \text{and} \quad v = G(\boldsymbol{x}, \boldsymbol{x_0}).$$

If the expressions of $u(\boldsymbol{x})$ and $G(\boldsymbol{x}, \boldsymbol{x_0})$ are substituted in the expression of (A.2), then one could end up with the following result:

$$\int_D u(\boldsymbol{x})\ \delta(\boldsymbol{x} - \boldsymbol{x_0}) - G(\boldsymbol{x}, \boldsymbol{x_0})\ Q(\boldsymbol{x})\ dV = \int_{\partial D} u(\boldsymbol{x})\ 0 - G(\boldsymbol{x})\ f(\boldsymbol{x})\ dS. \tag{A.3}$$

Notice that on $\int_D u(\boldsymbol{x})\ \delta(\boldsymbol{x} - \boldsymbol{x_0})\ dV$ the expression of (1.7) can be used, such that this integral expression becomes $u(\boldsymbol{x_0})$. After rearranging the above expression, the result shown in (A.4) could be constructed:

$$u(\boldsymbol{x_0}) = \int_D G(\boldsymbol{x}, \boldsymbol{x_0})\ Q(\boldsymbol{x})\ dV - \int_{\partial D} f(\boldsymbol{x})\ G(\boldsymbol{x}, \boldsymbol{x_0})\ dS. \tag{A.4}$$

In an equivalent way as the Dirichlet case the symmetric property of the Green's function will again be of great use:

$$\text{for all} \quad \boldsymbol{x}, \boldsymbol{x_0} \in D: \quad G(\boldsymbol{x}, \boldsymbol{x_0}) = G(\boldsymbol{x_0}, \boldsymbol{x}).$$

If the above property of Green's function is being used when interchanging $\boldsymbol{x}$ and $\boldsymbol{x_0}$ in expression (A.4), then the following result could be obtained:

$$u(\boldsymbol{x}) = \int_D G(\boldsymbol{x}, \boldsymbol{x_0}) Q(\boldsymbol{x_0})\, dV_0 - \int_{\partial D} f(\boldsymbol{x_0}) G(\boldsymbol{x}, \boldsymbol{x_0})\, dS_0. \tag{A.5}$$

Notice that in the first integral of this result one could find the product of Green's function $G(\boldsymbol{x}, \boldsymbol{x_0})$ with the function that made the Poisson's equation in-homogeneous $Q(\boldsymbol{x})$. And at the second integral one could find the find the product of the of the Green's function on the boundary $G(\boldsymbol{x}, \boldsymbol{x_0} \in \partial D)$ with the function that made the Neumann boundary condition in-homogeneous $f(\boldsymbol{x_0})$. So both terms do again combine to the final result $u(\boldsymbol{x})$ of the Partial Differential Equation in particular weighted integrals with Green's function.

Hence, if Green's function as defined in (A.2) can be found, then the inhomogeneous Poisson's problem with inhomogeneous Neumann boundary condition in (A.1) could be

solved. So the problem is transformed from solving the Poisson's Problem directly to finding a particular function called the Green's function which needs to satisfy the constraints in the definition of (A.2).

A.3. GREEN'S FUNCTIONS FOR NEUMANN INSIDE A SPHERE

The Green's function for the Dirichlet boundary conditions has been solved in chapter 3, so let us here give a look at the case of a Neumann boundary condition. The Neumann boundary condition is a almost a corollary to the Dirichlet boundary condition with a simple adaptation. On the radius of the spherical volume D for the Neumann boundary conditions it is required that $\frac{\partial G(\boldsymbol{x},\boldsymbol{x_0})}{\partial n} = 0$, for a sphere with radius a the outgoing normal surface vector is again $\hat{\boldsymbol{r}}$ such that the Neumann boundary condition says that $\frac{\partial G(\boldsymbol{x},\boldsymbol{x_0})}{\partial r} = 0$. This boundary condition is often translated to the phrase that the flux through the boundary needs to be 0. If the reader has some knowledge about the term flux, then this reader probably knows that the solution of 0 flux on the boundary is just the translation of the negative source $\boldsymbol{x_0^*}$ at the Dirichlet boundary condition into a positive source. Hence, the solution for the Neumann problem in spherical coordinates is given by:

$$G(r,\theta,\varphi,r_0,\theta_0,\varphi_0) = \frac{-1}{4\pi}\left[\frac{1}{\sqrt{r^2+r_0^2-2rr_0\cos\gamma}} + \frac{1}{\sqrt{r^2r0^2/a^2+a^2-2rr0\cos\gamma}}\right]. \tag{A.6}$$

The solution to the problem with Neumann boundary condition was given in the integral expression in (A.5) and transforming this integral to spherical coordinates and substituting the found Green's function in (A.6) gives:

$$u(\boldsymbol{x}) = \int_0^{2\pi}\int_0^{\pi}\int_0^{a} G(r,\theta,\varphi,r_0,\theta_0,\varphi_0)\; Q(r_0,\theta_0,\varphi_0)\; r^2\;\sin\theta\; dr_0 d\theta_0 d\varphi_0 \tag{A.7}$$

$$-\int_0^{2\pi}\int_0^{\pi} f(a,\theta_0,\varphi_0)\; G(r,\theta,\varphi,a,\theta_0,\varphi_0)\; a^2\;\sin\theta\;\; d\theta_0 d\varphi_0. \tag{A.8}$$

A.4. GREEN'S FUNCTIONS FOR NEUMANN OUTSIDE A SPHERE

The Green's function for the Neumann case does not depend on the direction of the outward unit vector, in comparison with the Dirichlet boundary condition, and the solution of the Neumann case outside the sphere is therefore similar to the one inside the sphere.

B

OBLATE SPHEROIDAL COORDINATES

In the discussion it was mentioned that an oblate spheroid is a volume that describes the body of the Earth more closely. In this part of the appendix an introduction to the oblate spheroidal coordinates are made and the reason why the Green's function is more difficult to evaluate in this case is discussed.

B.1. DEFINING THE ELLIPTICAL COORDINATES

An oblate spheroid is an ellipsoid that results from rotating a 2-dimensional elliptic surface about the non-focal axis of this elliptic surface. Because of this reason, it is useful to first take a look at an elliptical coordinate system in the x-z plane, and after this system is defined the oblate spheroidal coordinates can be found through a rotation. A representation of the ellipse for which the elliptical coordinates would like to be found is given in figure (B.1).

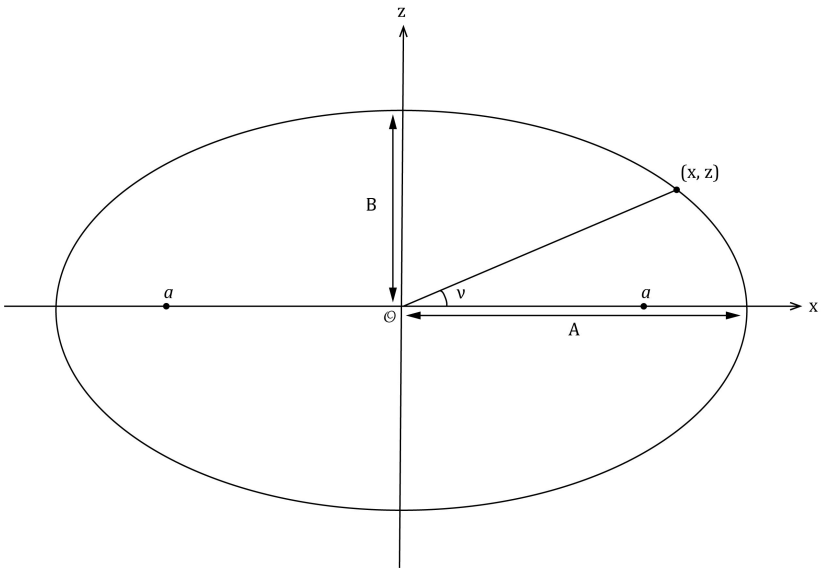

Figure B.1: In this figure, an example of an ellipse which is going to be used for clarification on the elliptical coordinates is shown. This ellipse has semi-major axis A, semi-minor axis B, and focal point a.

The ellipse in this figure has semi-minor axis A, semi-major axis B, and focal point a. Instead of deriving the elliptical coordinates by hand (which can be a long and a geometric cumbersome procedure), the elliptical coordinates will be stated and are then verified if

they agree with the elliptical formulae. The elliptical coordinates of an ellipse with focal point a in the x-z plane are given by:

$$\begin{aligned} x &= a\,\cosh\mu\,\cos\nu, \\ z &= a\,\sinh\mu\,\sin\nu. \end{aligned} \tag{B.1}$$

In these coordinates a is the focal point of the ellipse, μ is the elliptical surface parameter and ν is the angle parameter measured from the x-axis. The angle of $\nu = \pi/2$ therefore corresponds with the positive z-axis and $\nu = -\pi/2$ with the negative z-axis. What these parameters mean and how they behave will be examined later, first it is going to be verified if these parameters could portray an ellipse. A generic ellipse with semi-minor axis A and semi-major axis B needs to satisfy the following elliptical formulae:

$$\frac{x^2}{A^2} + \frac{z^2}{B^2} = 1. \tag{B.2}$$

Notice that in these elliptical coordinates $A = a\cosh\mu$ and $B = a\sinh\mu$. The following trigonometric identity shows that curves of constant μ form ellipses:

$$\frac{x^2}{(a\cosh\mu)^2} + \frac{z^2}{(a\sinh\mu)^2} = \cos^2\nu + \sin^2\nu = 1. \tag{B.3}$$

Hence, the elliptical coordinates with constant μ form elliptical curves. For a better understanding of the parameter μ some elliptical curves with different μ are constructed in Wolfram Mathematica 12.0 and are showed in figure (B.2).

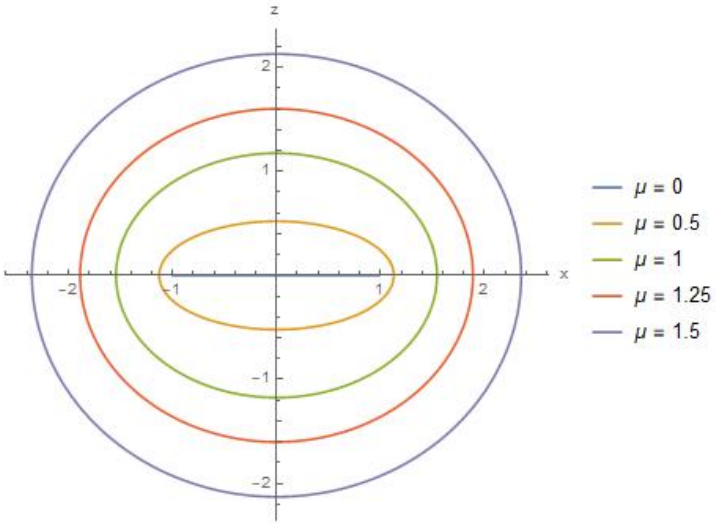

Figure B.2: In this figure, different ellipses with focal point $a = 1$ are plotted for different values of the surface parameter μ, to gain a better understanding of this parameter. The different values of μ can be found in the legend to the right of the figure.

In these ellipses, the focal point distance has been set to $a = 1$ for simplicity. In the plot it can be seen that the parameter μ functions like a parameter that sets the distance to the origin of a certain ellipse, the parameter $a\cosh\mu$ can therefore be thought of as the varying "radius" parameter of an ellipsoidal figure. Therefore, μ always needs to be positive. The conclusion of this section is that an ellipse in the x-z plane with focal point a can be described by the following elliptical coordinates:

$$x = a\,\cosh\mu\,\cos\nu,$$

$$z = a \sinh\mu \sin\nu,$$

with $\nu \in [-\pi, \pi]$ and with a constant $\mu \in [0, \infty)$.

B.2. DEFINING THE OBLATE SPHEROIDAL COORDINATES

An oblate spheroidal object is created when rotating an elliptical object given as in figure (B.1) around the nonfocal axis. In the case of figure (B.1), this nonfocal axis is given by the z-axis. A full rotation over 2π around the nonfocal axis would result in overlapping points, therefore only half of the ellipse on the positive x-axis will be rotated. For clarification this half ellipse is shown in figure (B.3).

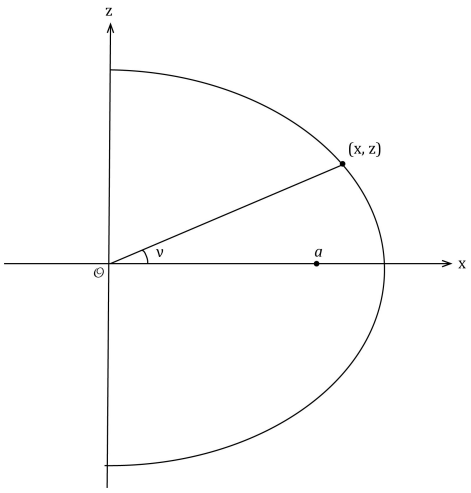

Figure B.3: In this figure, the ellipse with focal point a which is going to be rotated around the nonfocal axis, which is given by the z-axis, is shown. A schematic representation of the coordinates in this x-z plane together with accompanying angle ν can also be seen.

This figure can be constructed using the elliptical coordinates from the previous section, only now the angle is in the range $\nu \in [-\pi/2, \pi/2]$ instead of the range $[-\pi, \pi]$. This ellipse is going to be rotated around the z-axis over an angle φ which moves from 0 to 2π. The angle of $\varphi = 0$ corresponds to a half ellipse on the positive x-axis and after a rotation of 2π we are again at the positive x-axis. After rotation, a 3 dimensional object is constructed, and therefore following the right hand rule, the y-axis needs to has a direction into the paper. The rotation gives the oblate spheroidal coordinates (An oblate spheroid is defined as a spheroid which has two semi-major axis and one semi-minor axis.). The Cartesian coordinates (x, y, z) in oblate spheroidal coordinates (μ, ν, φ) are now given by:

$$\begin{aligned} x &= a \cosh\mu \cos\nu \cos\varphi, \\ y &= a \cosh\mu \cos\nu \sin\varphi, \\ z &= a \sinh\mu \sin\nu, \end{aligned} \tag{B.4}$$

with $\nu \in [-\pi/2, \pi/2]$, $\mu \in [0, \infty)$ and $\varphi \in [0, 2\pi)$. In the same way as the ellipse it can easily be seen that these coordinates satisfy the oblate spheroidal formulae with semi major axis, $A = a\cosh\mu$, in the x-y plane and semi minor axis, $B = a\sinh\mu$, at the z -axis:

$$\frac{x^2}{A^2} + \frac{y^2}{A^2} + \frac{z^2}{B^2} = \cos^2\nu \cos^2\varphi + \cos^2\nu \sin^2\varphi + \sin^2\nu = 1. \tag{B.5}$$

In the same way as with the elliptical surfaces, a constant μ gives rise to an oblate spheroidal surface. An example of how such an object looks like is given in figure (B.4).

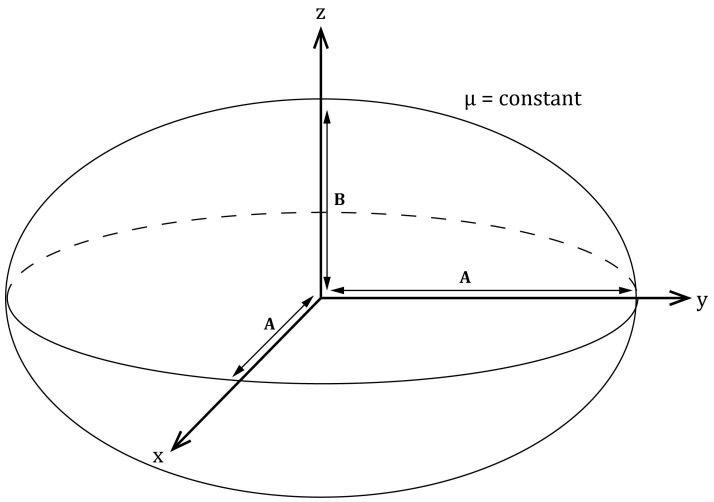

Figure B.4: In this figure, an example of an oblate spheroidal surface is shown. An oblate spheroidal surface is an object with a constant parameter μ in oblate spheroidal coordinates, this results in a spheroid with two semi-minor axis A and one semi-major axis B.

The oblate spheroidal coordinates and surfaces are now derived, and one can look at what for kind of Green's functions can be found with a boundary condition on such a oblate spheroidal surface.

B.3. GRAVITATIONAL POTENTIAL EXPRESSION FOR OBLATE SPHEROIDAL COORDINATES

After understanding the oblate spheroidal coordinates from the last chapter, one would like to find the Green's function for such an oblate spheroidal body. Let us first recapitulate the general expression of the gravitational potential for a general body D given in theorem (4.4).

The gravitational potential $\phi(\boldsymbol{x})$ of a self-gravitating rotating planet of volume D with mass density $\rho(\boldsymbol{x})$ which has been rotating for long enough such that it is in equilibrium (geoid) needs to satisfy:

$$\phi(\boldsymbol{x}) = \begin{cases} 4\pi G \int_D G(\boldsymbol{x},\boldsymbol{x_0})\rho(\boldsymbol{x_0})dV_0 + \int_{\partial D}\left[(-K-\phi_c(\boldsymbol{x_0}))\frac{\partial G(\boldsymbol{x},\boldsymbol{x_0})}{\partial n_0}\right]_{x_0\in\partial D} dS_0 & \text{if } \boldsymbol{x}\in D, \\ -\int_{\partial D}\left[(-K-\phi_c(\boldsymbol{x_0}))\frac{\partial \hat{G}(\boldsymbol{x},\boldsymbol{x_0})}{\partial n_0}\right]_{x_0\in\partial D} dS_0 & \text{if } \boldsymbol{x}\in D^c. \end{cases} \tag{B.6}$$

Let us transform this expression to oblate spheroidal coordinates. Therefore the Jacobian and the outgoing surface vector is needed,

$$\begin{aligned} \frac{\partial(x,y,z)}{\partial(\mu,\nu,\varphi)} &= \begin{vmatrix} \partial x/\partial\mu & \partial x/\partial\nu & \partial x/\partial\varphi \\ \partial y/\partial\mu & \partial y/\partial\nu & \partial y/\partial\varphi \\ \partial z/\partial\mu & \partial z/\partial\nu & \partial z/\partial\varphi \end{vmatrix} \\ &= \begin{vmatrix} a\sinh\mu\cos\nu\cos\varphi & -a\cosh\mu\sin\nu\cos\varphi & -a\cosh\mu\cos\nu\sin\varphi \\ a\sinh\mu\cos\nu\sin\varphi & -a\cosh\mu\sin\nu\sin\varphi & a\cosh\mu\cos\nu\cos\varphi \\ a\cosh\mu\sin\nu & a\sinh\mu\cos\nu & 0 \end{vmatrix} \\ &= a^3\cosh\mu\cos\nu\left(\sinh^2\mu+\sin^2\nu\right). \end{aligned} \tag{B.7}$$

Therefore it follows that:

$$dV_0 = a^3\cosh\mu_0\cos\nu_0\left(\sinh^2\mu_0+\sin^2\nu_0\right)\,d\mu_0\,d\nu_0\,d\varphi_0.$$

An oblate spheroid was created for a constant parameter μ, let us call this parameter for which the particular oblate spheroid follows M (capital μ). Hence, dS_0 is the surface for this M. So the outgoing surface vector is given by $\hat{\boldsymbol{n}} = \hat{\boldsymbol{\mu}}$, and therefore for oblate spheroidal coordinates $\boldsymbol{x} = (a\cosh\mu\cos\nu\cos\varphi, a\cosh\mu\cos\nu\sin\varphi, a\sinh\mu\sin\nu)^T$ it follows that for an oblate spheroid:

$$dS = dS_\mu = \left\| \frac{\partial \boldsymbol{x}}{\partial \nu} \times \frac{\partial \boldsymbol{x}}{\partial \varphi} \right\| d\nu\, d\varphi = a^2 \cosh^2\mu \cos\nu \sqrt{\sinh^2\mu + \sin^2\nu}\, d\nu\, d\varphi. \tag{B.8}$$

Substituting these result in the expression of the gravitational potential and having in mind that for oblate spheroidal coordinates $0 \le \mu \le M$, $-\pi/2 \le \nu < \pi/2$ and $0 \le \varphi < 2\pi$, then it follows that:

$$\phi(\mu,\nu,\varphi) = \begin{cases} 4\pi G \int_{-\pi/2}^{\pi/2}\int_0^{2\pi}\int_0^M G(\mu,\nu,\varphi,\mu_0,\nu_0,\varphi_0)\rho(\mu_0,\nu_0,\varphi_0) \\ \cdot a^3 \cosh\mu_0 \cos\nu_0 \left(\sinh^2\mu_0 + \sin^2\nu_0\right)\, d\mu_0\, d\nu_0\, d\varphi_0 + \\ \int_{-\pi/2}^{\pi/2}\int_0^{2\pi} (-K - \phi_c(M,\nu_0,\varphi_0)) \frac{\partial G(\mu,\nu,\varphi,\mu_0,\nu_0,\varphi_0)}{\partial \mu_0}\Big|_{\mu_0=M} \\ \cdot a^2 \cosh^2\mu_0 \cos\nu_0 \sqrt{\sinh^2\mu_0 + \sin^2\nu_0}\, d\nu_0\, d\varphi_0 & \text{if } \mu \le M, \\ \\ -\int_{-\pi/2}^{\pi/2}\int_0^{2\pi} (-K - \phi_c(M,\nu_0,\varphi_0)) \frac{\partial \hat{G}(\mu,\nu,\varphi,\mu_0,\nu_0,\varphi_0)}{\partial \mu_0}\Big|_{\mu_0=M} \\ \cdot a^2 \cosh^2\mu_0 \cos\nu_0 \sqrt{\sinh^2\mu_0 + \sin^2\nu_0}\, d\nu_0\, d\varphi_0 & \text{if } \mu > M. \end{cases} \tag{B.9}$$

In this expression $G(\mu,\nu,\varphi,\mu_0,\nu_0,\varphi_0)$ is the Green's function inside this volume D, $\hat{G}(\mu,\nu,\varphi,\mu_0,\nu_0,\varphi_0)$ is the Green's function outside this volume D and $\phi_c(M,\nu_0,\varphi_0)$ is the centrifugal potential. Remember that in expression (4.7) the centrifugal potential for Cartesian coordinates was found to be:

$$\phi_c(x,y,z) = -\frac{1}{2}\,\omega^2\,\left(x^2 + y^2\right). \tag{B.10}$$

Hence, the centrifugal potential for oblate spheroidal coordinates is given by:

$$\phi_c(\mu,\nu,\varphi) = -\frac{1}{2}\omega^2 a^2 \cosh^2\mu\, \cos^2\,\nu. \tag{B.11}$$

The only thing that is still missing in solving the gravitational potential for an oblate spheroidal body is the Green's function. This function is pretty difficult to find and is not evaluated in this report. In the next section the reason why the Green's function is difficult to find is described.

B.4. GREEN'S FUNCTION FOR OBLATE SPHEROIDAL VOLUME

In finding the Green's function, one could propose a similar method to that of the spherical case. There the method of images was used, such that the Green's function was given by:

$$\Delta G = \delta(\boldsymbol{x} - \boldsymbol{x_0}) - c\delta(\boldsymbol{x} - \boldsymbol{x_0^*}) \implies G = -\frac{1}{4\pi|\boldsymbol{x} - \boldsymbol{x_0}|} + \frac{c}{4\pi\left|\boldsymbol{x} - \boldsymbol{x_0^*}\right|}. \tag{B.12}$$

In this expression an image source $\boldsymbol{x_0^*}$ was placed outside the sphere to account for the fact that $G = 0$ for $\boldsymbol{x} \in \partial D$. The intuitive assumption was made that the image source $\boldsymbol{x_0^*}$ needs to be placed on the same line as the source term $\boldsymbol{x_0}$ or in mathematical terms:

$$\boldsymbol{x_0^*} = k\boldsymbol{x_0}. \tag{B.13}$$

In this expression k is a positive constant such that $\boldsymbol{x}_0^*$ is portrayed outside the surface of the oblate spheroid. For this condition of k the distance from the origin to a point of the oblate spheroidal surface is calculated:

$$\|\boldsymbol{x}\| = \sqrt{(a\cosh\mu\cos\nu\cos\varphi)^2 + (a\cosh\mu\cos\nu\sin\varphi)^2 + (a\sinh\mu\sin\nu)^2} \tag{B.14}$$

$$= a\sqrt{\cos^2\nu + \sinh^2\mu}. \tag{B.15}$$

Hence,

$$\boldsymbol{x} \in \partial D \iff \|\boldsymbol{x}\| = a\sqrt{\cos^2\nu + \sinh^2 M}. \tag{B.16}$$

One could again use the cosine rule on this expression and use the fact that the angle γ is the angle between $\boldsymbol{x}$ and $\boldsymbol{x_0}$ and also between $\boldsymbol{x}$ and $\boldsymbol{x}_0^*$. (This is completely similar to the spherical case described in (3.2). Solving for c and k after using the cosine rule gives and using the effect that the expression needs to be independent of γ, gives:

$$c = \frac{a\sqrt{\cos^2\nu + \sinh^2 M}}{|\boldsymbol{x_0}|}, \qquad k = \frac{a^2\left(\cos^2\nu + \sinh^2 M\right)}{|\boldsymbol{x_0}|^2}. \tag{B.17}$$

So the Green's function is given by:

$$G = -\frac{1}{4\pi|\boldsymbol{x}-\boldsymbol{x_0}|} + \frac{a\sqrt{\cos^2\nu + \sinh^2 M}}{|\boldsymbol{x_0}|}\frac{1}{4\pi\left|\boldsymbol{x} - \frac{a^2\left(\cos^2\nu+\sinh^2 M\right)}{|\boldsymbol{x_0}|^2}\boldsymbol{x_0}\right|}. \tag{B.18}$$

For the expression above, it is good to write out $\boldsymbol{x}$ and $\boldsymbol{x_0}$ in oblate spheroidal coordinates. However, this Green's function in (B.18) is in contrast with the beginning expression $\Delta G = \delta(\boldsymbol{x}-\boldsymbol{x_0}) - c\delta(\boldsymbol{x}-\boldsymbol{x}_0^*)$, This contrast arises because now c is not a constant parameter in terms of $\boldsymbol{x}$, but c is a function that depends on the angle ν. If the laplacian Δ is take from the expression in (B.18), then via the product rule an extra term shows up because of the dependency of c to ν. The same reason can also be given for the parameter k. So the expression in (B.18) does not satisfy the beginning point of method of Images.

In the book *Methods of theoretical* (Morse and Feshbach (1954)) it was stated that only close expressions for the method of images can be found for planes and spheres, and not for any other shape. In the case of other shapes, the method of images can also be used, only you will not find a close expression, and some eigenfunction expansions are needed. After some further investigation, it is found that the mathematical description to solve for an oblate spheroid with eigenfunction expansion is more complex in mathematical terms, and one needs to introduce a lot of new things before this can be done. (theory of Fourier Series and spherical harmonics). This part was omitted in this report because of the necessity in regard to time. Therefore, this part is recommended for further studies if one is interested in solving this problem and for gaining a better understanding of the gravitational profile of our Earth.

C

MATHEMATICA CODE

The Mathematica code is printed as a pdf file after this page occurs. In this Mathematica code, not all plots are made visible for keeping the code as short as possible. If someone is interested in the notebook file where this pdf is printed from, then it can be downloaded by clicking here Mathematica Code or going to the following link:

https://filesender.surf.nl/?s=download&token=b45ba86b-ca7c-426c-8965-cb03c4f32265

Gravitational Field of a spherical Earth

In this notebook the gravitational acceleration using Green's functions for a spherical Earth will be determined and evaluated. For this 3 different models of the density will be used: homogeneous density, linear density and the PREM model.

```
In[•]:= SetOptions[$FrontEndSession, NotebookAutoSave → True]
        NotebookSave[]
```

Parameters of the Earth:

```
In[•]:= massEarth = 5.9763 * 10^24;
        radiusEarth = 6.371 * 10^6;
        gravitationConstant = 6.6720 * 10^(-11);
        omega = 7.292116 * 10^(-5);
        geoPotentialConstant = 6.2637 * 10^7;
```

Spherical Coordinates:

```
In[•]:= x[r_, theta_, varphi_] :=
          {r Sin[theta] Cos[varphi], r Sin[theta] Sin[varphi], r Cos[theta]};
        x0[r0_, theta0_, varphi0_] := {r0 Sin[theta0] Cos[varphi0],
           r0 Sin[theta0] Sin[varphi0], r0 Cos[theta0]};
        angleBetween[theta_, varphi_, theta0_, varphi0_] :=
          Cos[theta] Cos[theta0] + Sin[theta] Sin[theta0] Cos[varphi - varphi0];
        dVolume[r_, theta_, varphi_] := r^2 Sin[theta];
```

Density models of the Earth:

Homogeneous Density Model:

```
In[•]:= volumeEarth = (4 / 3) Pi radiusEarth^3;
        densityHomogeneous = massEarth / volumeEarth;
```

Linear Density Model:

In the following linear model the density decreases linear with increasing radius, from rho0 at the center to rho1 at the surface (the condition we now must satisfy is: rho0 /4+ 3/4 rho1 = densityHomogeneous, because the Mass of Earth and Radius are constant), we choose the following values:

```
In[•]:= rho0 = 13088.5 (* same density at r=0 as PREM model in the next section *);
        rho1 = (4 / 3) (densityHomogeneous - (1 / 4) rho0);
        densityLinear[r_] := rho0 - (rho0 - rho1) r / radiusEarth;
```

let us check the condition:

```
In[•]:= (1 / 4) rho0 + (3 / 4) rho1 == densityHomogeneous;
```

Or an even more basic check,(volume integral over density = Mass):

```
In[•]:= Integrate[densityLinear[r] × dVolume[r, theta, varphi],
          {r, 0, radiusEarth}, {theta, 0, Pi}, {varphi, 0, 2 Pi}] == massEarth
Out[•]= True
```

PREM Density Model:

The PREM Density model is going to be more difficult, in this model all different layers of the earth will be examined, this has been done using waves inside the earth:

In[ ]:=
```
densityInnerCore[r_] := 13088.5 - 8838.1
    (r / radiusEarth)^2
  (* for r between 0 and 1221.5 km *);
densityOuterCore[r_] := 12581.5 - 1263.8 (r / radiusEarth) -
   3642.6 (r / radiusEarth)^2 - 5528.1 (r / radiusEarth)^3
  (* for r between 1221.5 and 3480.0 km *);
densityLowerMantle[r_] := 7956.5 - 6476.1 (r / radiusEarth) +
   5528.3 (r / radiusEarth)^2 - 3080.7 (r / radiusEarth)^3
  (* for r between 3480.0 and 5701.0 km *);
densityTransitionZone1[r_] := 5319.7 -
   1483.6 (r / radiusEarth)
  (* for r between 5701.0 and 5771.0 km *);
densityTransitionZone2[r_] := 11249.4 -
   8029.8 (r / radiusEarth)
  (* for r between 5771.0 and 5971.0 km *);
densityTransitionZone3[r_] := 7108.9 -
   3804.5 (r / radiusEarth)
  (* for r between 5971.0  and 6151.0 km *);
densityLVZ[r_] := 2691.0 + 692.4 (r /
     radiusEarth)
  (* for r between 6151.0 and 6346.6 km *);
densityCrust1[r_] :=
  2900
           (* for r between 6346.6 and 6356.0 km *);
densityCrust2[r_] :=
  2600
            (* for r between 6356.0 and 6368.0 km *);
densityOcean[r_] :=
  1020
              (* for r between 6368.0 and (radiusEarth) 6371.0 km *);
```

Now we can construct the density using a piecewise defined function (notice that *^3 is a short notation for *10^3)

In[•]:=
```
densityPREM[r_] =
 Piecewise[{{densityInnerCore[r], 0 ≤ r < 1221.5*^3}, {densityOuterCore[r],
    1221.5*^3 ≤ r < 3480.0*^3}, {densityLowerMantle[r], 3480.0*^3 ≤ r < 5701.0*^3},
   {densityTransitionZone1[r], 5701.0*^3 ≤ r < 5771.0*^3},
   {densityTransitionZone2[r], 5771.0*^3 ≤ r < 5971.0*^3},
   {densityTransitionZone3[r], 5971.0*^3 ≤ r < 6151.0*^3},
   {densityLVZ[r], 6151.0*^3 ≤ r < 6346.6*^3},
   {densityCrust1[r], 6346.6*^3 ≤ r < 6356.0*^3},
   {densityCrust2[r], 6356.0*^3 ≤ r < 6368.0*^3},
   {densityOcean[r], 6368.0*^3 ≤ r < radiusEarth}}]
```

Out[•]=

$13\,088.5 - 2.17743 \times 10^{-10}\, r^2$	$0 \le r < 1.2215 \times 10^6$
$12\,581.5 - 0.000198368\, r - 8.97421 \times 10^{-11}\, r^2 - 2.13773 \times 10^{-17}\, r^3$	$1.2215 \times 10^6 \le r < 3.48 \times 10^6$
$7956.5 - 0.0010165\, r + 1.362 \times 10^{-10}\, r^2 - 1.19131 \times 10^{-17}\, r^3$	$3.48 \times 10^6 \le r < 5.701 \times 10^6$
$5319.7 - 0.000232868\, r$	$5.701 \times 10^6 \le r < 5.771 \times 10^6$
$11\,249.4 - 0.00126037\, r$	$5.771 \times 10^6 \le r < 5.971 \times 10^6$
$7108.9 - 0.000597159\, r$	$5.971 \times 10^6 \le r < 6.151 \times 10^6$
$2691. + 0.00010868\, r$	$6.151 \times 10^6 \le r < 6.3466 \times 10^6$
2900	$6.3466 \times 10^6 \le r < 6.356 \times 10^6$
2600	$6.356 \times 10^6 \le r < 6.368 \times 10^6$
1020	$6.368 \times 10^6 \le r < 6.371 \times 10^6$
0	True

Let us make a plot of this density:

In[•]:=
```
plotDensityPREM =
 Plot[densityPREM[r], {r, 0, radiusEarth}, ExclusionsStyle → Black, Frame → True,
  FrameLabel → {"Radius (m)", "Density (kg/m^3)"}, PlotStyle → Black]
```

Out[•]=

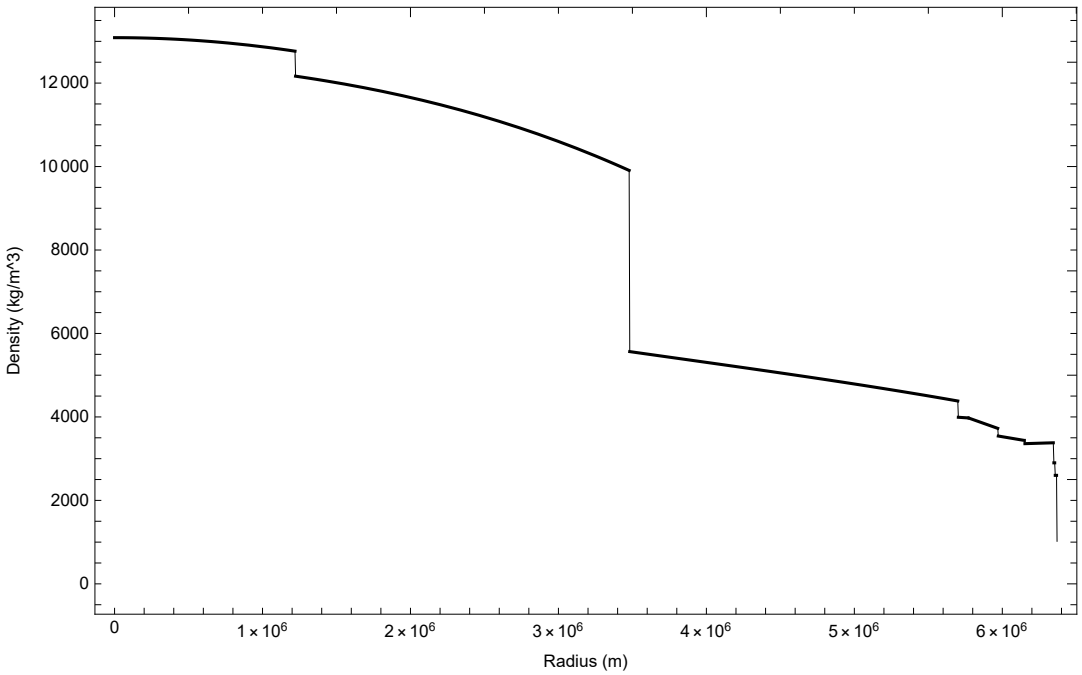

Let’s check how this expression with the total mass of the Earth:

```
In[•]:= Integrate[densityPREM[r] × dVolume[r, theta, varphi],
         {r, 0, radiusEarth}, {theta, 0, Pi}, {varphi, 0, 2 Pi}]
Out[•]= 5.97318 × 10^24

In[•]:= massEarth
Out[•]= 5.9763 × 10^24
```

Centrifugal Potential in spherical coordinates:

```
In[•]:= phiCentrifugal[r_, theta_, varphi_] := - (1 / 2) r^2 (omega)^2 (Sin[theta])^2;
```

Green Function in spherical coordinates:

The Green function for a sphere is given by:

```
In[•]:= greenFunction[r_, theta_, varphi_, r0_, theta0_, varphi0_] := (-1 / (4 * Pi))
          (1 / Sqrt[r^2 + r0^2 - 2 r r0 angleBetween[theta, varphi, theta0, varphi0] ] -
            1 / Sqrt[r^2 r0^2 / radiusEarth^2 + radiusEarth^2 -
                2 r r0 angleBetween[theta, varphi, theta0, varphi0] ]);
```

We also need the normal derivative of the Green's Function on the boundary, this is given by:

```
In[•]:= normalDerivativeGreenFunction[r_, theta_, varphi_, theta0_, varphi0_] :=
          (1 / (4 * Pi)) ((radiusEarth^2 - r^2) / (radiusEarth (r^2 + radiusEarth^2 -
                2 r radiusEarth angleBetween[theta, varphi, theta0, varphi0])^(3 / 2)));
```

We also need the gradient of these functions for the gravitational acceleration:

```
In[•]:= gradientGreenFunction[r_, theta_, varphi_, r0_, theta0_, varphi0_] =
          Part[{D[greenFunction[r, theta, varphi, r0, theta0, varphi0] , r],
            (1 / r) D[greenFunction[r, theta, varphi, r0, theta0, varphi0] , theta],
            (1 / (r Sin[theta]))
             D[greenFunction[r, theta, varphi, r0, theta0, varphi0] , varphi]}, 1];

In[•]:= gradientNormalDerivativeGreenFunction[
          r_, theta_, varphi_, theta0_, varphi0_] = Part[
          {D[normalDerivativeGreenFunction[r, theta, varphi, theta0, varphi0] , r], (1 / r)
            D[normalDerivativeGreenFunction[r, theta, varphi, theta0, varphi0] , theta],
           (1 / (r Sin[theta])) D[normalDerivativeGreenFunction[r, theta, varphi,
              theta0, varphi0] , varphi]}, 1];
```

Boundary Condition:

The assumption is made that the Earth is a geoid i.e. the surface of the earth needs to be an equipotential, this leads to the following boundary condition:

```
In[•]:= boundaryCondition[r_, theta_, varphi_] :=
          -geoPotentialConstant - phiCentrifugal[r, theta, varphi];
```

Gravitational Potential inside the Earth with Green's Function:

The boundary condition is independent of the density and will be evaluated first:

First the boundary condition inside the earth will be determined:

```
In[•]:= integrandBoundaryConditionInside[r_, theta_, varphi_, theta0_, varphi0_] :=
          normalDerivativeGreenFunction[r, theta, varphi, theta0, varphi0] ×
           boundaryCondition[radiusEarth, theta0, varphi0];

In[•]:= boundaryConditionIntegralInside[r_, theta_, varphi_] :=
          NIntegrate[integrandBoundaryConditionInside[r, theta, varphi, theta0, varphi0] ×
            dVolume[radiusEarth, theta0, varphi0], {theta0, 0, Pi}, {varphi0, 0, 2 Pi}];

In[•]:= numPlotBoundaryConditionIntegralInside =
         Plot[boundaryConditionIntegralInside[r, Pi / 4, Pi / 6], {r, 0, radiusEarth}]
```

Now the boundary condition outside the Earth will be determined, this is the same as the gravitational potential outside because there is no density outside the Earth:

```
In[•]:= integrandGravitationalPotentialOutside[r_, theta_, varphi_, theta0_, varphi0_] :=
          (-normalDerivativeGreenFunction[r, theta, varphi, theta0, varphi0])
           boundaryCondition[radiusEarth, theta0, varphi0];

In[•]:= gravitationalPotentialOustide[r_, theta_, varphi_] := NIntegrate[
           integrandGravitationalPotentialOutside[r, theta, varphi, theta0, varphi0] ×
            dVolume[radiusEarth, theta0, varphi0], {theta0, 0, Pi}, {varphi0, 0, 2 Pi}];

In[•]:= numPlotGravitationalPotentialOutside =
         Plot[gravitationalPotentialOustide[r, Pi / 4, Pi / 6],
          {r, 1.0001 radiusEarth, radiusEarth * 2}, PlotStyle → Black]
```

Numerical solution to the Gravitational Potential of the Earth with homogeneous density:

For clarification we first define the integrand:

```
In[•]:= integrandHomogeneousDensityInside[r_, theta_, varphi_, r0_, theta0_, varphi0_] :=
          4 Pi gravitationConstant
           greenFunction[r, theta, varphi, r0, theta0, varphi0] densityHomogeneous;
```

Now we will numerically integrate to get the gravitational potential inside the Earth:

```
In[•]:= densityHomogeneousIntegral[r_, theta_, varphi_] :=
          NIntegrate[integrandHomogeneousDensityInside[r, theta,
             varphi, r0, theta0, varphi0] × dVolume[r0, theta0, varphi0],
           {r0, 0, radiusEarth}, {theta0, 0, Pi}, {varphi0, 0, 2 Pi}];
```

```
In[•]:= numPlotDensityHomogeneousIntegral =
         Plot[densityHomogeneousIntegral[r, Pi / 4, Pi / 6], {r, 0, radiusEarth}]
```

The inside gravitational potential of a homogeneous sphere is then given by:

```
In[•]:= gravitationalPotentialHomogeneousInside[r_, theta_, varphi_] :=
          densityHomogeneousIntegral[r, theta, varphi] +
           boundaryConditionIntegralInside[r, theta, varphi];

In[•]:= numPlotGravitationalPotentialHomogeneousInside =
         Plot[gravitationalPotentialHomogeneousInside[r, Pi / 4, Pi / 6],
          {r, 0, 0.9999 radiusEarth}, PlotStyle → {Black, Dashed}]
```

We want to satisfy the conditions that the gravitational potential and the normal derivative of the gravitational potential are continuous across the surface, therefore we plot the homogeneous gravitational in- and outside of the sphere in one plot:

```
In[•]:= Show[numPlotGravitationalPotentialHomogeneousInside,
         numPlotGravitationalPotentialOutside, PlotRange -> All, Frame → True,
         FrameLabel → {"Radius (m)", "Gravitational Potential (J)"},
         GridLines → {{radiusEarth}, {}}]
```

Out[•]=

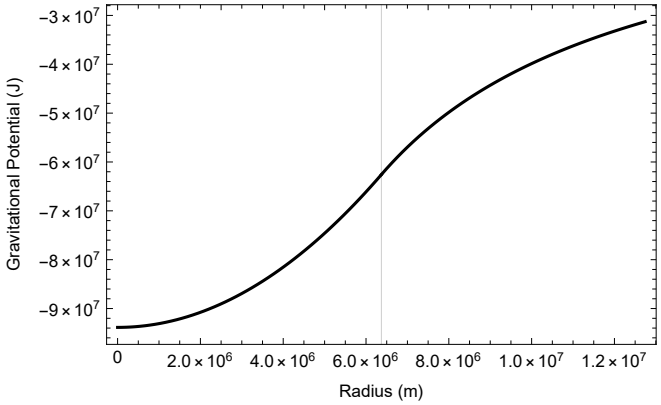

Let us also check on the varphi and theta dependencies for the homogeneous model:

```
In[•]:= numPlotGravitationalPotentialOutsideTheta = Plot[
          gravitationalPotentialOustide[1.001 radiusEarth, theta, Pi / 6], {theta, 0, Pi}]
```

In[•]:=
```
Show[numPlotGravitationalPotentialHomogeneousInsideTheta, Frame → True,
 FrameLabel → {"Polar Angle (radians)", "Gravitational Potential (J)"}]
```

Out[•]=

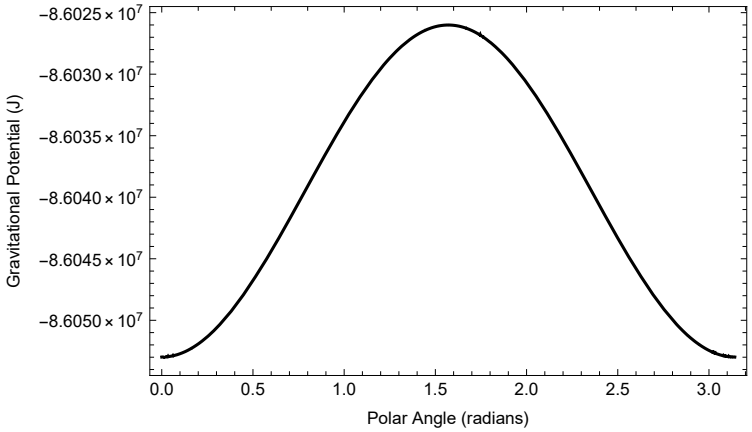

In[•]:=
```
numPlotGravitationalPotentialHomogeneousInsideVarphi =
 Plot[gravitationalPotentialHomogeneousInside[0.5 radiusEarth, Pi / 6, varphi],
  {varphi, 0, Pi}, PlotStyle → Black]
```

In[•]:=
```
Show[numPlotGravitationalPotentialHomogeneousInsideVarphi, Frame → True,
 FrameLabel → {"Azimuthal Angle (radians)", "Gravitational Potential (J)"}]
```

Out[•]=

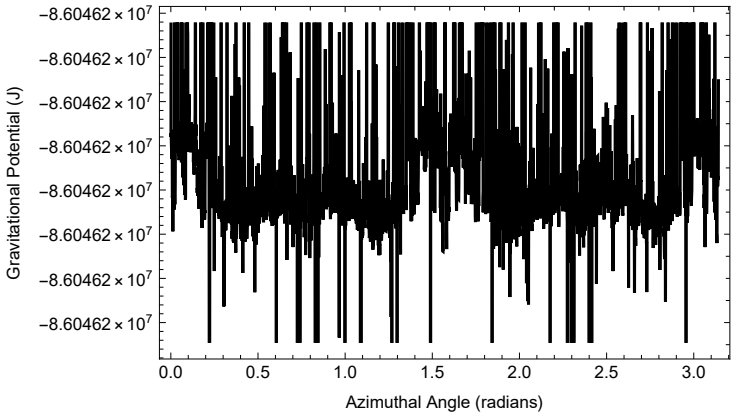

In[•]:=
```
numPlotGeoPotentialHomogeneousInsideVarphi =
 Plot[gravitationalPotentialHomogeneousInside[0.5 radiusEarth, theta, Pi / 6] +
  phiCentrifugal[0.5 radiusEarth, theta, Pi / 6], {theta, 0, Pi}]
```

Numerical solution to the Gravitational Potential of the Earth with linear density:

For clarification we first define the integrand:

In[•]:=
```
integrandLinearDensityInside[r_, theta_, varphi_, r0_, theta0_, varphi0_] :=
  4 Pi gravitationConstant
   greenFunction[r, theta, varphi, r0, theta0, varphi0] × densityLinear[r0];
```

Now we will numerically integrate to get the gravitational potential inside the Earth:

```
densityLinearIntegral[r_, theta_, varphi_] :=
  NIntegrate[integrandLinearDensityInside[r, theta, varphi, r0, theta0, varphi0] ×
    dVolume[r0, theta0, varphi0],
   {r0, 0, radiusEarth}, {theta0, 0, Pi}, {varphi0, 0, 2 Pi}];
```

```
numPlotDensityLinearIntegral =
 Plot[densityLinearIntegral[r, Pi / 4, Pi / 6], {r, 0, radiusEarth}]
```

```
$Aborted
```

The inside gravitational potential of a homogeneous sphere is then given by:

```
gravitationalPotentialLinearInside[r_, theta_, varphi_] :=
  densityLinearIntegral[r, theta, varphi] +
   boundaryConditionIntegralInside[r, theta, varphi];
```

```
numPlotGravitationalPotentialLinearInside =
 Plot[gravitationalPotentialLinearInside[r, Pi / 4, Pi / 6],
  {r, 0, 0.999 radiusEarth}, PlotStyle → {Black, Dotted}]
```

```
numPlotGravitationalPotentialLinearInsideTheta =
 Plot[gravitationalPotentialLinearInside[radiusEarth / 2, theta, Pi / 6],
  {theta, 0, Pi}, PlotStyle → Black]
```

```
Show[numPlotGravitationalPotentialLinearInsideTheta, Frame → True,
 FrameLabel → {"Polar Angle (radians)", "Gravitational Potential (J)"}]
```

```
numPlotGravitationalPotentialLinearInsideVarphi =
 Plot[gravitationalPotentialLinearInside[radiusEarth / 2, Pi / 6, varphi],
  {varphi, 0, 2 Pi}, PlotStyle → Black]
```

```
Show[numPlotGravitationalPotentialLinearInsideVarphi, Frame → True,
 FrameLabel → {"Azimuthal Angle (radians)", "Gravitational Potential (J)"}]
```

We want to satisfy the conditions that the gravitational potential and the normal derivative of the gravitational potential are continuous across the surface, therefore we plot the homogeneous gravitational in- and outside of the sphere in one plot:

```
Show[numPlotGravitationalPotentialLinearInside,
 numPlotGravitationalPotentialOutside, PlotRange -> All, Frame → True,
 FrameLabel → {"Radius (m)", "Gravitational Potential (J)"},
 GridLines → {{radiusEarth}, {}}]
```

Comparison of homogeneous against linear density gravitational plot

```
Show[numPlotGravitationalPotentialHomogeneousInside,
 numPlotGravitationalPotentialLinearInside, PlotRange → All]
```

PREM Density:

For clarification let us first define the integrand for the density integral in the PREM model:

```
In[•]:= integrandPREMDensityInside[r_, theta_, varphi_, r0_, theta0_, varphi0_] :=
          4 Pi gravitationConstant
           greenFunction[r, theta, varphi, r0, theta0, varphi0] × densityPREM[r0];
```

The density integral then becomes:

```
In[•]:= densityPREMIntegral[r_, theta_, varphi_] :=
          NIntegrate[integrandPREMDensityInside[r, theta, varphi, r0, theta0, varphi0] ×
            dVolume[r0, theta0, varphi0],
           {r0, 0, radiusEarth}, {theta0, 0, Pi}, {varphi0, 0, 2 Pi}];
```

The gravitational Potential for the PREM model will then be given by:

```
In[•]:= gravitationalPotentialPREMInside[r_, theta_, varphi_] :=
          densityPREMIntegral[r, theta, varphi] +
           boundaryConditionIntegralInside[r, theta, varphi];
```

Now let's make a plot of this:

```
In[•]:= numPlotGravitationalPotentialPREMInside =
         Plot[gravitationalPotentialPREMInside[r, Pi / 4, Pi / 6],
          {r, 0, 0.999 radiusEarth}, PlotStyle → {Black, DotDashed}]
```

Out[•]=

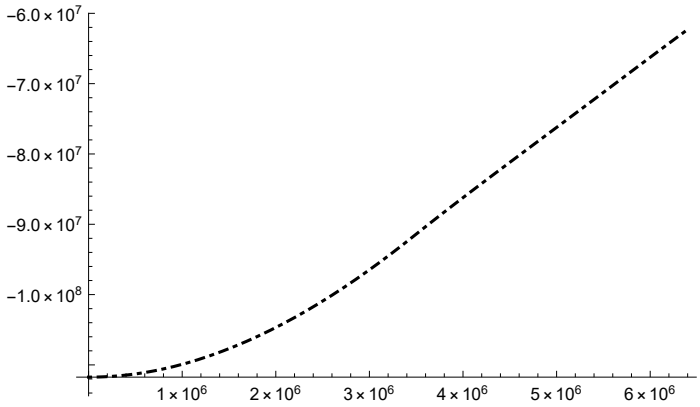

In[•]:=
```
Show[numPlotGravitationalPotentialPREMInside,
 numPlotGravitationalPotentialOutside, PlotRange -> All, Frame → True,
 FrameLabel → {"Radius (m)", "Gravitational Potential (J)"},
 GridLines → {{radiusEarth}, {}}]
```

Out[•]=

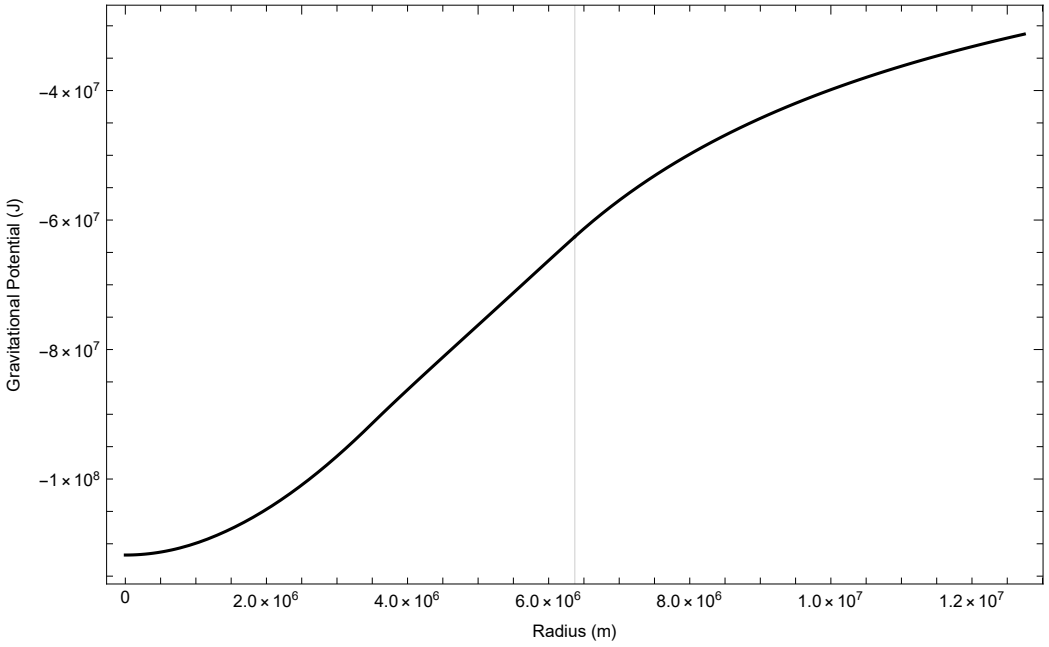

In[•]:=
```
numPlotGravitationalPotentialPREMInsideTheta =
 Plot[gravitationalPotentialPREMInside[radiusEarth / 2, theta, Pi / 6],
  {theta, 0, Pi}, PlotStyle → {Black}]
```

Out[•]=

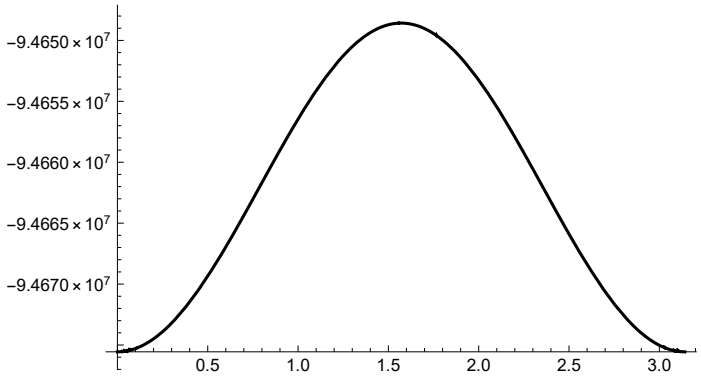

In[•]:=
```
Show[numPlotGravitationalPotentialPREMInsideTheta, Frame → True,
 FrameLabel → {"Polar Angle (radians)", "Gravitational Potential (J)"}]
```

In[ ]:=
```
numPlotGravitationalPotentialPREMInsideVarphi =
 Plot[gravitationalPotentialPREMInside[radiusEarth / 2, Pi / 4, varphi],
  {varphi, 0, 2 Pi}, PlotStyle → {Black}]
```

Out[ ]=

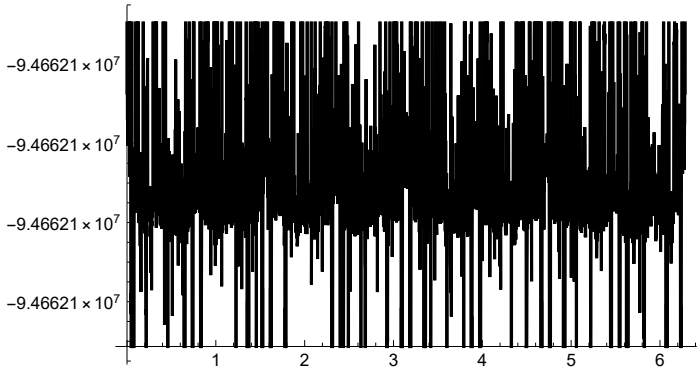

In[ ]:=
```
Show[numPlotGravitationalPotentialPREMInsideVarphi, Frame → True,
 FrameLabel → {"Polar Angle (radians)", "Gravitational Potential (J)"}]
```

Comparison of homogeneous, linear and PREM density gravitational plot:

In[ ]:=
```
Legended[Show[numPlotGravitationalPotentialHomogeneousInside,
  numPlotGravitationalPotentialLinearInside,
  numPlotGravitationalPotentialPREMInside,
  numPlotGravitationalPotentialOutside, PlotRange → All, Frame → True,
  FrameLabel → {"Radius (m)", "Gravitational Potential (J)"},
  GridLines → {{radiusEarth}, {}}], LineLegend[{Directive[Dashed, Black],
   Directive[Dotted, Black], Directive[DotDashed, Black], Black},
  {"homogeneous Density", "Linear Density", "PREM Density", "Outside Earth"}]]
```

Out[ ]=

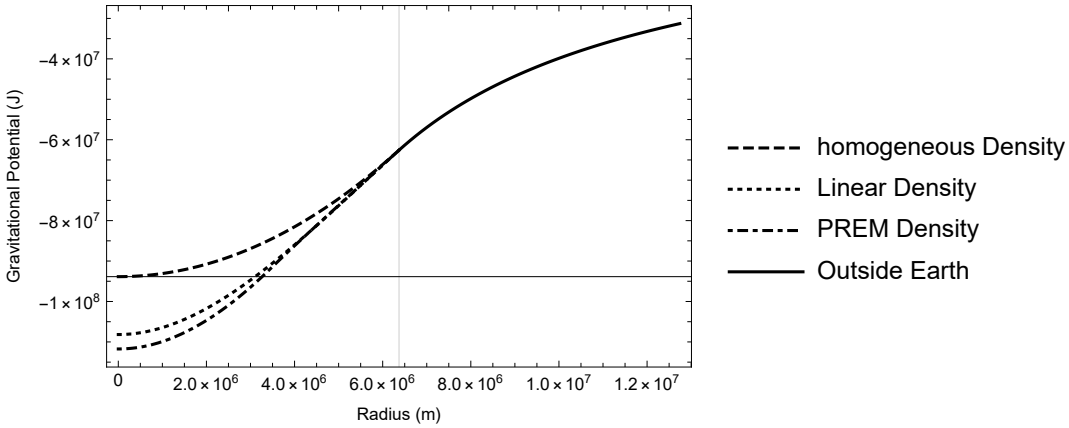

Gravitational Acceleration Outside the Earth

First we will evaluate the gravitational acceleration outside the Earth:

```
In[•]:= integrandGravitationalAccelerationBoundaryOutside[
          r_, theta_, varphi_, theta0_, varphi0_] :=
         (-gradientNormalDerivativeGreenFunction[r, theta, varphi, theta0, varphi0])
          boundaryCondition[radiusEarth, theta0, varphi0];

In[•]:= gravitationAccelerationOutside [r_, theta_, varphi_] :=
         NIntegrate[integrandGravitationalAccelerationBoundaryOutside[
            r, theta, varphi, theta0, varphi0] ×
           dVolume[radiusEarth, theta0, varphi0], {theta0, 0, Pi}, {varphi0, 0, 2 Pi}];

In[•]:= numPlotGravitationalAccelarationBoundaryOutside =
         Plot[gravitationAccelerationOutside[r, Pi / 2, 0],
          {r, 1.000001 radiusEarth, 1.001 radiusEarth}]
```

Out[•]=

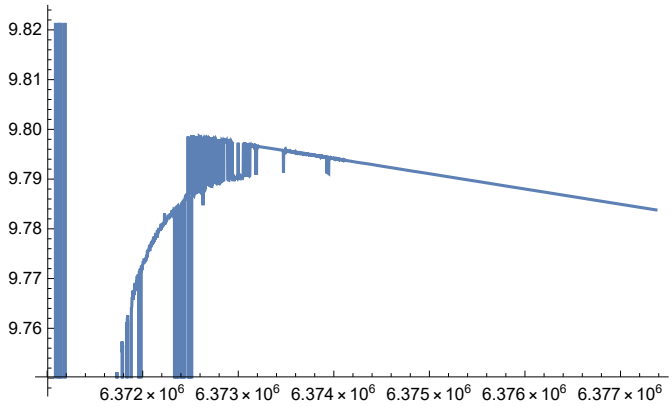


```
In[•]:= numPlotGravitationalAccelarationBoundaryOutsideHalfPi =
         Plot[gravitationAccelerationOutside[r, Pi / 2, 0],
          {r, 1.000001 radiusEarth, 1.001 radiusEarth}]

In[•]:= numPlotGravitationalAccelarationBoundaryOutsideOneThirdPi =
         Plot[gravitationAccelerationOutside[r, Pi / 3, 0],
          {r, 1.000001 radiusEarth, 1.001 radiusEarth}]

In[•]:= numPlotGravitationalAccelarationBoundaryOutsideOneQuarterPi =
         Plot[gravitationAccelerationOutside[r, Pi / 4, 0],
          {r, 1.000001 radiusEarth, 1.001 radiusEarth}]

In[•]:= numPlotGravitationalAccelarationBoundaryOutsideZeroPi =
         Plot[gravitationAccelerationOutside[r, 0, 0],
          {r, 1.000001 radiusEarth, 1.001 radiusEarth}]
```

Gravitational Acceleration Inside the Earth:

For all different densities we have the same boundary condition integral:

```
In[•]:= integrandGravitationAccelerationBoundaryInside [
          r_, theta_, varphi_, theta0_, varphi0_] :=
         (-gradientNormalDerivativeGreenFunction[r, theta, varphi, theta0, varphi0])
          boundaryCondition[radiusEarth, theta0, varphi0];
```

```
In[•]:= gravitationalAccelerationBoundaryInside[r_, theta_, varphi_] :=
          NIntegrate[integrandGravitationAccelerationBoundaryInside [
              r, theta, varphi, theta0, varphi0] ×
            dVolume[radiusEarth, theta0, varphi0], {theta0, 0, Pi}, {varphi0, 0, 2 Pi}];

        numPlotGravitationalAccelarationBoundaryInside =
         Plot[gravitationalAccelerationBoundaryInside[r, Pi / 2, Pi / 4],
          {r, 0.99 radiusEarth, radiusEarth}]
```

Homogeneous density:

```
In[•]:= integrandGravitationalAccelerationHomogeneousIntegral[
            r_, theta_, varphi_, r0_, theta0_, varphi0_] :=
          4 Pi gravitationConstant densityHomogeneous
           (- (- gradientGreenFunction[r, theta, varphi, r0, theta0, varphi0]));

In[•]:= gravitationAccelerationHomogeneous[r_, theta_, varphi_] :=
          NIntegrate[integrandGravitationalAccelerationHomogeneousIntegral[r,
              theta, varphi, r0, theta0, varphi0] × dVolume[r0, theta0, varphi0] ,
            {r0, 0, radiusEarth}, {theta0, 0, Pi}, {varphi0, 0, 2 Pi}] +
           gravitationalAccelerationBoundaryInside[r, theta, varphi];

        numPlotGravitationalAccelerationHomogeneous =
         Plot[gravitationAccelerationHomogeneous[r, Pi / 4, 0],
          {r, 0.999 radiusEarth, 0.999999 radiusEarth}, PlotStyle → Red]
```

Out[•]=

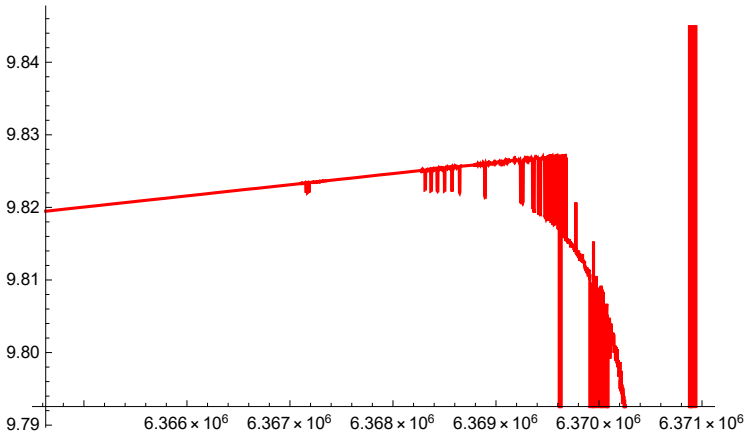


```
        numPlotGravitationalAccelerationHomogeneous =
         Plot[gravitationAccelerationHomogeneous[r, Pi / 3, 0],
          {r, 0.999 radiusEarth, 0.999999 radiusEarth}, PlotStyle → Black]
```

```
In[•]:= Legended[Show[numPlotGravitationalAccelarationBoundaryOutsideOneQuarterPi,
          numPlotGravitationalAccelerationHomogeneous, Frame → True,
          PlotRange → {{0.999 radiusEarth, 1.001 radiusEarth}, {9.81, 9.84}},
          FrameLabel → {"Radial Distance (m)", "Gravitational Accelaration (m/s^2)"},
          GridLines → {{radiusEarth}, {}}],
         LineLegend[{Directive[Line, Red], Directive[Line, Blue]},
          {"0.999 Radius Earth -> 0.999999 Radius Earth",
           "1.000001 Radius Earth -> 1.001 Radius Earth"}]
        ]
```

Out[•]=

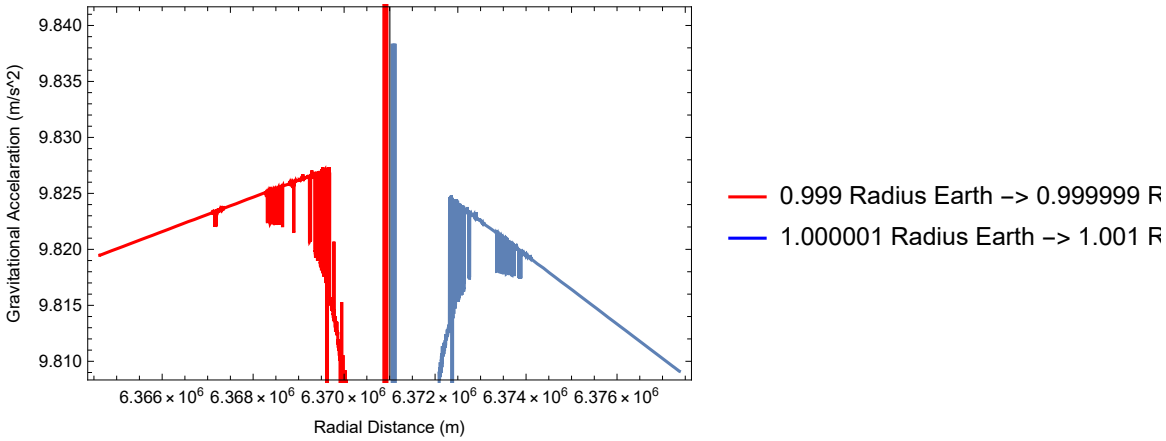


```
In[•]:= Show[numPlotGravitationalAccelerationHomogeneous,
         numPlotGravitationalAccelarationOutside, PlotRange → All, Frame -> True,
         FrameLabel → {"Radial Distance (m)", "Gravitational Accelaration (m/s^2)"},
         GridLines → {{radiusEarth}, {}}]

In[•]:= numPlotGravitationalAccelerationHomogeneousTheta =
         Plot[gravitationAccelerationHomogeneous[0.9999 radiusEarth, theta, Pi/6],
          {theta, 0, Pi}, PlotStyle → Black]

In[•]:= numPlotGravitationalAccelerationOutsideTheta =
         Plot[gravitationAccelerationOutside [1.001 radiusEarth, theta, Pi/6],
          {theta, 0, Pi}, PlotStyle → Black]
```

Linear density:

```
In[•]:= integrandGravitationalAccelerationLinearIntegral[r_, theta_, varphi_,
          r0_, theta0_, varphi0_] := 4 Pi gravitationConstant densityLinear[r0]
         (- (-gradientGreenFunction[r, theta, varphi, r0, theta0, varphi0]));

In[•]:= gravitationAccelerationLinear[r_, theta_, varphi_] :=
          NIntegrate[integrandGravitationalAccelerationLinearIntegral[r,
              theta, varphi, r0, theta0, varphi0] × dVolume[r0, theta0, varphi0] ,
           {r0, 0, radiusEarth}, {theta0, 0, Pi}, {varphi0, 0, 2 Pi}] +
          gravitationAccelerationOutside[r, theta, varphi];
```

In[•]:=
```
Show[numPlotGravitationalAccelerationLinear,
 numPlotGravitationalAccelarationOutside, PlotRange → All, Frame -> True,
 FrameLabel → {"Radial Distance (m)", "Gravitational Accelaration (m/s^2)"},
 GridLines → {{radiusEarth}, {}}]
```

Out[•]=

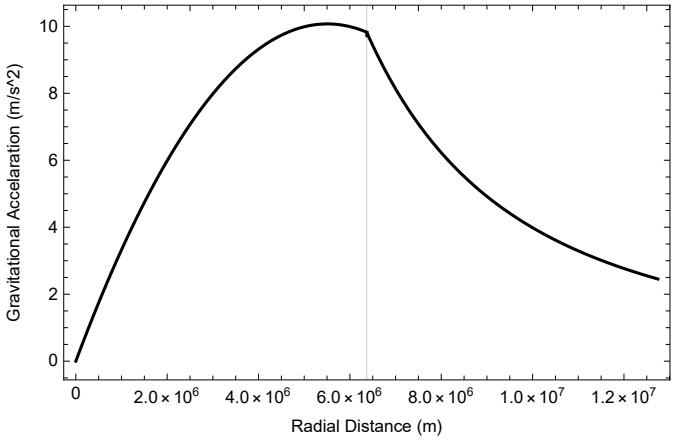

In[•]:=
```
numPlotGravitationalAccelerationLinearTheta =
 Plot[gravitationAccelerationLinear[0.999 radiusEarth, theta, Pi / 6],
  {theta, 0, Pi}, PlotStyle → Black]
```

In[•]:=
```
Legended[
 Show[ numPlotGravitationalAccelerationOutsideTheta,
  numPlotGravitationalAccelerationPremTheta, PlotRange → All, Frame → True,
  FrameLabel → {"Polar Angle (radians)", "Gravitational Acceleration (m/s^2)"}],
 LineLegend[{Directive[Black], Directive[Black]},
  { "1.001 Radius Earth", "0.999 Radius Earth"}]]
```

In[•]:=
```
numPlotGravitationalAccelerationlinearHalfPi =
 Plot[gravitationAccelerationLinear[r, Pi / 2, 0] ,
  {r, 0.999 radiusEarth, 0.999999 radiusEarth}, PlotStyle → Red]
```

In[•]:=
```
numPlotGravitationalAccelerationlinearOneThirdPi =
 Plot[gravitationAccelerationLinear[r, Pi / 3, 0] ,
  {r, 0.999 radiusEarth, 0.999999 radiusEarth}, PlotStyle → Red]
```

In[•]:=
```
numPlotGravitationalAccelerationlinearOneQuarterPi =
 Plot[gravitationAccelerationLinear[r, Pi / 4, 0] ,
  {r, 0.999 radiusEarth, 0.999999 radiusEarth}, PlotStyle → Red]
```

In[•]:=
```
numPlotGravitationalAccelerationlinearZeroPi =
 Plot[gravitationAccelerationLinear[r, 0, 0] ,
  {r, 0.999 radiusEarth, 0.999999 radiusEarth}, PlotStyle → Red]
```

In[ ]:=
```
Legended[Show[numPlotGravitationalAccelarationBoundaryOutsideZeroPi,
  numPlotGravitationalAccelerationlinearZeroPi, Frame → True,
  PlotRange → {{0.999 radiusEarth, 1.001 radiusEarth}, {9.83, 9.87}},
  FrameLabel → {"Radial Distance (m)", "Gravitational Accelaration (m/s^2)"},
  GridLines → {{radiusEarth}, {}}],
 LineLegend[{Directive[Line, Red], Directive[Line, Blue]},
  {"0.999 Radius Earth -> 0.999999 Radius Earth",
   "1.000001 Radius Earth -> 1.001 Radius Earth"}]
]
```

Out[ ]=

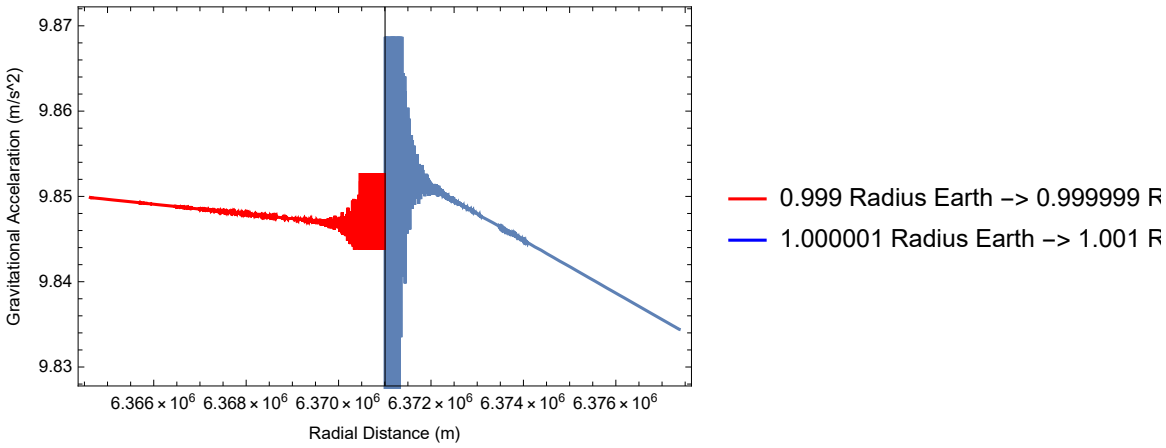

PREM Density:

In[ ]:=
```
integrandGravitationalAccelerationPREMIntegral[r_, theta_, varphi_,
   r0_, theta0_, varphi0_] := 4 Pi gravitationConstant densityPREM[r0]
  (-(-gradientGreenFunction[r, theta, varphi, r0, theta0, varphi0]));
```

In[ ]:=
```
gravitationAccelerationPREM[r_, theta_, varphi_] :=
  NIntegrate[integrandGravitationalAccelerationPREMIntegral[r, theta,
      varphi, r0, theta0, varphi0] × dVolume[r0, theta0, varphi0] ,
    {r0, 0, radiusEarth}, {theta0, 0, Pi}, {varphi0, 0, 2 Pi}] +
   gravitationAccelerationOutside[r, theta, varphi];
```

In[•]:=
```
Show[numPlotGravitationalAccelerationPREM,
 numPlotGravitationalAccelarationOutside, PlotRange → All, Frame -> True,
 FrameLabel → {"Radial Distance (m)", "Gravitational Accelaration (m/s^2)"},
 GridLines → {{radiusEarth}, {}}]
```

Out[•]=

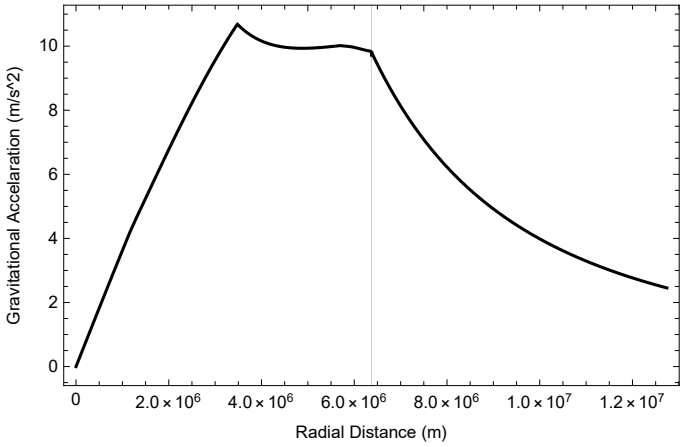

In[•]:=
```
Legended[
 Show[numPlotGravitationalAccelerationHomogeneous,
  numPlotGravitationalAccelerationLinear, numPlotGravitationalAccelerationPREM,
  numPlotGravitationalAccelarationOutside , PlotRange → All,
  AxesOrigin → {0, 0}, AxesLabel → {r, Abs[g]},
  PlotLabel → "Gravitational Models for a Spherical Earth"],
 LineLegend[{Directive[Dashed, Black], Directive[Dotted, Black],
   Directive[DotDashed, Black], Black},
  {"homogeneous Density", "Linear Density", "PREM Density", "Outside Earth"}]
]
```

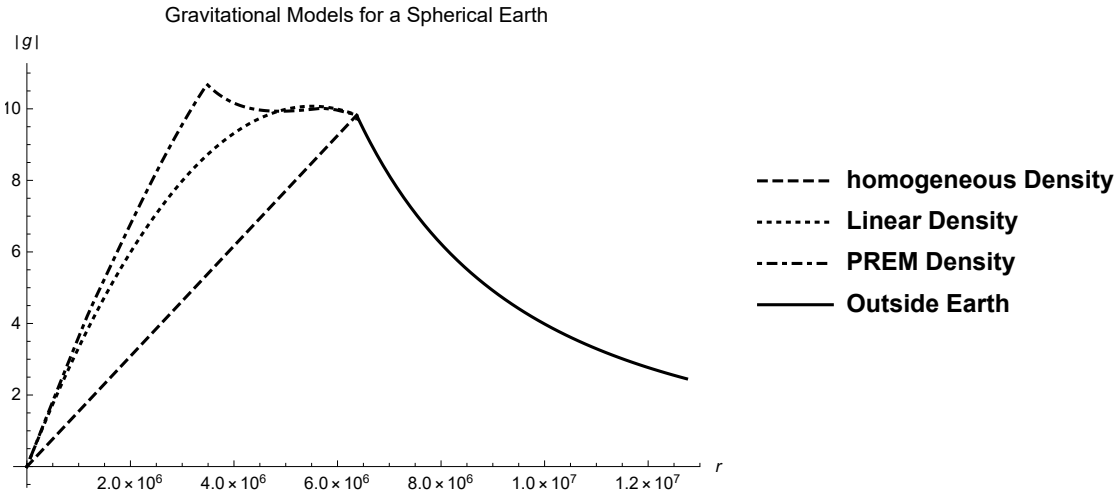

In[•]:=
```
numPlotGravitationalAccelerationPremTheta =
 Plot[gravitationAccelerationPREM[0.999 radiusEarth, theta, Pi / 6],
  {theta, 0, Pi}, PlotStyle → Black]
```

In[•]:=
```
numPlotGravitationalAccelerationPREMHalfPi =
 Plot[gravitationAccelerationPREM[r, Pi / 2, 0],
  {r, 0.999 radiusEarth, 0.999999 radiusEarth}, PlotStyle → Red]
```

In[ ]:=
```
Legended[Show[numPlotGravitationalAccelarationBoundaryOutsideHalfPi,
  numPlotGravitationalAccelerationPREMHalfPi, Frame → True,
  PlotRange → {{0.999 radiusEarth, 1.001 radiusEarth}, {9.78, 9.82}},
  FrameLabel → {"Radial Distance (m)", "Gravitational Accelaration (m/s^2)"},
  GridLines → {{radiusEarth}, {}}],
 LineLegend[{Directive[Line, Red], Directive[Line, Blue]},
  {"0.999 Radius Earth -> 0.999999 Radius Earth",
   "1.000001 Radius Earth -> 1.001 Radius Earth"}]
]
```

Out[ ]=

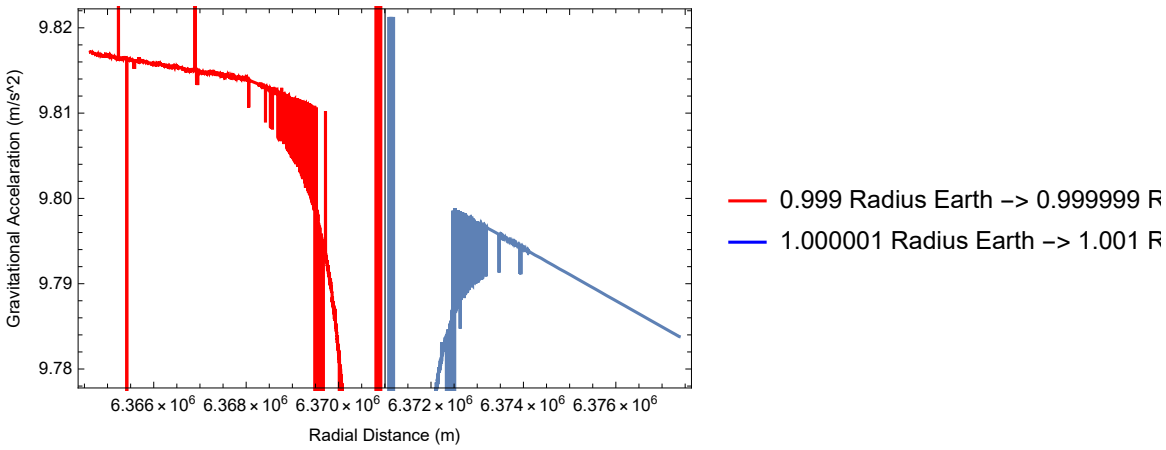

In[ ]:=
```
numPlotGravitationalAccelerationPREMOneThirdPi =
 Plot[gravitationAccelerationPREM[r, Pi/3, 0],
  {r, 0.999 radiusEarth, 0.999999 radiusEarth}, PlotStyle → Red]
```

In[ ]:=
```
numPlotGravitationalAccelerationPREMOneQuarterPi =
 Plot[gravitationAccelerationPREM[r, Pi/4, 0],
  {r, 0.999 radiusEarth, 0.999999 radiusEarth}, PlotStyle → Red]
```

In[ ]:=
```
numPlotGravitationalAccelerationPREMZeroPi =
 Plot[gravitationAccelerationPREM[r, 0, 0],
  {r, 0.999 radiusEarth, 0.999999 radiusEarth}, PlotStyle → Red]
```

BIBLIOGRAPHY

Abramowitz, M. and Stegun, I. A. (1948). *Handbook of mathematical functions with formulas, graphs, and mathematical tables*, volume 55. US Government printing office.

Aristotle (1956). *Aristotle's Metaphysics*, volume 1. Dent.

Buffett, B. A. (2010). Tidal dissipation and the strength of the earth's internal magnetic field. *Nature*, 468(7326):952–954.

Burša, M., Kouba, J., Raděj, K., True, S. A., Vatrt, V., and Vojtíšková, M. (1998). Mean earth's equipotential surface from topex/poseidon altimetry. *Studia Geophysica et Geodaetica*, 42(4):459–466.

Carothers, N. L. (2003). *Real Analysis*. Cambridge University Press.

Chambat, F. and Valette, B. (2001). Mean radius, mass, and inertia for reference earth models. *Physics of the Earth and Planetary Interiors*, 124(3-4):237–253.

Chandrasekhar, S. (1969). *Ellipsoidal Figures of Equilibrium*. Yale University Press, New Haven and London, first edition.

Clement, B. M. (2004). Dependence of the duration of geomagnetic polarity reversals on site latitude. *Nature*, 428(6983):637–640.

de Pagter, B. and Groenevelt, W. (2015). *Analysis 2*. Electrical Engineering, Mathematics and Computer Science.

Denis, C., Rogister, Y., Amalvict, M., Delire, C., Denis, A. I., and Munhoven, G. (1997). Physics of the Earth and Planetary Interiors. *Elsevier*, pages 195–206.

Dziewonski, A. M. and Anderson, D. L. (1981). Preliminary reference earth model. *Physics of the Earth and Planetary Interiors*, 25(4):297–356.

Glatzmaier, G. (2013). *Introduction to Modeling Convection in Planets and Stars*. Princeton University Press.

Glatzmaier, G. A. and Roberts, P. H. (1995). A three-dimensional self-consistent computer simulation of a geomagnetic field reversal. *Nature*, 377(6546):203–209.

Glatzmaier, G. A. and Roberts, P. H. (1996). Rotation and magnetism of earth's inner core. *Science*, 274(5294):1887–1891.

Groten, E. (1999). Report of the iag. *Special Commission SC3, Fundamental Constants, XXII IAG General Assembly*.

Haberman, R. (2003). *Applied partial differential equations with Fourier series and Boundary Value Problems*. Pearson, fifth edition edition.

Hinze, W. J., von Frese, R. R. B., and Saad, A. H. (2018). *Gravity and Magnetic Exploration*. Cambridge University Press.

Ifan G. Hughes, T. P. A. H. (2010). *Measurements and their Uncertainties A practical guide to modern error analysis*. Oxford University Press.

Isakov, V. (2017). *Inverse Problems for Partial Differential Equations*. Springer International Publishing.

Jackson, J. D. (2007). *Classical electrodynamics*. John Wiley & Sons.

Lobo, F. S. N. and Visser, M. (2004). Fundamental limitations on 'warp drive' spacetimes. *Classical and Quantum Gravity*, 21(24):5871–5892.

Luzum, B., Capitaine, N., Fienga, A., Folkner, W., Fukushima, T., Hilton, J., Hohenkerk, C., Krasinsky, G., Petit, G., Pitjeva, E., Soffel, M., and Wallace, P. (2011). The IAU 2009 system of astronomical constants: the report of the IAU working group on numerical standards for fundamental astronomy. *Celestial Mechanics and Dynamical Astronomy*, 110(4):293–304.

Malkin, Z. and Miller, N. (2009). Chandler wobble: two more large phase jumps revealed.

McComb, W. D. (1999). Dynamics and relativity. *Dynamics and relativity., by McComb, WD. Oxford University Press, Oxford (UK), 1999, XIX+ 372 p., ISBN 0-19-850112-9,.*

Milyukov, V. and Fan, S.-h. (2012). The newtonian gravitational constant: modern status of measurement and the new codata value. *Gravitation and Cosmology*, 18(3):216–224.

Misner, C. W., Thorne, K. S., Wheeler, J. A., et al. (1973). *Gravitation*. Macmillan.

Moritz, H. (1988). Geodetic reference system 1980. *Bulletin géodésique*, 62(3):348–358.

Morse, P. M. and Feshbach, H. (1954). *Methods of theoretical physics*, volume 22. American Association of Physics Teachers.

Sharp, T. (2014). Bridgmanite—named at last. *Science*, 346(6213):1057–1058.

Singer, B. S., Jicha, B. R., Mochizuki, N., and Coe, R. S. (2019). Synchronizing volcanic, sedimentary, and ice core records of earth's last magnetic polarity reversal. *Science Advances*, 5(8):eaaw4621.

Trenberth, K. E. and Smith, L. (2005). The mass of the atmosphere: A constraint on global analyses. *Journal of Climate*, 18(6):864–875.

van der Toorn, R. (1997). *Geometry, Angular Momentum and the Intrinsic Drift of Oceanic Monopolar Vortices*. Universiteit Utrecht.

van der Toorn, R. and Zimmerman, J. T. F. (2008). On the spherical approximation of the geopotential in geophysical fluid dynamics and the use of a spherical coordinate system. *Geophysical & Astrophysical Fluid Dynamics*, 102(4):349–371.

William C. Elmore, M. H. (1985). *The Physics of Waves*. Dover Publications Inc.